THE UNIVERSITY *of* EDINBURGH

Investigating the Mechanism by which Thalamocortical Projections Reach the Cerebral Cortex

Yijing Chen

Thesis submitted for the Degree of Doctor of Philosophy at the University of Edinburgh

2011

This thesis is dedicated to my family

Declaration

I declare that this thesis was composed by me, and that the work presented in this thesis has been conducted by me unless otherwise specifically mentioned in the text. This work has not been submitted for any other degree or professional qualification except as specified.

Acknowledgments

I would like to thank my great supervisors David Price and Tom Pratt for providing excellent advice and guidance throughout my PhD. Thanks also to my thesis committee member John Mason for his helpful input. I am very grateful to Dario Magnani and Thomas Theil for collaboration and technical support. Thanks Dario Magnani particularly for demonstrating the techniques of *in vitro* transplant culture and performing certain amounts of transplant culture to contribute to the N number for the transplantation experiment. I am also grateful to Katy Gilles, Mike Molinek and Rowena Smith for technical guidance.

Big thanks go to Trudi Gillespie for helping with the confocal imaging. I also want to thank Martine Manuel, Vassiliki Vfotaki, Petrina Georgala, Natasha Tian, Vlad Ivaniutsin, Chris Conway, Nikky Yu-Ting Huang, Da Mi, Tom Nowakowski, Hayden Selvadurai, Jim Clegg, Gosia Borkowska, Kevin Adutwum-Ofosu and other lab members for friendship and helps. Thanks Hayden Selvadurai particularly for proof reading the main result chapters.

Thanks Dorothy Tse, Jing Qiu, Weijia Liu, Danlei Bi, Xin Ma and many others for being great friends and share the fun and joy of life in Edinburgh.

I would like to thank my dear parents. Thank you so much for having been giving me endless support and encouragement throughout my PhD.

Finally I would like to thank MRC and ORSAS organization for the funding!

Table of contents

Abbreviations

An – angle region
ANR – anterior neural ridge
Apc – Adenomatous Polyposis coli
CGE – caudal ganglionic eminence
CNS – central nervous system
CP – cortical plate
CTAs – corticothalamic axons
Cx – cortex
DTB - diencephalic-telencephalic boundary
FACS – Fluorescence Activated Cell Sorting
FAP – Familial Adenomatous Polyposis
GP - globus pallidus
Ht – hypothalamus
IC – internal capsule
IZ – intermediate zone
LGE – lateral ganglionic eminence
LP – lateral pallium
MGE – medial ganglionic eminence
MP – medial pallium
PCR – Polymerase Chain Reaction
PPL – preplate
PSPB – Pallial-Subpallial boundary
Str – striatum
SVZ – subventricular zone
TCAs – thalamocortical axons
Th – thalamus
VP – ventral pallium
vTel – ventral telencephalon
VZ – ventricular zone
Zli – zona limitans intrathalamica

Abstract

This thesis provides insights into the mechanism by which thalamocortical axons (TCAs) approach the cortex from their origin in the thalamus. Previous studies suggested that the reciprocal projections from the prethalamus and the ventral telencephalon guide TCAs to descend through the prethalamus and cross the diencephalic-telencephalic boundary (DTB), after which TCAs navigate through permissive corridor cells in the ventral telencephalon and cross the pallial-subpallial boundary (PSPB) before reaching their final targets in the cortex. The 'Handshake Hypothesis' proposed that pioneer axons from cortical preplate neurons guide TCAs into corresponding cortical areas. However, there is a lack of convincing evidence on whether TCAs need any guidance to cross the PSPB.

In the current study, Adenomatous polyposis (Apc) gene is conditionally deleted from the cortex, by using $Emx1^{Cre}$-APC^{loxP} recombination technology. *Apc* is widely expressed in the nervous system including the cortical plate of the cortex and regulates axonal growth and neuronal differentiation. Deleting *Apc* may block neurite extension and/or affect the formation of attractive or repulsive cues in the cortex. By using DiI tracing as well as L1 immunohistochemistry techniques, I showed that in the *Apc* mutants cortical axons are absent and that TCAs initially navigate into the ventral telencephalon normally but fail to complete their journey into the cortex. They stop as they approach the PSPB, although the PSPB doesn't seem to be directly affected by the mutation of *Apc* in the cortex. Additionally, Ig-Nrg1 (Neuregulin-1), the secreted protein that was suggested to play long-range roles in attracting TCAs towards the cortex, is present in the *Apc* mutant. This implies that Ig-Nrg1 is not sufficient for guiding TCAs into the cortex, and that additional guidance factors are needed. Moreover, my *in vitro* explant culture experiments show that the mutant cortex neither repel nor inhibit thalamic axonal outgrowth, indicating that the failure of TCAs in reaching the cortex is not due to the change of repulsive cues secreted by the mutant cortex. It rather indicates that the guidance factors for TCAs are likely to function through cell-cell contact mediated mechanisms. The *Apc* mutant cortex lacks these guidance factors, which might be the cortical axons.

In conclusion, my data reveal a choice point for TCAs at the PSPB. Guidance factors from the cortex are needed for TCAs to cross the PSPB, which are absent in the *Apc* mutant. TCAs may need the direct contact with cortical axons and use them as an axonal scaffold to navigate into the cerebral cortex.

Chapter 1. Introduction

1.1 Forebrain development

The forebrain (or prosencephalon) is a large structure located at the rostral-most part of the brain. It has important functions such as information processing, reasoning, memorising, emotion controlling, etc. The forebrain derives from a simple sheet of neuroepithelial cells in anterior neuroectoderm. During embryonic development, cells at the anterior border of the neural plate-the anterior neural ridge (ANR) provide a source of signals to induce markers of procencephalic identity in the anterior neuroectoderm and promote telencephalic gene expression. The interaction of signalling centers produces gradients of signalling molecules (e.g. Fgfs, Wnts, BMPs, Shh) thus transforming the forebrain into discrete structures including the telencephalon, diencephalon and hypothalamus (Hoch et al., 2009; Wilson and Houart, 2004).

1.1.1 Dorsoventral patterning of the telencephalon

The mutually exclusive expression of different kinds of signalling molecules further determine the dorsoventral patterning of the telencephalon. The roof plate produces Wnts and Tgf-β (include Bmps) which dorsalize the neural tube, whereas the floor plate generates ventralizing signals including Sonic Hedgehog (Shh), Chordin and Noggin (Briscoe and Ericson, 2001; Lee et al., 1998). Subsequently the telencephalon develops into dorsal telencephalon (pallium) and ventral telencephalon (subpallium).

Gli3 and Shh are important factors in specifying the characteristics of the dorsal and ventral telencephalon. Transcription factor *Gli3* is initially expressed in the whole area of the telencephalon and then is downregulated in the ventral region. *Gli3* plays a role in dorsalizing the telencephalon, while *Shh* promotes ventral identity by restricting the dorsalizing function of *Gli3* (Hebert and Fishell, 2008). The expression of *Shh* starts in the hypothalamus and then extends to the ventral

telencephalon. Shh signalling induces the expression of ventral telencephalic markers such as *Nkx2.1*, *Gsh2* and *Dlx2*, etc (Corbin et al., 2003).

Fgfs act downsteam of Shh to generate ventral telencephalic cell types. As a telencephalic organizer, Fgf signalling specifies the patterning of both dorsal and ventral telencephalon, through collaboration with transcription factor Foxg1 (Hebert and Fishell, 2008).

The dorsal telencephalon can be further partitioned into the medial pallium (MP), which gives rise to the hippocampus; the dorsal pallium (DP), which develops into the neocortex; the lateral pallium (LP), which forms the olfactory cortex; the ventral pallium (VP), which generates the claustroamygdaloid complex (Schuurmans and Guillemot, 2002). The ventral telencephalon is composed of lateral ganglionic eminence (LGE) and the caudal ganglionic eminence (CGE), which gives rise to the striatum; the medial ganglionic eminence (MGE), which generates the pallidum. The LGE can be subdivided into dorsal and ventral LGE, which express different levels of *Pax6*, *Gsh2*, *Dlx2* and *Mash1*. These genes show higher expression in the dorsal LGE (dLGE) (Figure1).

1.1.2 Formation of the pallial-subpallial boundary (PSPB)

At approximately E12/13, the pallial-subpallial boundary (PSPB) forms in the murine telencephalon, separating the dorsally located cortex from the ventrally located ganglionic eminence (GE) (Inoue et al., 2001; Stoykova et al., 1997). In addition to its anatomical characteristics to be a physical boundary, the PSPB also appears to be a molecular boundary, since a number of transcription factors such as *Pax6*, *Ngn2*, *Gsh2*, *Dlx2*, *Mash1*, *Dbx1* and cell adhesion molecules such as the *cadherin* family display distinct expression patterns in either the pallial or subpallial side of the PSPB from E10.5 onwards (Figure 2) (Carney et al., 2006; Carney et al., 2009; Chapouton et al., 2001; Inoue et al., 2001; Puelles et al., 2000; Stoykova et al., 2000).

Previous studies have revealed that *Pax6* and *Gsh2* cooperate to regulate the proper positioning of the PSPB by genetically cross repressing each other, and specify proper cortical and striatal identity on either side of the PSPB (Carney et al., 2009).

Figure 1

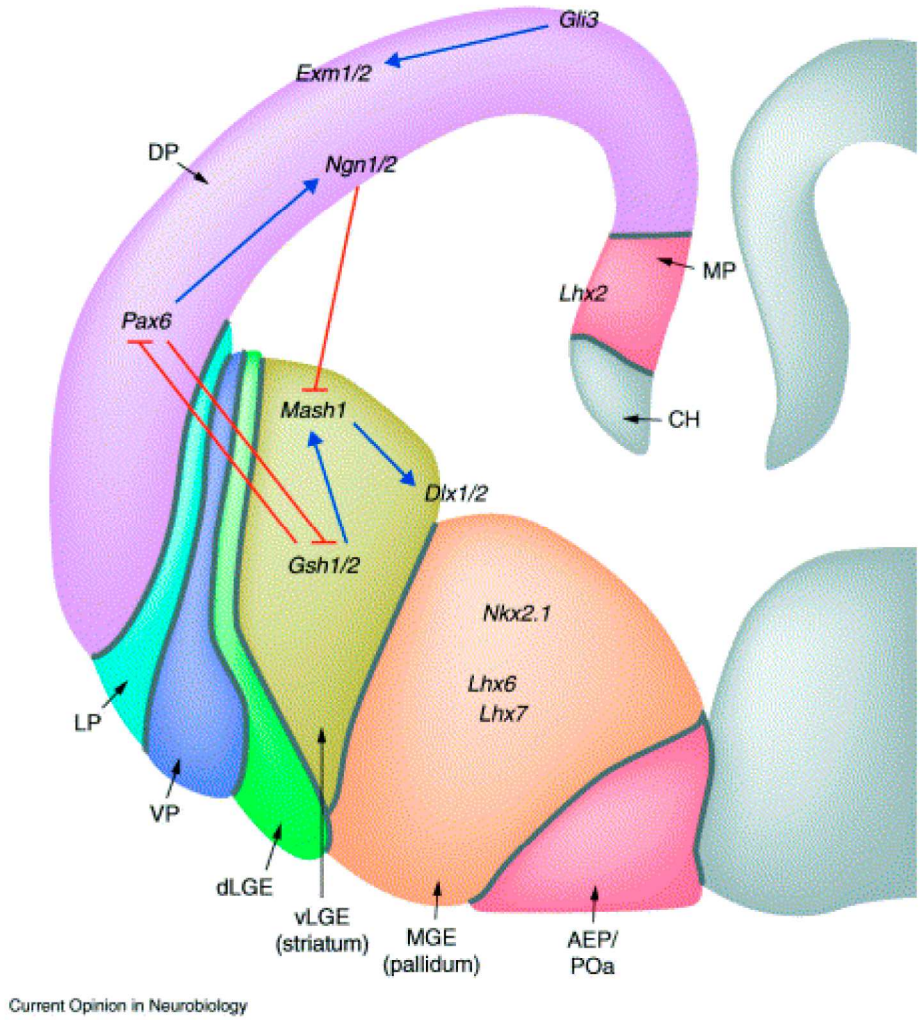

(From Schuurmans and Guillemot, 2002)

Figure 1. A schematic diagram showing dorsoventral patterning of the telencephalon. The dorsal telencephalon can be further partitioned into the medial pallium (MP), which gives rise to the hippocampus; the dorsal pallium (DP), which develops into the neocortex; the lateral pallium (LP), which forms the olfactory cortex; the ventral pallium (VP), which generates the claustroamygdaloid complex. The ventral telencephalon is composed of lateral ganglionic eminence (LGE) and the caudal ganglionic eminence (CGE), which gives rise to the striatum; the medial ganglionic eminence (MGE), which generates the pallidum. The LGE can be subdivided into dorsal and ventral LGE, which express different levels of *Pax6*, *Gsh2*, *Dlx2* and *Mash1*. These genes show higher expression in the dorsal LGE (dLGE).

Figure 2

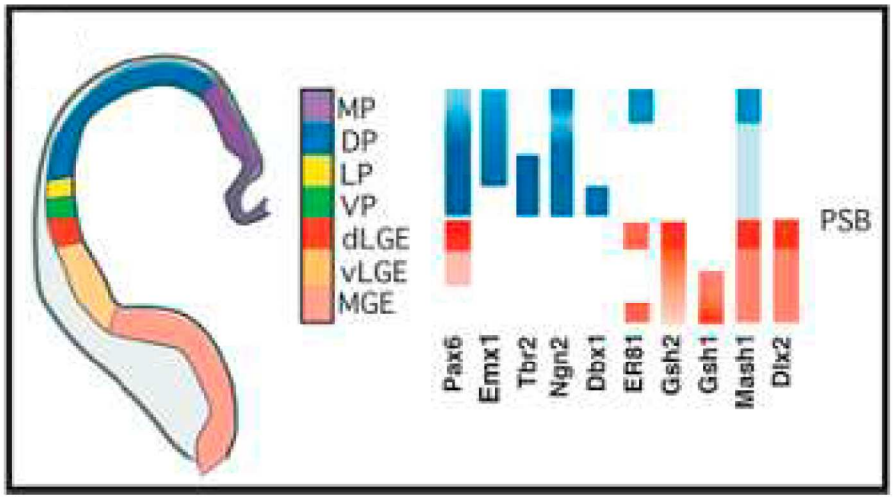

(From Yun *et al*., 2001)

Figure 2. A schematic diagram showing maker gene expressions in the telencephalon. A number of transcription factors such as Pax6, Ngn2, Gsh2, Dlx2, Mash1, Dbx1 display distinct expression patterns in the progenitor cells at the PSPB from E10.5 onwards.

Thus the PSPB is also defined as the boundary where high *Pax6* expression closely apposes to *Gsh2* expression (Carney et al., 2009). While *Pax6* is required for the differential regulation of individual VP markers (*Sfrp2*, *Tgfα*), *Gsh2* is required for the differential regulation of individual dLGE markers (*mTsh1*, *Sp8*). In the absence of *Pax6* in *Sey* mutant mice, a number of subpallial markers such as *Gsh2*, *Mash1*, *Dlx1*, *Dlx2*, expand into the pallium (Stoykova et al., 1997; Stoykova et al., 2000; Yun et al., 2001). In contrast, the lack of *Gsh2* in *Gsh2* mutant mice results in an expansion of pallial markers such as *Pax6*, *Ngn2*, *Tbr1* ventrally into the LGE (Yun et al., 2001).

It is also proposed that the differential expression of cadherin cell adhesion molecules is responsible for maintaining the cortico-striatal compartment boundary (Inoue et al., 2001). Prior to the formation of the PSPB, cadherins restrict ventral to dorsal and dorsal to ventral cell migration. By E10.5, the interface between *R-cadherin* and *cadherin-6* expression at the PSPB defines the boundary for cell lineage restriction. While *R-cadherin* delineates the future cerebral cortex, *cadherin-6* delineates the lateral ganglionic eminence (LGE).

Despite the presence of the unique boundary structure at the cortico-striatal border, its functions in restricting the migration of dorsal and ventral cells are different. While many cells migrate into the cerebral cortex from the ventral ganglionic eminence (GE), hardly any cortical cells cross the boundary into the GE. However, in *neurogenin* $2^{-/-}$ mice where *neurogenin 2* is absent in the dorsal telencephalon, cells derived from the cortex aberrantly migrate into the ventral region of the GE. Since migration of cells from the GE into the cortex is not affected in *neurogenin* $2^{-/-}$ mutants, it is speculated that transcription factor *neurogenin 2* is required for boundary features recognised specifically by cortical cells (Chapouton et al., 2001).

Progenitor cells from the pallial (VP) and subpallial (dLGE) sides of the PSPB have functions in generating migratory cells that target and populate other regions in the forebrain. For instance, cells derived from the pallial side of the PSPB migrate into the cerebral cortex. It has been reported that one of the two main subgroups of Cajal-

Retzius neurons in the pallium is generated by the tangential migration of Dbx1-expressing progenitors at the ventral pallium (VP) (Bielle et al., 2005). Moreover, progenitors from the pallial and subpallial sides of the PSPB provide a source for the lateral cortical stream (LCS), a population of migrating neurons that target the basal telencephalic limbic system, including the amygdala and the piriform and olfactory cortices. The progenitor cells from the subpallial side of the PSPB (dLGE) also contribute to the rostral migratory stream (RMS) of migrating neurons, which target in the olfactory bulb (OB) and populate the diverse subtypes of OB interneurons (Carney et al., 2006).

The LCS is comprised of a mix of Pax6-positive pallial-derived and Dlx2-positive subpallial-derived neural progenitor cells. During the early stage of brain development, a distinct $RC2^+$ radial glial scaffold is observed extending from the corticostriatal border to the ventrolateral telencephalic pial surface, with the putative migrating cells of the LCS appearing to follow this trajectory (Carney et al., 2006). $Pax6^+$ cells arising from the LCS are observed accumulating in the prospective basolateral complex, cortical and basomedial nuclei of the amygdala, as well as the olfactory tubercle and ventral pallidum, with a small population of cells present in the piriform cortex. Similar to the $Pax6^+$ cells, $Dlx2^+$ cells migrate along the route of LCS and accumulate in the basolateral complex, basomedial and cortical nuclei of the amygdala, and the piriform cortex (Carney et al., 2006).

It appears that the majority of migrating cells of the LCS target in the major structure of the basal telencephalon, the amygdala. The amygdala (or amygdalar complex) is a highly differentiated and complex region of the mammalian limbic system, and is comprised of at least 10 functionally and anatomically distinct subnuclei. The amygdala nuclei can be subdivided into two basic functional groups: those that contain excitatory neurons and those that contain inhibitory projection neurons (inhibitory interneurons exist in all amygdala nuclei). Thus, it is hypothesized that the amygdala consists of both pallial- and supallial-derived cells (Swanson and Petrovich, 1998). This is supported by the observations that the LCS appears to provide a source of both pallial- and subpallial-derived cells for the amygdala. It is

conceivable that $Pax6^+$ cells of the LCS will give rise to excitatory cells of the basal telencephalic limbic system and the $Dlx2^+$ cells will give rise to inhibitory neurons (Carney et al., 2006).

1.1.3 The lamination of the cerebral cortex

In the neocortex, most neurons are derived from the progenitor cells in the ventricular and subventricular zones (VZ/SVZ). After exit of the cell cycle, the first post mitotic neurons migrate to the pial surface of the cortex and form a new layer of cells called the preplate (PP). Subsequently, more and more post mitotic cells generated in the VZ/SVZ migrate along the processes of radial glia to form the cortical plate (CP), which splits the preplate into the marginal zone (MZ) and the subplate (SP). Through successive rounds of cell division and migration, the cortex develops into a six-layer structure (Allendoerfer and Shatz, 1994; Cecchi and Boncinelli, 2000).

1.1.4 The development of the diencephalon

The diencephalon consists of thalamus, prethalamus, eminentia thalami, epithalamus and pretectum (Lim and Golden, 2007; Puelles and Rubenstein, 2003). The prethalamus and thalamus are separated by a boundary called the zona limitans intrathalamica (ZLI). As a signalling center for numerous signalling molecules including Shh, Fgf, and Wnt, the ZLI is proposed to be an essential organizer in the anterior-posterior (AP) patterning of the diencephalon (Lim and Golden, 2007). During development, neural progenitor cells in the ventricular zone of the diencephalon exit the cell cycle and differentiate into post mitotic cells. The mature neurons migrate to the mantle zone and form distinct thalamic nuclei.

In the thalamus, various nuclei generate connections with different regions of the cortex. For instance, the dorsal lateral geniculate nucleus (dLGN) sends projections to the visual cortex, while the ventrobasal complex (VB) and the medial geniculate

nucleus project to the primary somatosensory cortex and the primary auditory cortex, respectively (Allendoerfer and Shatz, 1994; Lopez-Bendito and Molnar, 2003).

1.2 The formation of reciprocal connections between cortex and thalamus

Thalamic nuclei serve as relays receiving the inputs from sense organs (e.g. visual and acoustic organs) and the subcortical motor centers, and then delivering them to the relevant cortical regions through which the sensory information is processed. Two major axonal tracts are involved in communication between the thalamus and cortex in mammals: thalamocortical axons (TCAs) and corticothalamic axons (CTAs). TCAs project from the thalamus and target the cerebral cortex whereas CTAs originate from the cerebral cortex and project to the thalamus. The mechanisms that control TCA targeting and areal specialization in the cortex have been the subject of research on early brain development for many years, but are still not fully understood. It is suggested that all cortical areas receive inputs from thalamic cells and send outputs to lower motor centers. The communications between cortical areas are through direct corticocortical and corticothalamocortical pathways. The transthalamic pathways provide an important route for corticocortical communication (Sherman and Guillery, 2011).

There are two chemically defined classes of thalamocortical relay neurons in primates: calbindin-positive matrix cells and parvalbumin-positive core cells (Jones, 2001). Matrix cells extend throughout the thalamus and project to superficial layers of the cortex over wide areas. Core cells are only present in some thalamic nucleus and they project to middle layers of the cortex in a topographically ordered area-specific manner. After the activation of a population of cortical cells by an external or internal stimulus, the signal is transferred back to the matrix cells of the thalamic relay nucleus through the corresponding corticothalamic fibers. The diffuse projections of the matrix cells to the superficial layers of the cerebral cortex could then trigger the adjacent populations of cortical cells. The corticothalamic feedback

from these cells to the matrix cells of their thalamic relay nuclei, and so on, could be used to form links across wide regions of cortex and thalamic nuclei.

Whereas all thalamic relay cells receive a feedback input from cortical layer VI, some also receive a feedforward input from layer V. For example, in primates layer VI of area 17 sends corticothalamic projections to the lateral geniculate nucleus, whereas corticothalamic axons projecting from layer V cells of various areas reach other thalamic nuclei, e.g. from the visual cortex to the pulvinar, from the primary auditory cortex to the dorsal and magnocellular medial geniculate nuclei, and from the primary somatosensory area to the intralaminar nuclei and the anterior pulvinar nucleus (Jones, 2001). The transthalamic corticocortical pathways allow the information being processed in one cortical area and transferred to other cortical areas.

1.2.1 The early development of corticothalamic and thalamocortical axons in rodents

A number of studies have been carried out to reveal the development of axonal fibers between the cerebral cortex and the thalamus by placing carbocyanine dyes such as 1,1'-dioctadecyl-3, 3, 3', 3'-tetramethyl-indocarbocyanine perchlorate (DiI) or 4-(4-dihexadecylaminostyryl)-*N*-methylpyridinium iodide (DiA) into the cerebral cortex, the thalamus or the subcortical regions in the forebrain (Auladell et al., 2000; Metin and Godement, 1996; Molnar et al., 1998a; Molnar and Blakemore, 1995; Molnar and Cordery, 1999). Carbocyanine dyes are fluorescent lipophilic dyes that can diffuse along the lipid membranes of cells. Thus dyes placed in the brain tissue can be picked up by the cells located at the dye placement sites and anterogradely label axons projecting from the cell bodies. Additionally, dyes can also be picked up by the axons passing through the dye crystal placement sites and retrogradely label cell bodies that are located in a distance from the dye placement sites.

Here I introduce the early development of CTAs and TCAs based on carbocyanine dye tracing experiments in rodents. Since the animal model that I use in the current

study is mouse, this introduction mainly focuses on mouse models, but also mentions the equivalent developmental stage in rats and hamsters.

1.2.1.1 Early outgrowth of corticothalamic projections

Following DiI placements in the neocortex of E12 mouse embryos, corticofugal axons are observed navigating through the intermediate zone (Figure 3A-C) (Auladell et al., 2000). However, some cortical axons navigate further than others, depending on the DiI placement sites in the cortex. For instance, DiI placements in the lateral part of the neocortex label a small amount of cortical axons that have made a sharp turn at the exit of the cortex and reach the basal telencephalon at E12 (arrows, Figure 3A). When DiI crystals are placed in the medial part of the neocortex, however, the labelled cortical axons are short and none of them have left the cortex (arrows, Figure 3C). At this early stage of development, cortical axons are tipped with large and bifurcated growth cones (arrowheads, Figure 3A,C).

At E13, numerous cortical axons run through the lowest intermediate zone and turn into the corpus striatum, displaying a scattered pattern (arrows, Figure 3D). The cortical axons progress further into the basal telencephalon at E13, compared to E12, and most of them are tipped with complex branching growth cones (arrowheads, Figure 3D,F). In the LGE, sparsely distributed cell bodies are observed near the front of cortical efferents (Figure 3J,K,L), suggesting that the LGE projects axons into the neocortex during early embryonic stages (Magnani et al., 2010; Metin and Godement, 1996).

At E14, the earliest corticofugal axons have travelled though the internal capsule and straight up to the thalamus, as revealed by DiI placements in the lateral part of the cortex (arrows, Figure 3G). Occasionally, retrogradely labelled cells are detected in the thalamus, indicating that the earliest thalamic axons have reached the lateral cortex at E14 (Figure 3G). Shortly after that, at E14.5, large numbers of retrogradely labelled cells are seen in the thalamus (arrows, Figure 3H,I), indicating that a large amount of thalamic axons have arrived at the lateral cortex at E14.5.

The development of corticofugal efferents was also studied in the golli-tau-GFP transgenic mice where tau-GFP protein expresses in cortical preplate and subplate neurons and their axonal projections (Jacobs et al., 2007). Similar to DiI labelling results in E13.5 mouse embryos, golli-tau-GFP labelled corticofugal fibers pass the PSPB and terminate at the lateral part of the internal capsule. However, the cortical fibers in the golli-tau-GFP mice appear to pause in the presumptive neostriatum between E13.5 and E15.5, before progressing rapidly to the medial aspect of the pallidum at E16.5. Golli-tau-GFP labelled corticofugal efferents pause and gather at the DTB between E16.5 and E17.5, and then pass through the thalamic reticular nucleus to enter the thalamus at E18.5. The observation that Golli-tau-GFP positive cortical fibers do not invade the thalamus until just prior to birth is different from the above DiI results, where DiI-labelled pioneer corticofugal axons have reached the thalamus by E14 (Figure 3G).

1.2.1.2 Early outgrowth of thalamocortical projections

At E12, DiI placements in the thalamus of mouse embryos label a bundle of thalamic axons descending through the prethalamus into the internal capsule. By E13, a large amount of thalamic axons have passed the diencephalic-telencephalic boundary (DTB) and turned laterally into the basal telencephalon. At this time some single thalamic fibers have already entered the lateral part of the neocortex through the intermediate zone (arrows, Figure 4B), bearing large and complex growth cones at their tips (arrowheads, Figure 4B). At this stage, these early thalamic axons have not yet invaded the overlying cortical preplate. This occurs one day later (E14), when more thalamic fibers have arrived at the lateral cortex and start to invade the cortical plate at the lateral part of the cortex (arrows, Figure 4D). Growth cones are observed at the tips of these thalamic fibers (arrowheads, Figure 4D).

Taken together, corticothalamic and thalamocortical axons project from the cerebral cortex and the thalamus synchronously, and meet on the way towards their targets,

after which they continue their journey to the thalamus and the cerebral cortex, respectively, in a reciprocal manner (Figure 5).

Figure 3

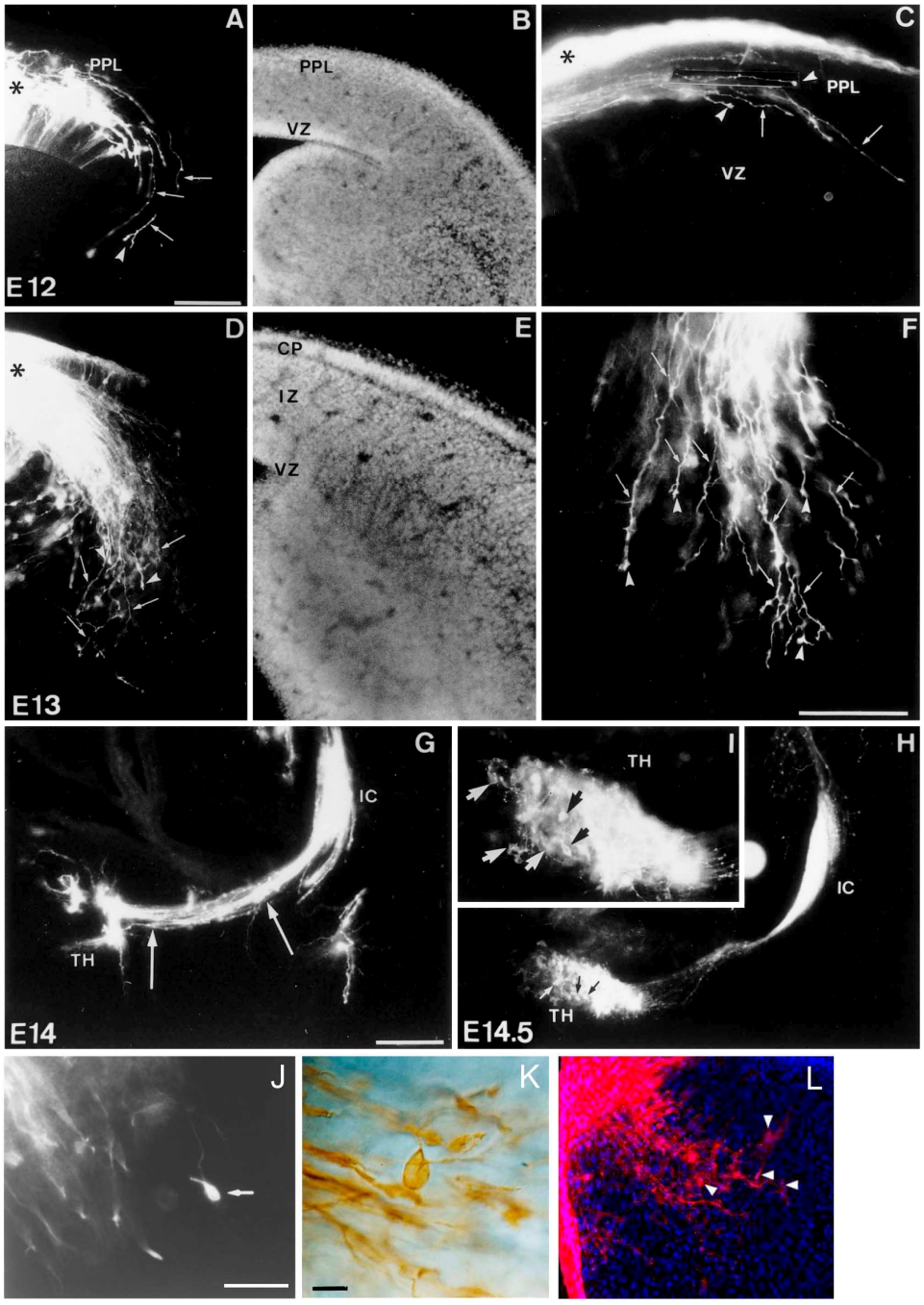

Figure 3. Early outgrowth of CTAs in mouse. (A & C) Following DiI placements in the neocortex of E12 mouse embryos, corticofugal axons are observed navigating through the intermediate zone. **(A)** DiI placements in the lateral part of the neocortex label a small amount of cortical axons that have made a sharp turn at the exit of the cortex and reach the basal telencephalon at E12 (arrows). **(B)** Same section as shown in A, stained with bisbenzimide. **(C)** When DiI crystals are placed in the medial part of the neocortex, the labelled cortical axons are short and none of them have left the cortex (arrows). At this early stage of development, cortical axons are tipped with large and bifurcated growth cones (arrowheads, A & C). **(D & F)** At E13, numerous cortical axons run through the lowest intermediate zone and turn into the corpus striatum, displaying a scattered pattern (arrows). The cortical axons progress further into the basal telencephalon at E13, compared to E12, and most of them are tipped with complex branching growth cones (arrowheads). **(E)** Same section as shown in A, stained with bisbenzimide. **(G)** At E14, the earliest corticofugal axons have travelled though the internal capsule and straight up to the thalamus, as revealed by DiI placements in the lateral part of the cortex (arrows). Occasionally, retrogradely labelled cells are detected in the thalamus, indicating that the earliest thalamic axons have reached the lateral cortex at E14. **(H & I)** At E14.5, large numbers of retrogradely labelled cells are seen in the thalamus (arrows), indicating that a large mount of thalamic axons have arrived at the lateral cortex at E14.5. **(J-L**) Cell bodies are observed in the LGE, near the front of the cortical axons. PPL-preplate; VZ-ventricular zone; CP-cortical plate; IZ-intermediate zone; IC-internal capsule; TH-thalamus. Scale bars: (A-E) 150 µm; (F, I) 100 µm; (G, H) 100 µm; (J) 50 µm; (K) 10 µm.

Figure 4

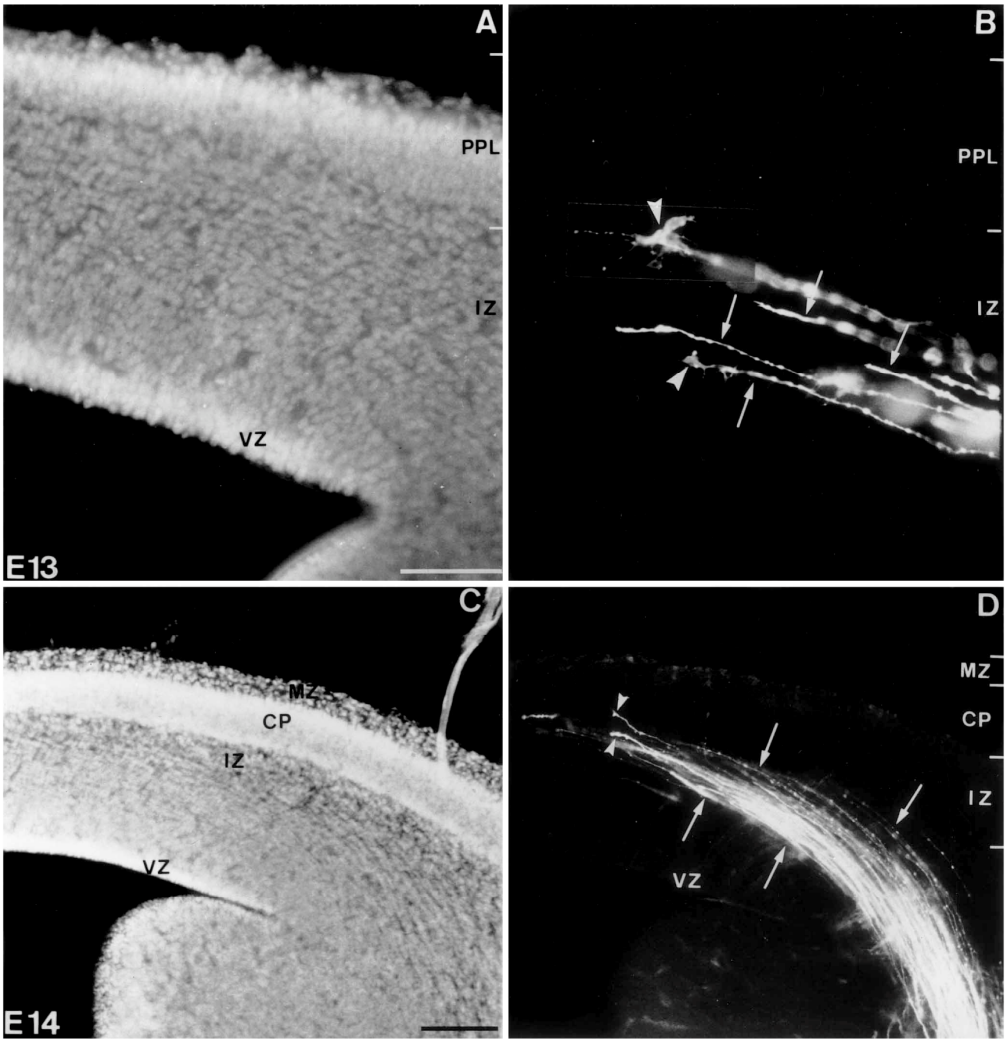

(From Auladell *et al*., 2000)

Figure 4. Early outgrowth of TCAs in mouse (Auladell et al., 2000). (A) Same section as shown in B, stained with bisbenzimide. **(B)** At E13, a large amount of thalamic axons have passed the diencephalic-telencephalic boundary (DTB) and turned laterally into the basal telencephalon. At this time some single thalamic fibers have already entered the lateral part of the neocortex through the intermediate zone (arrows), bearing large and complex growth cones at their tips (arrowheads). **(C)** Same section as shown in D, stained with bisbenzimide. **(D)** At E14, more thalamic fibers have arrived at the lateral cortex and start to invade the cortical plate at the lateral part of the cortex (arrows). Growth cones are observed at the tips of these thalamic fibers (arrowheads). PPL-preplate; VZ-ventricular zone; CP-cortical plate; IZ-intermediate zone; MZ-marginal zone. Scale bars: (A, B) 50 µm; (C, D) 150 µm.

Figure 5

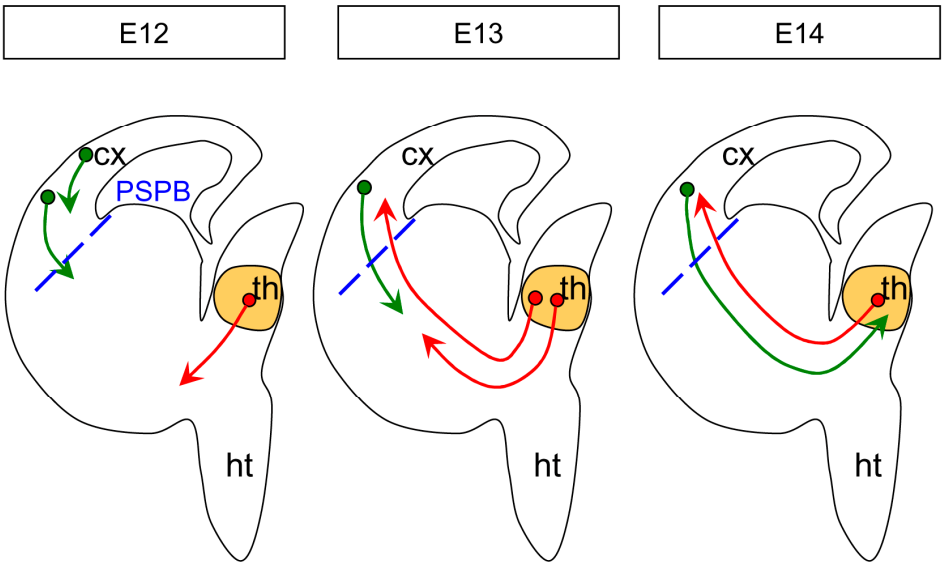

Figure 5. A schematic diagram showing the early development of CTAs and TCAs. Corticothalamic and thalamocortical axons project from the cerebral cortex and the thalamus synchronously, and meet on the way towards their targets, after which they continue their journey to the thalamus and the cerebral cortex, respectively, in a reciprocal manner. cx-cortex; th-thalamus; ht-hypothalamus; PSPB-pallial-subpallial boundary.

1.2.2 The mechanisms by which the corticothalamic and thalamocortical axons find the way to their targets

Both CTAs and TCAs display distinct growth patterns during their trajectory towards the thalamus and the cortex, respectively. The normal development of CTAs and TCAs has been proposed to be regulated by numerous guidance factors en route (Bolz et al., 2004; Dufour et al., 2003; Garel and Rubenstein, 2004; Lakhina et al., 2007; Lett et al., 2009; Little et al., 2009; Lopez-Bendito et al., 2002; Lopez-Bendito and Molnar, 2003; Ma et al., 2002; Marin et al., 2002; Price et al., 2006; Torii and Levitt, 2005; Uemura et al., 2007; Wright et al., 2007). A number of chemo-attractant molecules expressed in a gradient are suggested to direct the advance of CTAs and TCAs, while chemo-repellent molecules help to prevent axons from invading the improper areas in the forebrain. Additionally, transient pioneer axons are hypothesised to serve as axonal scaffolds for CTAs and TCAs to navigate along to reach their targets (Figure 6). Here I introduce several mechanisms by which CTAs and TCAs find the way to their targets.

1.2.2.1 Chemo-repellent molecules prevent CTAs and TCAs from invading the improper locations in the forebrain

During early brain development, numerous guidance molecules are expressed along the route of CTAs and TCAs. Some of these molecules such as Slits, Semaphorins and Ephrins are chemo repellents to axons and hence prevent CTAs and TCAs from growing towards improper locations in the brain (Bagri and Tessier-Lavigne, 2002; Bolz et al., 2004; Braisted et al., 1999; Dufour et al., 2003; Garel and Rubenstein, 2004; Powell et al., 2008; Torii and Levitt, 2005). These molecules function by interacting with receptors expressed on the growth cones of CTAs and TCAs or along the axonal fibers.

In vivo evidence that Slits and Robos cooperate to prevent CTAs and TCAs from invading the improper regions in the forebrain

Figure 6

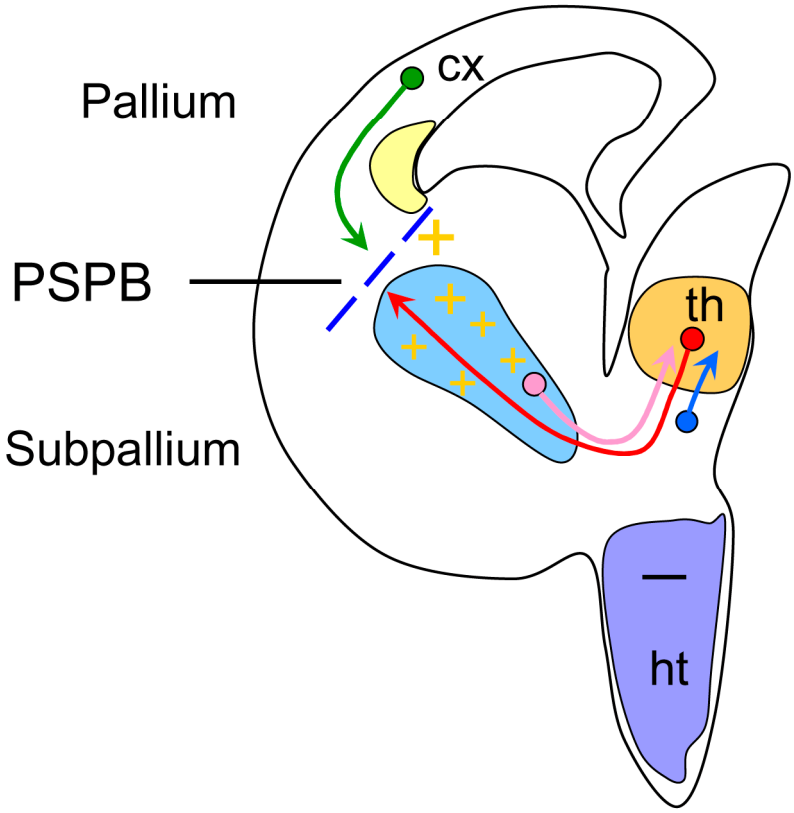

Figure 6. The guidance factors for the development of CTAs and TCAs. A number of chemo-attractant molecules expressed in a gradient are suggested to direct the advance of CTAs and TCAs, while chemo-repellent molecules help to prevent axons from invading the improper areas in the forebrain. Additionally, transient pioneer axons are hypothesised to serve as axonal scaffolds for CTAs and TCAs to navigate along to reach their targets.

Slits and their Robo receptors cooperate to prevent TCAs from invading the hypothalamus or crossing the midline of the forebrain (Andrews et al., 2006; Bagri et al., 2002; Braisted et al., 2009). The expression patterns of *Slit* genes and their *Robo* receptors are correlated with the development of CTAs and TCAs (Bagri et al., 2002). In E14.5 mouse embryos, *Robo1* is expressed in the cortical plate while *Robo2* is expressed in the subplate and intermediate zone of the cerebral cortex, in a pattern complementary to that of *Robo1*. Both *Robo1* and *Robo2* are expressed in the developing thalamus, in a decreasing gradient from the neuroepithelium to the mantle region. *Slit1* is expressed in the cortical plate and in the proliferative zone of the thalamus, hypothalamus, lateral and medial ganglionic eminences and septum. *Slit1* is also expressed in the mantle region of the septum and preoptic area. *Slit2* is expressed in the neuroepithelium of the medial cortex and in the proliferative zone of the thalamus, hypothalamus, preoptic area and septum. *Slit2* is also expressed in the mantle region of the hypothalamus (Bagri et al., 2002).

As cortical axons descend through the intermediate zone of the cerebral cortex and make a sharp turn into the ventral telencephalon, they avoid the proliferative regions of the ganglionic eminences, which express high levels of *Slit1* mRNA (Bagri et al., 2002). Instead, cortical fibers navigate within the mantle region of the ganglionic eminences and form the internal capsule. On their way toward the thalamus, cortical axons avoid the ventral region of the basal telencephalon and the midline, which also express high levels of *Slit1* and *Slit2* mRNA. On reaching the thalamus, cortical axons avoid approaching the proliferative zone of the thalamus, which expresses high levels of *Slit1* and *Slit2* mRNA. The trajectory of TCAs is largely reciprocal to that of CTAs. TCAs descend through the prethalamus and make a sharp turn into the ventral telencephalon, avoiding the hypothalamus, where *Slit1* and *Slit2* mRNA expression is high. Once in the ventral telencephalon, TCAs grow through the internal capsule to reach the cortex, and avoid crossing the midline or approaching the ventral region of the basal telencephalon and the proliferative zone of the ganglionic eminences, which express high levels of *Slit1* and *Slit2* mRNA (Bagri et al., 2002).

While *Slit1*$^{-/-}$ mutants do not show obvious defects of CTAs and TCAs during development, *Slit2*$^{-/-}$ mutants display dramatic defects of both CTAs and TCAs. In *Slit2*$^{-/-}$ mutant embryos, CTAs reach the thalamus following an abnormally ventral and caudally extended path in the ventral telencephalon (Bagri et al., 2002). Some TCAs do reach the cortex, but the amount is dramatically reduced compared to the wild-type. Instead, most TCAs projecting from the midline thalamic nuclei turn ventrally and caudally to enter the hypothalamus. In *Slit1*$^{-/-}$*Slit2*$^{-/-}$ double mutant embryos, CTAs follow a very caudal and ventral path in the ventral telencephalon before most of them turn into the diencephalon, while some of them fail to ascend toward the thalamus and instead project into the anterior hypothalamus (Bagri et al., 2002). A large number of descending TCAs are able to enter the telencephalon but most of them fail to reach the internal capsule, turning instead toward the midline. Additionally, a lot of TCAs descend into the hypothalamus rather than turning into the telencephalon. Taken together, the defects of CTAs and TCAs trajectory observed in the *Slit2*$^{-/-}$ and *Slit1*$^{-/-}$*Slit2*$^{-/-}$ double mutants suggest that the expression of *Slit1* and *Slit2* genes in the ventral region of the basal telencephalon, the hypothalamus and the midline is important for preventing axonal entry into ventral regions of the telencephalon as well as into the hypothalamus and across the midline (Figure 7) (Bagri et al., 2002). The fact that CTAs and TCAs invade the midline in *Slit1*$^{-/-}$*Slit2*$^{-/-}$ double mutants but not in *Slit2*$^{-/-}$ single mutants indicates that Slit1 does have an effect in preventing the improper invasion of CTAs and TCAs towards the midline. However, this Slit1 function is associated with the presence of Slit2, since there are no axonal defects observed in *Slit1*$^{-/-}$ single mutants.

In *Robo1*$^{-/-}$ mutant mice, both CTAs and TCAs arrive at their targets at least 1 day earlier than controls, indicating that Robo1 plays a delaying role in the timely projection of TCAs and CTAs (Andrews et al., 2006). Nevertheless, while CTAs show an aberrant trajectory crossing the midline of the forebrain in *Slit1*$^{-/-}$*Slit2*$^{-/-}$ double mutants, such phenotypes of CTA targeting are not observed in *Robo1* mutants, indicating that additional ligands, receptors or receptor partners are likely to be involved in Slit/Robo signalling, i.e. Robo2.

Figure 7

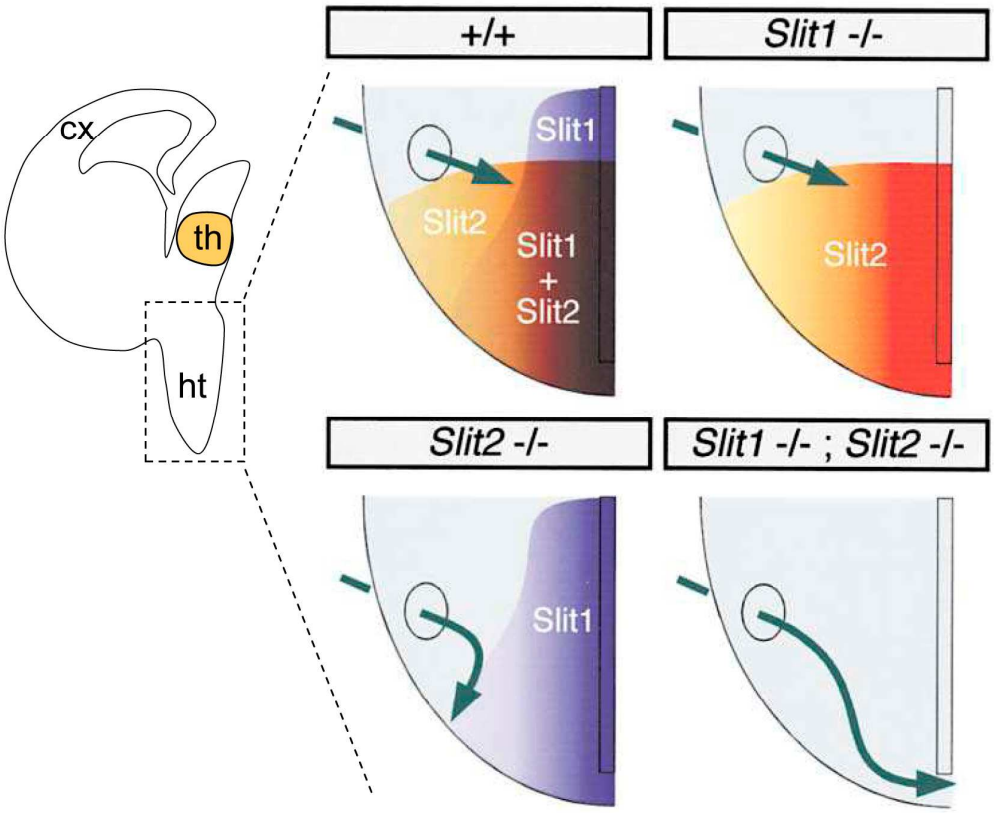

(Revised from Bagri *et al*., 2002)

Figure 7. A summary of axonal pathfinding defects in the *Slits* mutants. A simplified diagram of a coronal section of the forebrain on the left and a higher magnification of the boxed area on the right showing the axonal trajectory in the hypothalamus of wild type and Slits mutants. The defects of CTAs and TCAs trajectory observed in the *Slit2* and *Slit1;Sli2* double mutants suggest that the expression of *Slit* genes in the hypothalamus and the midline is important for preventing axonal entry into the hypothalamus and across the midline. Cx-cortex; th-thalamus; ht-hypothalamus.

In *Robo2*$^{-/-}$ mutant mice, some thalamocortical axons fail to enter the telencephalon and instead invade the hypothalamus. Some thalamocortical and corticothalamic axons navigate through the ventral telencephalon, but enter ventral regions that they normally avoid (Lopez-Bendito et al., 2007).

In *Robo1*$^{-/-}$*Robo2*$^{-/-}$ double mutants, only a few cortical axons reach the thalamus, while most of them abnormally grow toward the midline and cross it. Additionally, numerous thalamic axons fail to turn into the telencephalon and instead aberrantly project toward the hypothalamus (Lopez-Bendito et al., 2007).

Thus, similar to *Slit1*$^{-/-}$*Slit2*$^{-/-}$ double mutants, *Robo1*$^{-/-}$*Robo2*$^{-/-}$ double mutants also show abnormal invasion of cortical and thalamic projections at the midline. Since *Robo1* or *Robo2* single mutants do not show prominent defects as seen in *Robo1*$^{-/-}$ *Robo2*$^{-/-}$ double mutants, it is likely that Robo1 and Robo2 compensate each other's function in the absence of one of the receptors. It is conceivable that Slit1 and Slit2 prevent midline crossing of cortical and thalamic projections in the mammalian forebrain through both Robo1 and Robo2 receptors (Lopez-Bendito et al., 2007). However, there are defects in *Robo2* mutants that cannot be compensated by Robo1 function, for example the corticofugal and thalamocortical axons run ventrally in the basal telencephalon. These results suggest that Robo1 and Robo2 functions may not be completely redundant. Slit2 binding to Robo2 may be more effective than it is to Robo1, therefore may not be able to maintain the normal dorsoventral position of cortical and thalamic axons in *Robo2* mutants through repulsion (Lopez-Bendito et al., 2007). Consistent with this possibility, *in vitro* experiments show that Slit2 binds more effectively to Robo2 than to Robo1.

Other than Robos, Slits also bind the heparin sulphate (Liang et al., 1999; Ronca et al., 2001), which in turn enhances the affinity of Slits for Robo receptors. Similar to Robo1 and Robo2, heparin sulphate proteins are expressed in corticofugal and thalamocortical projections, and it is suggested that heparin sulphate may also

contribute to the guidance of these major forebrain projections along with Slit/Robo signalling.

In vitro evidence that Slits are chemorepellents for TCAs

When thalamic explants are co-cultured with hypothalamus, thalamic axon outgrowth is biased away from the hypothalamus, which indicates that the hypothalamus releases a diffusible activity that can repel TCAs at a distance (Braisted et al., 1999). Additionally, co-culture of thalamic explants with Slit2-expressing cell aggregates show the decrease of thalamic axonal outgrowth on the explant side facing Slit2-expressing cells, and the overall reduction of total thalamic axonal outgrowth. Thus, Slits are likely to be the chemorepellents for TCAs endogenous to hypothalamus and steer TCAs from diencephalon into ventral telencephalon (Braisted et al., 2009).

1.2.2.2 Ventral telencephalic chemoattractants help direct TCAs through the ventral telencephalon

In vivo evidence that Netrin-1 is required for normal TCA navigation in the ventral telencephalon

While TCAs avoid the repulsive cues derived from the hypothalamus and make a sharp turn into the ventral telencephalon, some chemoattractive molecules such as Netrin-1 are expressed in the ventral telencephalon and help direct the advance of TCAs (Bonnin et al., 2007; Braisted et al., 2000; Powell et al., 2008).

Netrin-1 is expressed in a cluster of cells in the internal capsule zone, which are in close proximity to the fascicles of TCAs in the internal capsule. *DCC* and *neogenin,* receptors implicated in mediating the attractant effects of netrin-1, are expressed in the thalamus, whereas *unc5h2* and *unc5h3*, netrin-1 receptors implicated in repulsion, are not. These findings may reveal the role of netrin-1 as an attractant for TCAs to grow into and/or through the internal capsule (Braisted et al., 2000). In netrin-$1^{-/-}$

mutant mice, TCAs can grow out of the thalamus and travel through the prethalamus to turn into the ventral telencephalon normally. However, fascicles of TCAs are disorganized and abnormally restricted to the dorsomedial half of the internal capsule/striatum when they are passing through the ventral telencephalon. Moreover, the amount of TCA projection reaching the neocortex is reduced in the netrin-$1^{-/-}$ mutants (Braisted et al., 2000). These findings demonstrate that Netrin-1 is required for the normal trajectory of TCAs through the ventral telencephalon.

In vitro evidence that netrin-1 has a growth-promoting effect on TCAs

In vitro, thalamic axons show biased growth toward a source of netrin-1, which can be abolished by netrin-1 blocking antibodies. Additionally, when thalamic explants are cultured *in vitro* with soluble recombinant netrin-1 protein added to the growth medium, there is a significant increase in both the number and the length of thalamic axon fascicles compared to control conditions. These data show that netrin-1 has a growth-promoting effect on thalamic axon outgrowth *in vitro* (Braisted et al., 2000).

When thalamic explants are co-cultured with medial ventral telencephalic explants, thalamic axon outgrowth is biased toward the ventral telencephalon, which indicates that the medial aspect of the ventral telencephalon releases a diffusible attractant activity for TCAs (Braisted et al., 1999). To test whether netrin-1 is the medial ventral telencephalic attractant for TCAs, thalamic explants were cultured with the medial ventral telencephalic explants, with a netrin-1-blocking antibody added to the culture medium (Braisted et al., 2000). The bias in thalamic axon outgrowth toward the ventral telencephalon was diminished in these cultures, but the change was not statistically significant. One possibility is that the blocking antibody is not completely effective at neutralizing the action of netrin-1. Another explanation would be that netrin-1 is not solely responsible for the attractant effect of the medical ventral telencephalon on TCAs. Netrin-1 may act combinatorially with other guidance cues in the ventral telencephalon to direct the growth of TCAs (Braisted et al., 2000).

Through these *in vitro* data it is proposed that *in vivo* the ventral telencephalic chemoattractants including netrin-1, together with the hypothalamic chemorepellents Slit1 and Slit2, promotes the sharp turning of TCAs away from hypothalamus and into the ventral telencephalon (Braisted et al., 1999).

1.2.2.3 The subcortical region provides a permissive environment for TCAs

1.2.2.3.1 TCAs navigate through a corridor generated by tangential migration

In vivo evidence

At around E13, TCAs navigate through a corridor between the progenitor zones of the MGE and the developing globus pallidus (Figure 8). The MGE corridor cells do not express genes characteristic of the MGE, such as *Nkx2.1* or *Lhx6*, but instead express markers of the LGE derivatives such as *Islet1*, *Ebf1* and *Meis2*. The idea that the MGE corridor cells may be derived from tangential migration of LGE cells into the MGE comes from the observation of progressive expansion of LGE markers such as *Islet1* and *Ebf1* into the MGE between E11.5 and E13.5. Subsequently TCAs are observed to be in close contact with corridor cells by using double immunohistochemistry with TCA marker Calretinin and corridor cell marker Islet1 (Lopez-Bendito et al., 2006).

In vitro evidence

The *in vitro* culture experiments where GFP-positive LGE progenitor zones are transplanted into wild-type host slices show that the LGE generates a stream of GFP-expressing cells migrating tangentially into the MGE, expressing the LGE marker Islet1. This ventral migration of LGE derivatives is blocked by inserting a semipermeable membrane between the LGE and the MGE in E11.5-E12 telencephalic slices, and interestingly, this leads to a drastic reduction in TCA

navigation in the MGE (Lopez-Bendito et al., 2006). In *Mash1*$^{-/-}$ mutant embryos the MGE corridor does not form or is severely reduced and the TCAs fail to grow into the ventral telencephalon (Tuttle et al., 1999). However, a graft of wild-type LGE progenitor zones into the *Mash1* mutant slices *in vitro* can rescue the formation of the corridor in the MGE and restore the growth of TCAs into the *Mash1*$^{-/-}$ mutant MGE region (Lopez-Bendito et al., 2006). Taken together, these results show that the MGE corridor is generated by tangential migration of cells from the LGE into the MGE, and that this tangential migration is required for TCAs to travel through the MGE (Lopez-Bendito et al., 2006).

1.2.2.3.2 Territories derived from the MGE are nonpermissive for TCAs

In vitro evidence

When GFP-expressing thalamic explants are positioned in the wild-type telencephalic slices, GFP-positive TCAs preferentially grow into the Islet1-positive corridor of the MGE, avoiding the MGE ventricular and subventricular zones and globus pallidus. Secondly, TCAs show widespread growth through the striatum. However, when explants of the MGE ventricular and subventricular zones or globus pallidus are inserted into the striatum, TCAs avoid the heterotypic MGE ventricular and subventricular zones or globus pallidus transplants. Thus the *in vitro* brain slice culture shows that the MGE corridor and the LGE striatum are highly permissive for the growth of TCAs, while the MGE ventricular and subventricular zones and globus pallidus are relatively nonpermissive to TCA outgrowth (Lopez-Bendito et al., 2006).

1.2.2.3.3 Different isoforms of Nrg1 cooperate to control TCA pathfinding

In vivo evidence

CRD-Nrg1, the membrane bound isoform of the *Neuregulin-1* (*Nrg1*) gene, is highly expressed in the LGE-derived corridor within the MGE, while Ig-Nrg1, the diffusible

isoform of *Nrg1*, is highly expressed by progenitor cells in the most ventral region of the pallium (the angle region) (Figure 8) (Lopez-Bendito et al., 2006). In the *Foxg1*-Cre/*Nrg1*-LoxP conditional mutants where all forms of *Nrg1* are disrupted specifically in the telencephalon, TCAs enter the telencephalon normally but defasciculate through the MGE corridor and largely fail to navigate toward the cortex (Lopez-Bendito et al., 2006).

In vitro evidence

In order to test the role of the Ig-Nrg1 expressing angle region in TCA guidance, brain slice culture experiments were carried out where the angle region was ablated, and the consequence was that TCAs failed to reach the cortex. Interestingly, addition of Ig-Nrg1-expressing COS cells to the ablated angle region in the slice cultures rescued the growth of TCAs toward the cortex (Lopez-Bendito et al., 2006). In another experiment where thalamic explants were cocultured with Ig-Nrg1-expressing COS cell aggregates, the outgrowth of thalamic axons was dramatically increased. However, thalamic axons did not specifically extend toward the source of Nrg1 (Lopez-Bendito et al., 2006). This indicates that Ig-Nrg1 is a growth promoter for thalamic axons, but it does not affect the direction of thalamic axonal outgrowth.

These results show that CRD-Nrg1 and Ig-Nrg1 proteins cooperate to guide TCAs through the MGE corridor to the cortex. While CRD-Nrg1 expression in corridor cells contributes to the navigation of TCAs within the ventral telencephalon, Ig-Nrg1 helps to direct TCAs towards the cortex, acting as a long-range attractant (Lopez-Bendito et al., 2006).

1.2.2.3.4 ErbB4, an Nrg1 receptor, is required for TCAs navigation

ErbB4 receptors are expressed by thalamic neurons. Deletion of *ErbB4* in the thalamus results in a similar phenotype to the *Nrg1* mutants, in which TCAs enter the telencephalon but fail to advance toward the cortex. These results indicate that ErbB4 signalling in TCAs is required for their normal navigation in the ventral

telencephalon and support the hypothesis that Nrg1 mediates its function in axon guidance through ErbB4 (Lopez-Bendito et al., 2006).

1.2.2.3.5 Normal subcortical environment is crucial for TCAs entry

Celsr3 conditional mutants reveal the importance of the ventral telencephalon in CTAs and TCAs navigation

Conditional knockout of Celsr3 in various regions of the forebrain reveals the importance of the normal subcortical environment in the guidance of CTAs and TCAs. In Foxg1-Cre/Celsr3-LoxP conditional mutants where Celsr3 is inactivated in the telencephalon driven by Foxg1-Cre, TCAs either run aberrantly along the edge of the basal telencephalon or cross the midline ventrally, and none of the TCAs reach the cerebral cortex (Zhou et al., 2008). In Dlx5/6-Cre/Celsr3-LoxP conditional mutants where Celsr3 is deleted in Dlx5/6 expressing cells in the ventral region of the telencephalon and diencephalon, a subpopulation of TCAs run aberrantly through the pallidum and amygdala after crossing the diencephalic-telencephalic boundary, and fail to grow toward the cerebral cortex. CTAs in the Dlx5/6-Cre/Celsr3-LoxP conditional mutants cross the pallial-subpallial boundary and enter the lateral part of the ventral telencephalon, but terminate and form an abnormal mass in the dorsal striatum and protrude into the lateral ventricle. In Emx1-Cre/Celsr3-LoxP conditional mutants where Celsr3 is inactivated in the cerebral cortex driven by Emx1-Cre, both CTAs and TCAs develop normally and reach their targets (Figure 9). These observations indicate that the normal environment of the subcortical areas maintained by ventral telencephalic cells is important for the normal trajectory of CTAs and TCAs.

Figure 8

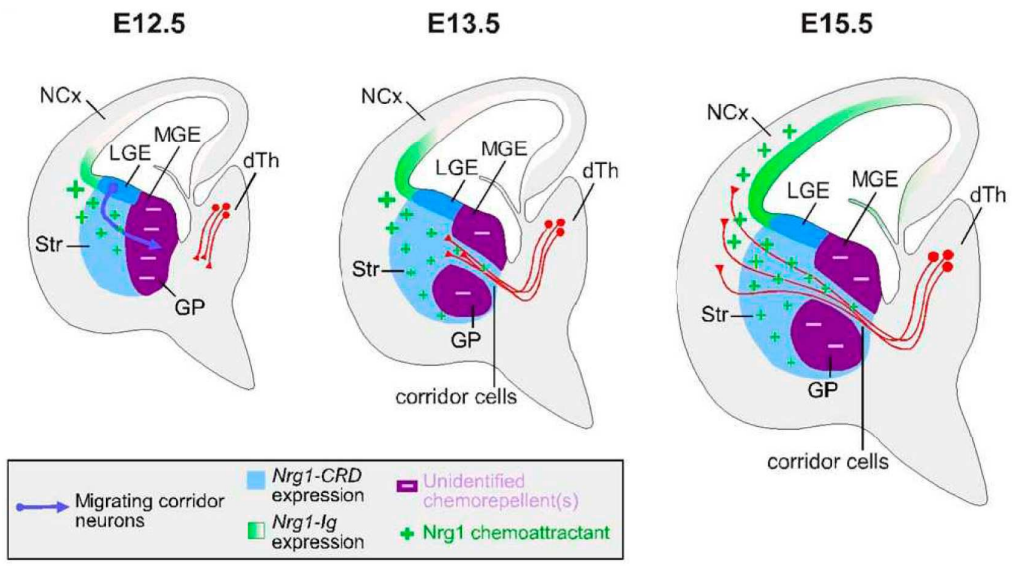

(From Lopez-Bendito *et al*., 2006)

Figure 8. A group of cells form a 'corridor' in the ventral telencephalon that allows TCAs to traverse through it. The corridor cells are composed of a subset of GABAergic interneurons migrating from the LGE to the MGE, and they express Islet 1, Ebf1 and CRD-Nrg1. Additionally, Ig-Nrg1, which is highly expressed by progenitor cells in the most ventral region of the pallium-the angle region, has been suggested to guide TCAs through the ventral telencephalon and towards the cerebral cortex, acting as a long-range attractant. Ncx-neocortex; dTh-dorsal thalamus; LGE-lateral ganglionic eminence; MGE-medial ganglionic eminence; Str-striatum; GP-globus pallidus.

TCAs fail to enter the telencephalon in *Foxg1*$^{-/-}$ mice

In *Foxg1*$^{-/-}$ mutants embryos which lack recognizable ventral telencephalic structures, TCAs navigate through the thalamus but fail to turn laterally into the telencephalon; instead, TCAs descend into the lateral hypothalamus (Pratt et al., 2002). No back labelled cell bodies were detected in the ventral telencephalon of *Foxg1*$^{-/-}$ mutant embryos after DiI placements into the thalamus, indicating the absence of transient projections from the ventral telencephalon towards the thalamus. These findings indicate that a normal ventral telencephalon is required for the turning of TCAs from the diencephalon into the telencephalon. Additionally, the abnormal invasion of TCAs into the lateral part of the hypothalamus in *Foxg1*$^{-/-}$ mutants suggests that repulsion by the hypothalamus in vivo is not sufficient to divert TCAs laterally into the ventral telencephalon (Pratt et al., 2002).

1.2.2.4 The guidance from axonal scaffolds *en route*

1.2.2.4.1 The roles of the transient projections from the LGE and MGE

The observation of LGE projections to the cortex and MGE projections to the thalamus comes from DiI/DiA tracing experiments. Placements of DiI crystals in the cerebral cortex label the descending cortical axons, with cell bodies located in the cortical preplate and the large growth cones at the tips of the axonal fibers. However, DiI labelled cell bodies are also observed near the front of the cortical axons in the LGE (simplified diagram in Figure10). These cells can be clearly distinguished from the surrounding growth cones by their chromatin content shown by bisbenzimide nuclear staining (Molnar et al., 1998a). The explanation for these DiI labelled cells in the LGE would be that these cells project axons towards the cerebral cortex, and pick up DiI at the crystal placement sites (Metin and Godement, 1996). In a telencephalic vesicle culture experiments where dye crystals were placed into the cortex, sparse cell bodies were back labelled in the LGE, suggesting that cells from the LGE project axons towards the cortex in these explants.

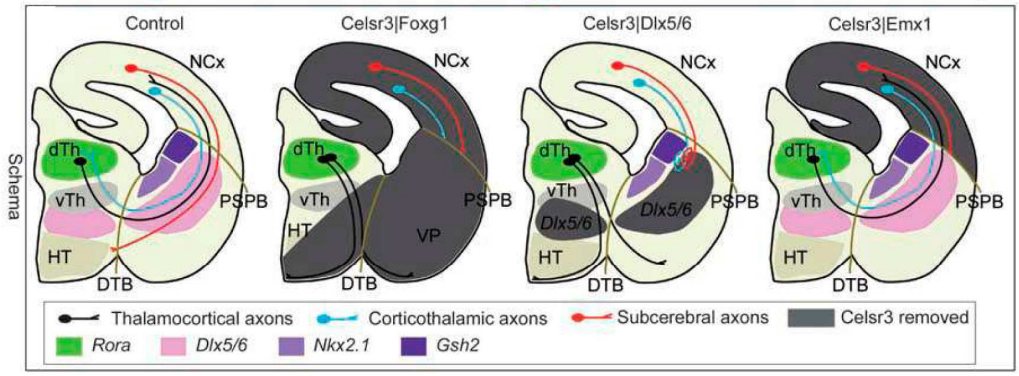

(From Zhou *et al*., 2008)

Figure 9. A summary of axonal developmental patterns in *Celsr3* conditional mutants. When *Celsr3* is inactivated in the telencephalon driven by *Foxg1*-Cre, TCAs either run aberrantly along the edge of the basal telencephalon or cross the midline ventrally, and none of the TCAs reach the cerebral cortex. When *Celsr3* is deleted in *Dlx5/6* expressing cells in the ventral region of the telencephalon and diencephalon, a subpopulation of TCAs run aberrantly through the pallidum and amygdale after crossing the diencephalic-telencephalic boundary, and fail to grow toward the cerebral cortex. CTAs in the *Dlx5/6*-Cre-driven *Celsr3* deficient mice cross the pallial-subpallial boundary and enter the lateral part of the ventral telencephalon, but terminate and form an abnormal mass in the dorsal striatum and protrude in the lateral ventricle. When *Celsr3* is inactivated in the cerebral cortex driven by *Emx1*-Cre, both CTAs and TCAs develop normally and reach their targets.

Similarly, DiA placements in the thalamus not only anterogradely label the descending thalamic axons, but also retrogradely label cells in the MGE, indicating that cells in the MGE send out axons towards the thalamus (simplified diagram in Figure10). Additionally, the prethalamus has been suggested to project axons towards the thalamus, since cell bodies are observed in the prethalamus when DiI crystals are placed in the thalamus (Braisted et al., 1999; Molnar et al., 1998a; Molnar and Cordery, 1999; Tuttle et al., 1999).

The functions of these transient early projections from the LGE and the MGE are not clear. Since they share the same compartment with the descending CTAs and TCAs, respectively, it is hypothesised that the reciprocal projections from the LGE and the MGE serve as axonal scaffolds for the early CTAs and TCAs to navigate along and be directed into the basal telencephalon (Figure 10). Thus the pioneer cortical and thalamic axons grow independently from each other to enter the ventral telencephalon (Metin and Godement, 1996).

LGE axons are absent in *Pdn/Pdn* mutant mice, delaying the entry of CTAs into the ventral telencephalon

In the *Gli3* hypomorphic mouse mutant *Polydactyly Nagoya* (*Pdn*), LGE pioneer neurons were not detected by DiI placements in the neocortex, suggesting that LGE pioneer neurons either fail to send projections toward the cortex or do not form properly in *Pdn* mutants (Magnani et al., 2010). At E14.5, cortical DiI placements in *Pdn/Pdn* mutant embryos showed no labelled axons entering or leaving the cortex, while normally cortical efferents would have crossed the PSPB and enter the ventral telencephalon. However, corticofugal axons penetrate the ventral telencephalon of the *Pdn* mutants at P0, suggesting that the LGE pioneer neurons and their projections might be important for the correct timing of CTAs to cross the PSPB and that CTAs would be guided into the ventral telencephalon by the later-arriving thalamocortical axons in the absence of LGE axons (Magnani et al., 2010).

Figure 10

(From Metin and Godement, 1996)

Figure 10. Early steps of CTAs and TCAs development. 1. CTAs and TCAs project from the cerebral cortex and the thalamus synchronously. Additionally, the LGE and the MGE send transient pioneer axons towards the cerebral cortex and the thalamus, respectively. **2.** CTAs and TCAs meet in the ventral telencephalon, after which they continue their journey towards the thalamus and the cortex, respectively. **3.** CTAs and TCAs have reached their targets. The transient projections from the LGE and MGE gradually disappear.

MGE axons are absent in *Mash-1*$^{-/-}$ mice and TCAs fail to enter the telencephalon

In *Mash-1*$^{-/-}$ mutants, many TCAs fail to pass through the prethalamus; instead, they form a dense bundle at the border between the thalamus and the prethalamus. A small number of TCAs in the *Mash-1*$^{-/-}$ mutants extend through the prethalamus and reach the border between the prethalamus and the hypothalamus, but few of these axons are able to cross the diencephalic-telencephalic boundary to enter the ventral telencephalon (Figure 11 e). The reciprocal projections from the ventral telencephalic cells are also absent in the *Mash-1*$^{-/-}$ mutants. These findings might indicate that the ventral telencephalic neurons and their axons are important for guiding TCAs through the prethalamus and into the ventral telencephalon (Tuttle et al., 1999).

However, apart from the ventricular zone of the MGE, LGE and CGE, *Mash-1* is also expressed in the ventricular zone of hypothalamus, prethalamus and ZLI. Alterations in the expression of genes such as *Pax6* and *RPTPδ* are detected in the prethalamus and hypothalamus of *Mash-1*$^{-/-}$ mutants, which contribute to the more inhibitory environment for TCA growth than in the wild type (Tuttle et al., 1999). Thus the failure of TCAs to navigate into the ventral telencephalon in *Mash-1*$^{-/-}$ mutants might be due to the change of guidance cues in the diencephalon rather than or in addition to the absence of reciprocal projections from the ventral telencephalic cells.

1.2.2.4.2 TCAs meet with pioneer preplate axons in the ventral telencephalon and use them as an axonal scaffold to enter the cortex

It has been speculated that TCAs meet with the earliest cortical preplate axons in the ventral telencephalon, after which TCAs navigate along the pioneer corticofugal axons descending from the corresponding cortical areas and reach their final targets in the neocortex. This is described as the ‘Handshake’ hypothesis

Figure 11

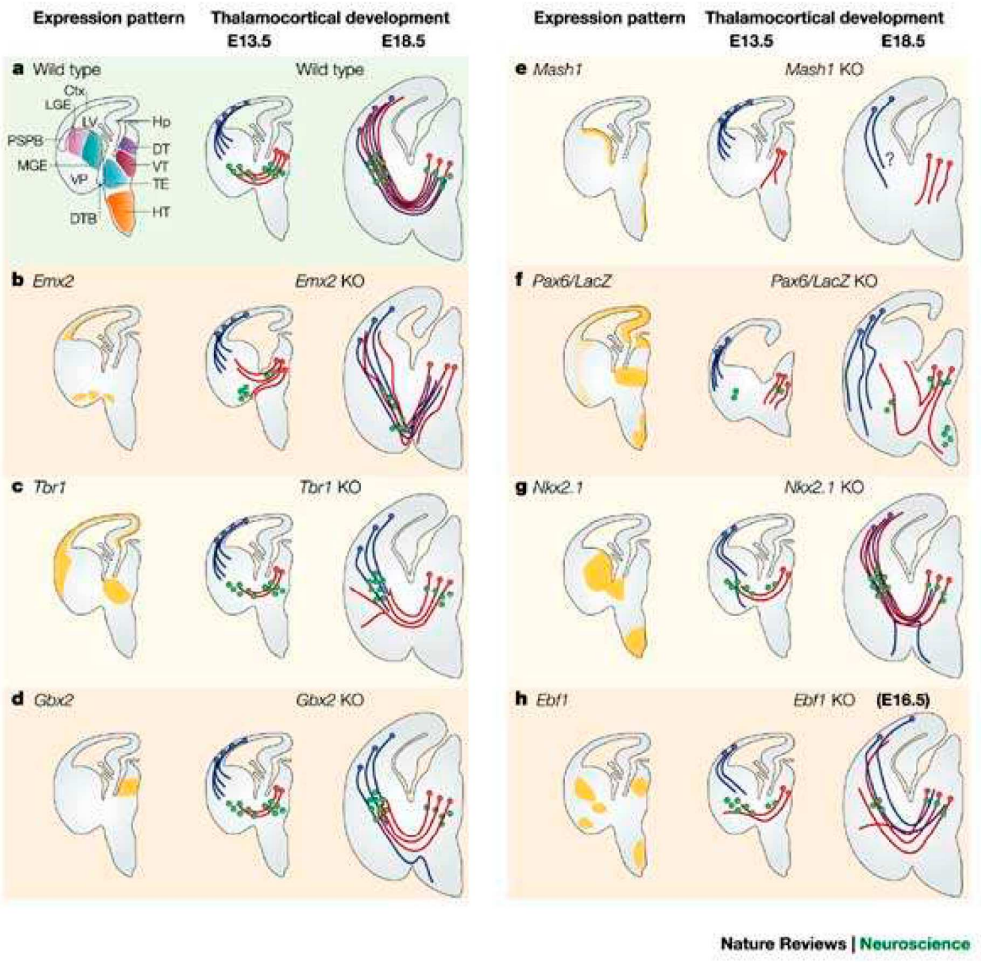

(From Lopez-Bendito and Molnar, 2003)

Figure 11. A schematic diagram showing the defects of CTAs and TCAs in mutant animal models where different transcription factor genes are inactivated. (a) Normal thalamocortical development in the wild type. **(b)** *Emx2* expression pattern and its mutant model. **(c)** *Tbr1* expression pattern and its mutant model. **(d)** *Gbx2* expression pattern and its mutant model. **(e)** *Mash1* expression pattern and its mutant model. **(f)** *Pax6/LacZ* expression pattern and its mutant model. **(g)** *Nkx2.1* expression pattern and its mutant model. **(h)** *Ebf1* expression pattern and its mutant model.

(Allendoerfer and Shatz, 1994; Molnar et al., 1998a; Molnar et al., 1998b; Molnar and Blakemore, 1995; Molnar and Cordery, 1999). But the exact location of the 'Handshake' event remains to be clarified. It has been proposed that the location where TCAs and subplate axons meet and establish intimate association is at the basal telencephalon (Molnar and Blakemore, 1995).

Evidence of the intermingling between cortical and thalamic axons came from the double labelling experiments where DiI and DiA crystals were placed in the cortex and the thalamus, respectively (Molnar et al., 1998a). Bundles of labelled corticofugal and thalamocortical axons are mixed and juxtaposed in the ventral telencephalon and intermediate zone. Cross-sectioning of the mixed bundles reveals the close association of the cortical and thalamic axons, which are often lying side-by side, literally in contact (Molnar et al., 1998a). However, cortical and thalamic axons labelled by this double labelling strategy are also shown to lay close to each other within the intermediate zone but do not overlap extensively (Miller et al., 1993). The observations of spatially separate groups of labelled cortical and thalamic fibers can be explained by the misalignment of dye placements in the cortex and the thalamus, since the handshake hypothesis demands that thalamic axons only intermingle with cortical axons from the corresponding region of the cortex (Molnar et al., 1998a).

It is also suggested that thalamic and cortical fibers run in separate, adjacent compartments close to the target area in the cortex, with ascending thalamic axons navigating within the subplate layer, whereas descending cortical efferents run below the subplate (Bicknese et al., 1994). However, dye placement in the internal capsule clearly labels identifiable thalamic axons running in close association with cortical efferents within the intermediate zone, following them right up to the subplate (Molnar et al., 1998a).

1.2.2.4.2.1 The importance of the intermingling between CTAs and TCAs in the ventral telencephalon

Since previously identified mutants with cortical axonal defects usually display reciprocal TCA defects, the intermingling of TCAs and cortical axons may be important for both sets of axons to reach their targets. However, caution is needed when the cause of the CTA and TCA defects in the mutants is being interpreted, since most mutations tend to affect multiple forebrain regions, making it hard to isolate primary defects.

Absence of *Tbr1* in the cortex causes CTAs and TCAs defects in the ventral telencephalon

However, the contact and association of CTAs and TCAs do not seem to guarantee the success of their subsequent journey towards their targets, as is the case in the *Tbr1*$^{-/-}$ mutants, where CTAs and TCAs associate in the internal capsule but fail to continue their pathfinding to the thalamus and cortex, respectively (Fig. 11 c). *Tbr1* is a T-box transcription factor gene that expresses in the cortex but not the thalamus of mouse embryos. In the cerebral cortex, *Tbr1* is strongly expressed in early-born cortical neurons, including layer 6, subplate, and Cajal-Retzius cells (Hevner et al., 2001). In *Tbr1*$^{-/-}$ mutants, CTAs enter the LGE normally at E14.5, similar to the controls. TCAs in *Tbr1*$^{-/-}$ mutants meet with CTAs in the internal capsule at the ventral telencephalon but deviate laterally through the middle of the internal capsule and curve toward the external capsule (Hevner et al., 2002). By E16.5, *Tbr1*$^{-/-}$ CTAs slow down or stop their growth in the midportion of the subpallium, without entering the diencephalon, while TCAs remain mainly in the internal capsule, the external capsule, and the amygdalar region, without innervating the cerebral cortex. Interestingly, the defects of CTAs and TCAs in *Tbr1*$^{-/-}$ mutants are observed in occipital, parietal, temporal, and sensorimotor cortex but not in the prefrontal or cingulate cortex regions where CTAs and TCAs are preserved (Hevner et al., 2002). This implies that the development of CTAs and TCAs is regulated by various mechanisms corresponding to different cerebral cortical regions.

Absence of *Gbx2* in the thalamus causes CTAs and TCAs defects in the ventral telencephalon

Another example that shows the defects of both CTAs and TCAs is the *Gbx2* mutant (Fig.11 d). *Gbx2* is a homeobox gene that is expressed in the thalamus but not the cortex of mouse embryos. In *Gbx2* mutants, the number of TCAs that project into the internal capsule is reduced at E14.5, while the growth of CTAs into the ventral telencephalon is normal at this age. At E16.5, TCAs in the *Gbx2* mutants end in the middle of the ventral telencephalon, while CTAs either end in the internal capsule or continue into the cerebral peduncle, without growing into the thalamus. At E18.5, TCAs in the *Gbx2* mutants still tangle in the internal capsule and fail to enter the cortex, while CTAs grow into the cerebral peduncle but none enter the thalamus (Hevner et al., 2002).

Taken together, *Tbr1* or *Gbx2* mutant mice show developmental defects of CTAs and TCAs, with no CTAs or TCAs reaching their final targets independently of each other. In both *Tbr1*$^{-/-}$ and *Gbx2*$^{-/-}$ mutants, CTAs and TCAs first grow into the ventral telencephalon independently without contact between each other. However, CTAs and TCAs fail to form intimate connections with each other in the subpallium of *Gbx2*$^{-/-}$ mutants and they both end mainly in the middle of the subpallium. In *Tbr1* mutants, although CTAs and TCAs are closely apposed and occupy the same fiber bundles once they meet in the subpallium, they fail to reach the thalamus and cortex, respectively. Since *Tbr1* is expressed in the cortex but not in the thalamus, the lack of Tbr1 is not likely to affect the thalamic nuclei and TCAs. Therefore, one explanation for this phenotype in *Tbr1*$^{-/-}$ mutants is that the expression of bidirectional signalling molecules is impaired in CTAs, so that CTAs and TCAs intermingle but lose the ability to signal to each other. Thus, not only the intermingling between CTAs and TCAs in the subpallium but also the recognition and bidirectional signalling between CTAs and TCAs might be important to direct the axons toward their final targets (Hevner et al., 2002).

Additionally, in *Tbr1*$^{-/-}$ and *Gbx2*$^{-/-}$ mutants CTAs are capable of crossing the PSPB and navigating into the middle of the internal capsule before meeting TCAs in the ventral telencephalon, indicating that CTAs are guided through the PSPB by non-

TCA factors. During normal development in mice, cortical pioneer axons cross the PSPB and enter the ventral telencephalon at approximately E13.5, and have reached the middle of the internal capsule by E14.5, but appear to pause in the neostriatum for 24-48 hrs (Bloom et al., 2007). It is speculated that this pause in the neostriatum provides the time for CTAs and the corresponding TCAs to gather and match up with each other (Jacobs et al., 2007).

1.2.2.4.2.2 The PSPB is a choice point for CTAs and TCAs

Before entering the cerebral cortex, TCAs have to cross the pallial-subpallial boundary (PSPB) between the dorsal and the ventral telencephalon, also known as the cortico-striatal border (CSB). It is unclear whether the PSPB is a barrier for TCAs, and whether TCAs need the guidance from CTAs to get through the PSPB. In rats, CTAs and TCAs have been shown to pause at the PSPB before crossing it, and their axonal fasciculation patterns change when they are crossing the PSPB (Lopez-Bendito and Molnar, 2003; Molnar et al., 1998a; Molnar and Butler, 2002; Molnar and Cordery, 1999). For example, DiI crystals placed into the dorsal cortex of E14 rat brain label numerous descending corticofugal axons that reach the boundary between the pallium and the subpallium where they terminate in large growth cones (Molnar and Cordery, 1999). At E15, more corticofugal axons arrive at the lateral entrance of the internal capsule, but only a few begin to cross the border between the intermediate zone and the lateral edge of the internal capsule (Molnar and Cordery, 1999). As TCAs leave the diencephalon, they form a thick bundle to enter the internal capsule. When TCAs navigate through the corpus striatum, they are slightly separated into distinct fascicles, which open up in a fan-shape pattern. As TCAs reach the border between the corpus striatum and the intermediate zone of the cortex, they defasciculate and form a fairly uniform array of individual fibers. Afterwards TCAs remain more or less parallel as they ascend through the intermediate zone into the cortex (Molnar et al., 1998a).

In hamster embryos, thalamic axons arrive at the striatum at E12.5, and their growth cones accumulate at the boundary between the striatum and the lateral cortical wall (Metin and Godement, 1996).

In mouse embryos, carbocyanine dye tracing shows that CFAs and TCAs temporarily pause at E14.5 at the PSPB, before they continue towards their targets (Jones et al., 2002). The cortical fibers in the golli-tau-GFP mice appear to pause in the presumptive neostriatum between E13.5 and E15.5, before progressing rapidly to the medial aspect of the pallidum at E16.5 (Jacobs et al., 2007).

Interestingly, the PSPB also seems to be a lateral border for the ventral telencephalic cells that project axons toward the thalamus (Molnar and Cordery, 1999). In rat embryos, DiI placements in the diencephalon back-label a large number of internal capsule cells under both medial and lateral ganglionic eminences. These back-labelled internal capsule cells respect a sharp border slightly medial to the PSPB and thus the lateral edge of the back-labelled cell group never extends laterally to the adjacent cortical intermediate or subplate zones.

Phr1$^{-/-}$ mice reveal the PSPB as a choice point for CTAs

The PSPB has been suggested to be a choice point for CTAs, as revealed by the defects of CTAs in the *Phr1*$^{-/-}$ mutants (Bloom et al., 2007). *Phr1* (for *PAM*, *highwire*, *rpm-1*) is the single well-conserved murine ortholog of the human gene *PAM* (encoding Protein Associated with Myc) and the invertebrate ubiquitin ligase genes *highwire* (in *Drosophila*) and *rpm-1* (in *Caenorhabditis elegans*), which functions cell-autonomously to regulate synapse growth and morphology. *Phr1* is widely expressed in the developing and adult mouse CNS. In constitutive *Phr1* knockout mice (*Phr1* KO) where deletion of the floxed *Phr1* gene is driven by *β-actin*-Cre expression, neither CTAs nor TCAs are able to grow into the ventral telencephalon. CTAs descend through the cerebral cortex of the constitutive *Phr1* knockout mice but terminate at the edge of the corticostriatal boundary and fail to enter the subpallium, while TCAs descend within the diencephalon along the

boundary between telencephalon and hypothalamus and fail to cross the diencephalic-telencephalic boundary into the ventral telencephalon (Figure 12).

However, in the *Phr1* cortical-knockout mice (Phr1 cortical-KO) where *Phr1* deletion is restricted in the cerebral cortex by using *Emx1*-Cre, CTAs and TCAs develop normally and target the thalamus and cortex, respectively, as in controls (Figure 12). Therefore the failure of CTAs to cross the corticostriatal boundary in the constitutive *Phr1* knockout mice is not due to the absence of *Phr1* in either cerebral cortical neurons or *Emx1*-expressing glial cells. Instead, the presence of Phr1 in an uncharacterized population of neurons or glia in the subcortical telencephalon may be required to make the corticostriatal boundary passable to CTAs (Bloom et al., 2007).

In *Coup-tfI*$^{-/-}$ mice very few TCAs reach the cerebral cortex

There are examples where the subplate axonal scaffold is intact but TCAs fail to enter the cerebral cortex, e.g. *Coup-tf1*$^{-/-}$ mutants. Chicken ovalbumin upstream promoter-transcription factors (COUP-TFs) are orphan members of the nuclear receptor superfamily. *Coup-tfI*, one of the two *Coup-tf* homologs, is widely expressed in the developing central and peripheral nervous systems (CNS and PNS). At E11.5, *Coup-tfI* is detected in the dorsocaudal telencephalon and diencephalon. At E14.5, *Coup-tfI* is expressed in the thalamus, prethalamus and hypothalamus, the lateral and medial ganglionic eminence. In *Coup-tfI* mutants, TCAs projecting from the ventrobasal thalamus (VB) navigate into the internal capsule normally, but very few TCAs grow out of the internal capsule, toward the striatum (Zhou et al., 1999). Even fewer TCAs are able to project into the intermediate zone of the cerebral cortex, and those TCAs that turn into the intermediate zone of the cortex follow a disorganized route, with some axons turning early and crossing with other axons in mutants. The vast majority of TCAs in mutants are stunted after growing out of the internal capsule and some almost turn backward and never project to their cortical targets. However, the subplate neurons are able to project pioneer axons toward the thalamus normally in *Coup-tf1*$^{-/-}$ mutants, indicating that the subplate scaffold alone

Figure 12

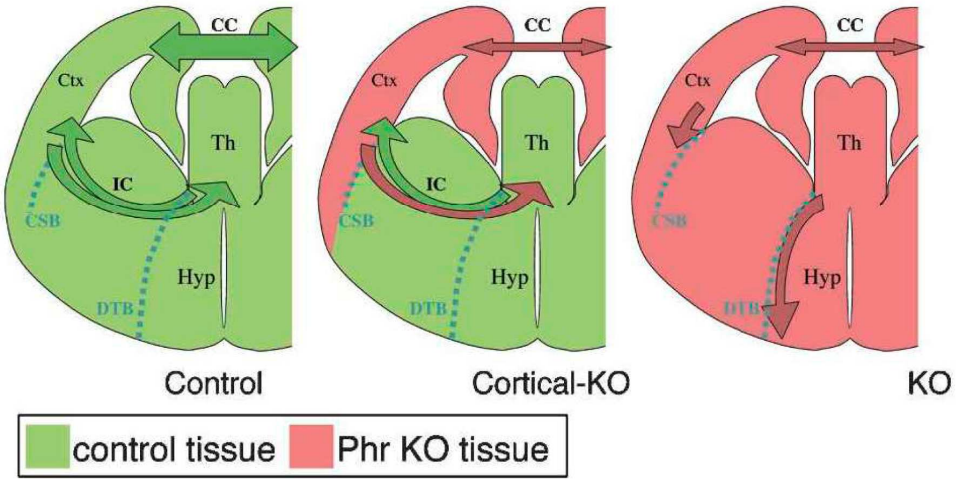

(From Bloom *et al*., 2007)

Figure 12. A summary of axonal developmental patterns in *Phr1* conditional mutants. In constitutive *Phr1* knockout mice (*Phr1* KO) where deletion of the floxed *Phr1* gene is driven by β-actin-Cre expression, neither CTAs nor TCAs are able to grow into the ventral telencephalon. CTAs descend through the cerebral cortex of the constitutive *Phr1* knockout mice but terminate at the edge of the corticostriatal boundary and fail to enter the subpallium, while TCAs descend within the diencephalon along the boundary between telencephalon and hypothalamus and fail to cross the diencephalic-telencephalic boundary into the ventral telencephalon. However, in the *Phr1* cortical-knockout mice (Phr1 cortical-KO) where *Phr1* deletion is restricted in the cerebral cortex by using *Emx1*-Cre, CTAs and TCAs develop normally and target the thalamus and cortex, respectively, as in controls (Bloom et al., 2007).

is not sufficient to guide TCAs in *Coup-tf1*$^{-/-}$ mutants, although the improper subplate neuron differentiation in *Coup-tfI* mutants may also lead to TCA defects. On the other hand, intrinsic defects in the thalamus cannot be ruled out since *Coup-tfI* is also expressed in the thalamus (Zhou et al., 1999).

Pax6 $^{-/-}$ mice show defects of CTAs and TCAs at the PSPB

For example, in mice lacking *Pax6*, both CTAs and TCAs project towards the PSPB but fail to cross this cortico-striatal boundary (Figure 11 f) (Hevner et al., 2002; Jones et al., 2002). In *Pax6*$^{-/-}$ mice, CTAs descend ventrolaterally through the developing lateral pallium and extend towards the base of the ventral pallium (the amygdaloid region). Most CTAs fail to cross the PSPB, while some of them enter into the subpallium in large bundles at more caudal levels. Instead of turning into the telencephalon from the diencephalon through the internal capsule as in a wild-type, the majority of the TCAs in *Pax6*$^{-/-}$ mice project aberrantly into the hypothalamus. Additionally, TCAs are seen emerging abnormally from the base of the ventral telencephalon and turn dorsomedially towards the proliferative zone of the ganglionic eminence, but fail to cross the PSPB. What's more, double DiI/DiA labelling experiments with DiA placed in the cortex and DiI in the thalamus indicate that no interactions occur between TCAs and CTAs within the internal capsule and the PSPB.

In the *Pax6*$^{-/-}$ brains, the cells within the PSPB domain appear to be more densely packed than in wild-type brains. These densely packed adhering cells at the PSPB of the *Pax6*$^{-/-}$ brains might not be penetrable for TCAs or CTAs, thus making an additional obstacle for the TCAs and CFAs to cross the PSPB (Jones et al., 2002). Additionally, the ventricular cellular mass and the atypical PSPB do not express glial cell markers GFAP or vimentin, and do not express calbindin or GABA, but express neuronal marker b-tubulin class III, suggesting that they comprise undifferentiated neurons (Jones et al., 2002).

In the *Pax6*$^{-/-}$ brains, the altered expression pattern of axonal guidance molecules including *Sema3c* and *Sema5a* in the pallium is also suggested to be responsible for the aberrant development of CFAs and TCAs (Jones et al., 2002). In wild-type brains, Sema3c is expressed in the SVZ and intermediate zone of the dorsal, lateral and ventral pallial domains. In *Pax6*$^{-/-}$ brains, *Sema3c* is still detected in the dorsal pallium, but the expression is shifted into the most superficial zone of the cortical plate. In the region of the ventral and lateral pallium of the *Pax6*$^{-/-}$ brains, however, the expression of *Sema3c* is completely abolished.

In wild-type brains, *Sema5a* is expressed in the VZ of the rostral pallium with a lateral (high) to medial (low) expression gradient. A prominent hybridization signal of *Sema5a* is seen within the VZ at the PSPB. In the *Pax6*$^{-/-}$ brains, lower expression level of *Sema5a* is preserved in the medial pallium, but not in the VZ at the PSPB (Jones et al., 2002).

Since *Pax6* is expressed in cortex, PSPB, basal telencephalon, and prethalamus, the absence of *Pax6* in *Pax6*$^{-/-}$ mice may affect the molecular characteristics of cortex, PSPB, basal telencephalon, and prethalamus. Thus the defects of TCAs and CTAs in *Pax6*$^{-/-}$ mice could be due to the defects of the guidance cues in multiple brain regions, as well as the autonomous defects of TCAs and CTAs themselves.

To test whether there is an autonomous defect of cells in the thalamus that affects the normal outgrowth of TCAs in *Pax6*$^{-/-}$ mice, in vitro explant culture experiments were applied where thalamic explants from *Pax6*$^{+/+}$ or *Pax6*$^{-/-}$ embryos were co-cultured with wild-type ventral telencephalic explants (Pratt et al., 2000). Whereas *Pax6*$^{+/+}$ thalamic explants showed strong innervation of wild-type ventral telencephalon in a pattern that is reminiscent of the in vivo trajectory of thalamic axons as they grow through the internal capsule, *Pax6*$^{-/-}$ explants did not, indicating that the mutant thalamic cells are unable to respond to guidance cues normally present in ventral telencephalon.

To further investigate the role of Pax6 in the normal development of CTAs and TCAs, recent years have seen the use of the Cre-LoxP system to conditionally knock out *Pax6* in the cortex driven by *Emx1*-Cre (Pinon et al., 2008) and in the basal telencephalon driven by *Six3*-Cre (Simpson et al., 2009).

Cortex-specific *Pax6* knockout mice show normal TCAs and CTAs connections

In cortex-specific conditional Pax6 knock-out mice (*Emx1*-Cre/*Pax6*-LoxP cKO), the caudal cortical areas (putative visual and somatosensory) are expanded while the rostral cortical domain (putative motor) is severely reduced (Pinon et al., 2008). Despite the rostral shift of graded expression of areal markers in the cerebral cortex and the accumulation of cells along the PSPB extending from the cortical intermediate zone to beneath the lateral cortex and amygdala, TCAs and CTAs develop normally in *Emx1*-Cre/*Pax6*-LoxP cKO mice. TCAs originating from VA, VB, and dLGN correctly target the putative motor, somatosensory, and visual cortical areas, respectively. CTAs projecting from different cortical areas descend through the intermediate zone in an organized topographic order, and they are capable of passing the PSPB and reaching the thalamus. These results indicate that molecular regionalization and thalamic targeting in cortical areas are possibly not strictly interdependent processes.

Deletion of *Pax6* in the ventral telencephalon causes CTAs and TCAs defects

When *Pax6* is deleted in the ventral telencephalon close to the internal capsule, driven by the *Six3*-Cre expression, some CTAs and TCAs derail from the normal trajectory when they grow through the ventral telencephalon (Simpson et al., 2009). Many TCAs take aberrant routes, either failing to turn laterally into the ventral telencephalon or exiting the developing internal capsule ventrally (Figure 13). Some CTAs are misrouted to the lateral telencephalon. In *Six3*-Cre/*Pax6*-loxP cKO mice, the corridor in the ventral telencephalon appears to be broader and less dense than

Figure 13

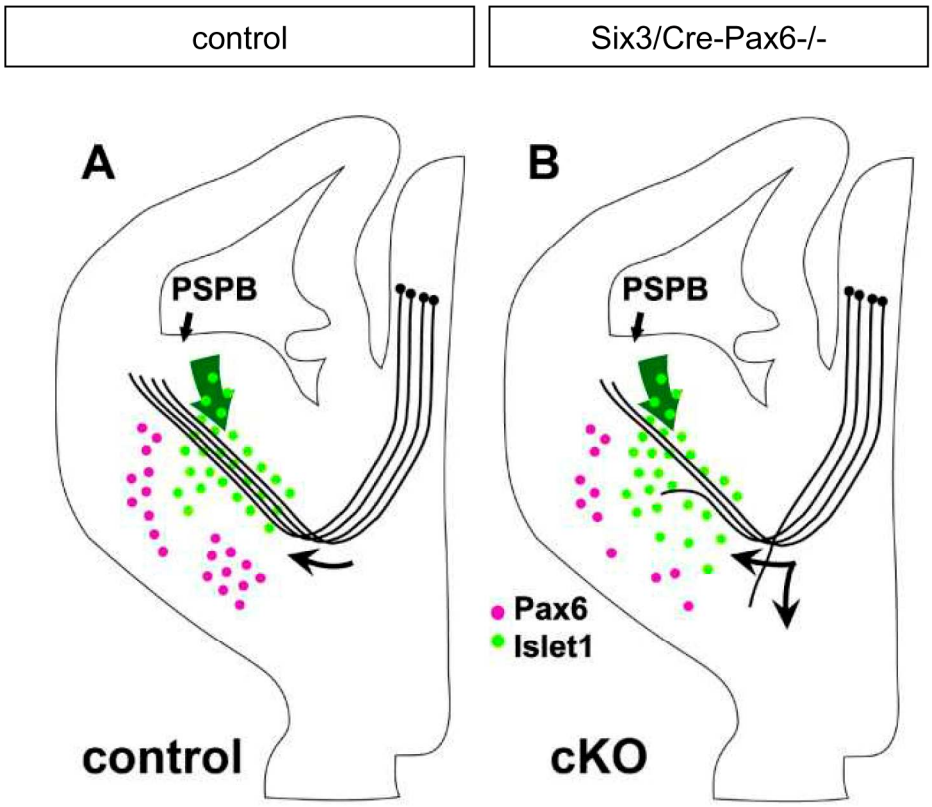

(From Simpson *et al*., 2009)

Figure 13. **A summary of axonal pathfinding defects in *Pax6* conditional mutants.** When *Pax6* is deleted in the ventral telencephalon close to the internal capsule, driven by the *Six3*-Cre expression, some CTAs and TCAs derail from the normal trajectory when they grow through the ventral telencephalon (Simpson et al., 2009).

normal, as revealed by Islet1-expressing cells, indicating that Pax6 is important for formation of the Islet1-expressing corridor in the ventral telencephalon. In *Pax6*$^{-/-}$ mice, no retrogradely labelled cells are detected in the ventral telencephalon after DiI placements into the thalamus, indicating the absence of transient thalamic afferents from the ventral telencephalon (Pratt et al., 2002). However, the pioneer axons that project from the ventral telencephalon to thalamus are present in *Six3*-Cre/*Pax6*-loxP cKO mice. These results indicate that the expression of Pax6 in the ventral telencephalon is important for formation of the Islet1-positive corridor and the thalamic and cortical axons that navigate through the ventral telencephalic corridor (Simpson et al., 2009).

Summary

A number of previously identified mutants with CTA defects usually display reciprocal TCA defects (Bloom et al., 2007; Hevner et al., 2002; Jones et al., 2002; Komuta et al., 2007; Lopez-Bendito and Molnar, 2003; Tissir et al., 2005; Wang et al., 2002; Zhou et al., 1999; Zhou et al., 2008), although in most cases the gene is expressed in more than one location, which makes it harder to interpret if the defects of TCAs and CTAs are cell autonomous or non autonomous and whether they are associated. This prompted us to generate a mutant animal model with a gene specifically knocked out in the cortex but not in the PSPB and other subcortical structures, which may lead to the defects of CTA outgrowth as well as the formation of guidance cues from the cortex. By examining the growth pattern of TCAs during their trajectory towards the thalamus in the conditional mutant, we may get some insights into the importance of the cortex in the guidance of TCAs, and whether TCAs are able to enter the cortex normally when CTAs are disrupted. It would also be interesting to delete a gene specifically in the thalamus, which may disrupt the outgrowth of TCAs as well as the generation of guidance factors from the thalamus. Examining the growth pattern of CTAs in the conditional mutant may reveal how important the thalamus is in the guidance of CTAs. In the current work the candidate

gene that I chose for specific cerebral cortical deletion as well as thalamic inactivation is Adenomatous polyposis coli (*Apc).*

1.3 Adenomatous polyposis coli (APC)

Adenomatous popyposis coli (APC) was originally identified as the gene mutated in Familial Adenomatous Polyposis (FAP), a disease characterized by the development of multiple colorectal adenomas (Groden et al., 1991).

1.3.1 The functions of APC

APC is well characterized as a tumor-suppressor that plays an important role in controlling the stability and subcellular localization of β-catenin (β-cat), and subsequently affects the Wnt signalling pathway. In the absence of APC, β-catenin may enter the nucleus, binds LEF-1/TCF proteins, and activates Wnt target genes (Sierra et al., 2006).

Additionally, APC has been suggested to be involved in a variety of cellular processes such as cell migration, cell-cell adhesion, mitotic spindle assembly and chromosome segregation, cell cycle progression, etc (Hanson and Miller, 2005).

During early brain development, APC is highly expressed in some regions of the cortex where the newly born postmitotic neurons are located, which indicates that APC may be important for the maturation of postmitotic cells (Bhat et al., 1994). APC has been shown to play important roles in the normal growth and differentiation of the cerebral cortex, regulating the cell number, interkinetic nuclear migration, cell polarity, cell type specification, neuronal differentiation, axonal outgrowth, axonal extension, etc (Ivaniutsin et al., 2009; Yokota et al., 2009). It has been shown that APC localizes to the end of microtubules in axons and stabilizes microtubule polymerization, which is regulated by NGF-PI3K-GSK-3β pathway (Zhou et al., 2004).

1.3.2 *Emx1*-Cre/*Apc*-LoxP as a model to understand the importance of the cerebral cortex in the guidance of TCAs

Since APC is involved in neuronal differentiation and axonal outgrowth and extension, deleting *Apc* in the cortex may lead to defects of CTA outgrowth as well as the formation of guidance cues from the cortex. This would allow me to examine the importance of CTAs and some cortical molecules in guiding TCAs into the cortex. In order to remove Apc specifically in the cerebral cortex but not in any other areas, I used *Emx1*-Cre/*Apc*-LoxP mice, in which the expression of *Emx1*-Cre confers the recombination of loxP target loci, and subsequently results in the specific knockout of the gene at the loxP loci, in this case, the *Apc* gene.

As a member of the *Emx* family, *Emx1* is a homeodomain transcription factor expressed by progenitor cells of the embryonic cortex, in a low rostrolateral to high caudomedial gradient (Bishop et al., 2002), and its expression begins from E9.5 (Cecchi and Boncinelli, 2000). Hence the deletion of the *Apc* gene in the relevant part of the neocortex of the *Emx1*-Cre/*Apc*-LoxP conditional mutants may start at E9.5.

In this work I examined the development of CTAs and TCAs, as well as the expression of some cerebral cortical guidance molecules in the *Apc* conditional mutant.

1.3.3 *RORα*-Cre/*Apc*-LoxP as a model to understand the importance of the thalamus in the guidance of CTAs

In the current work I used the *RORα*-Cre/*Apc*-LoxP mouse to generate a conditional mutant model where *Apc* was inactivated specifically in the thalamus. Deleting *Apc* in the thalamus may interrupt TCA development as well as the formation of guidance cues from the thalamus. This would allow me to study the importance of the thalamus in the guidance of CTAs, and test whether CTAs are able to reach the thalamus in the absence of the guidance from the descending TCAs.

Investigating the thalamocortical tract system in the *Apc* conditional mutants may give some insights into the principles of thalamocortical development, the development of communication between the cortex and thalamus, and the causal relationships between signal molecules and the cortical and thalamic patterns. Furthermore, it may provide some clues into the reasons for some neurological diseases during early brain development, and may provide a theoretical foundation for therapy attempts.

The results of the current study are described in Chapter 3, 4 and 5. In Chapter 3, I demonstrate the growth pattern of CTAs and TCAs in *Emx1*-Cre/*Apc*-LoxP conditional mutant mice where *Apc* is specifically inactivated in the cerebral cortex. My results show that in the absence of Apc in the neocortex, corticofugal axons fail to grow, and that thalamic axons stop proximal to pallial-subpallial boundary (PSPB). Instead of entering the cortex, thalamic axons turn ventrally in the basal telencephalon. These results reveal the PSPB as a choice point for TCAs, and that TCAs need guidance from the cortex to cross the PSPB.

To further investigate what guidance cues are necessary to guide TCAs into the cortex, I examined the gene expression pattern of some attractive molecules and used *in vitro* explant culture assay to detect the possible upregulation of repulsive cues in the *Emx1*-Cre/*Apc*-LoxP mutant cortex. As described in chapter 4, my results show that some attractive molecules for TCAs are still present in the mutant cortex. Thus the failure of TCAs to enter the cerebral cortex in the conditional mutant is less likely to be ascribed to the lack of attractive molecules secreted by the cortex. Additionally, the explant culture experiments show that the mutant cortex does not repel or inhibit thalamic axonal outgrowth, and that the angle region of the mutant cortex still has growth promoting effects on thalamic axons. Thus the failure of TCAs to enter the cortex of the conditional mutant might be due to the loss of descending CTAs in the cortex. In support of this hypothesis, in the *in vitro* brain slice culture experiments where mutant cortex was replaced with control cortex, cortical axons regenerate from the control cortex and rescue thalamic axon growth into the cortex. These results

indicate that descending cortical axons are important in directing thalamic axons into the cerebral cortex.

In Chapter 5 I describe the grow pattern of TCAs and CTAs in the *RORα*-Cre/*Apc*-LoxP conditional mutant mice where Apc is deleted in the primary sensory nuclei of the thalamus. No dramatic defects of CTAs and TCAs are observed in this mutant, indicating that the deletion of Apc in postmitotic neurons in the thalamus may not affect axonal development between the cortex and the thalamus.

Chapter 2. Materials & Methods

2.1 Animals

Mice harbouring different transgenic alleles were used in this study: Apc^{580S}, $Emx1^{Cre}$ and $ROR\alpha^{Cre}$. To generate $Emx1^{Cre/+}Apc^{580S/580S}$ progeny, $Emx1^{Cre/+}Apc^{580S/+}$ were intercrossed with $Emx1^{+/+}Apc^{580S/580S}$. To generate $ROR\alpha^{Cre/+}Apc^{580S/580S}$ progeny, $ROR\alpha^{Cre/+}Apc^{580S/+}$ were intercrossed with $ROR\alpha^{+/+}Apc^{580S/580S}$. The first day of vaginal plug was designated as E0.5. Pregnant females were killed by anesthesia and cervical dislocation. The embryos were removed immediately by caesarean surgery, and their heads were immersed in cold fixative. In this manuscript, 'control' embryos were double heterozygotes ($Emx1^{Cre/+}Apc^{580S/+}$ and $ROR\alpha^{Cre/+}Apc^{580S/+}$, respectively), which are phenotypically normal. $Emx1^{Cre/+}Apc^{580S/580S}$ and $ROR\alpha^{Cre/+}Apc^{580S/580S}$ embryos were designated as 'conditional mutant'.

2.2 In Situ Hybridization

Brains of mouse embryos were fixed overnight in 4% paraformaldehyde in phosphate buffered saline (PBS) before processing to wax blocks. Wax sections were cut at 10 µm and collected on TESPA-coated slides. DNA templates for RNA probes were prepared by digesting the plasmids with Hind III and cleaning up using QIAquick Gel Extraction Kit (50), Cat. No.28704. RNA probes were labelled with digoxigenin. *In situ* hybridizations for *Ig-Nrg1* were performed as previously described (Flames et al., 2004).

2.3 Immunohistochemistry

Embryonic heads were fixed overnight in 4% paraformaldehyde in PBS. Heads were either embedded in wax and cut into sections at 10 µm thick or embedded in agarose and cut into vibratome sections at 100 µm thick. The GFP explant cultures were fixed in 4% paraformaldehyde 0.1M PBS for 1 hr on ice before undertaking a GFP immuno. Immunofluorescence was performed as previously described [Ivaniutsin et

al.]. The following primary antibodies were used: Affiniti NA1297 rabbit polyclonal anti-neurofilament cocktail, 1:500 (www.biomol.com), rabbit anti-GAP43 (AB5220), 1:1000 (Chemicon International, Temecula, CA), mouse anti-Map2, 1:500 (Sigma, UK), mouse anti-RC2, 1:500 (DSHB), rat anti-L1, 1:500 (Chemicon International, Temecula, CA), rabbit anti-GFP, 1:3000 (Abcam), and rabbit anti-calbindin, 1:2000. The secondary antibodies included: polyclonal goat anti-rabbit immunoglobulins /biotinylated (E0432, DakoCytomation), polyclonal goat anti-mouse immunoglobulins /biotinylated (E0433, DakoCytomation). ABC kit Strepavidin was used to amply signal. The fluorescent secondary antibodies were as follows: goat anti-rabbit IgG Alexa Fluor 568, 1:200 (Molecular Probes), goat anti-rat IgG Alexa Fluor 568, 1:200 (Molecular Probes) and goat anti-mouse IgM Alexa Fluor 488, 1:200 (Molecular Probes).

2.4 Tracing experiments

In the present study, carbocyanine dyes were used as tracers in formaldehyde-fixed brains (Godement et al., 1987). Using DiI and DiA crystal placements, we should be able to trace the navigation pattern of CTAs and TCAs and the projections from LGE domain in mouse embryos, since DiI and DiA are fluorescent dyes that specifically label axons and their cell bodies anterogradely or retrogradely. Tracing experiments on the brains of embryos were performed as previously described (Métin et al., 1996).

Brain fixation. After dissection in cold PBS (0.1M), brains were fixed overnight in PFA (4% paraformaldehyde in 0.1M phosphate buffer, at 4°C).

Labeling. For each embryo, the brain was separated into two halves by cutting along the midline. Tips of glass micropipettes coated with DiI were used to impale the embryonic neocortex after the pia was removed. In order to anterogradely label cortical axons and retrogradely label projections from LGE, two DiI placements were applied in the dorsal-lateral cortex, at the anterior and posterior part of the telencephalon. To anterogradely label thalamic axons and retrogradely label

projections from MGE or ventral telencephalon, DiI and DiA were placed in the thalamus, with DiI at the anterior part and DiA at the posterior part of the thalamus. The brains were then returned to fixative and kept for 4 weeks at room temperature before analysis.

Analysis of labelling. Brains were embedded in 4% agarose, and serial sections were cut with a vibratome in the frontal plane at 100 µm. Sections were collected in 0.1M PBS. Nuclei were counterstained with Hoechst or TO-PRO-3 iodide (Invitrogen) at 1 µM. Before observation, the sections were rinsed in PBS and mounted in Mowiol or Vectashield. Images were acquired by using an epifluorescence microscope and digital camera (Leica, Nussloch, Germany) or a TCS NT confocal microscope (Leica).

2.5 Explant cultures

Mice harbouring different transgenic alleles were used in the explant culture experiments: Apc^{580S} and $Emx1^{Cre}$. To generate $Emx1^{Cre/+}Apc^{580S/580S}$ progeny, $Emx1^{Cre/+}Apc^{580S/+}$ mice were intercrossed with $Emx1^{+/+}Apc^{580S/580S}$ mice. To generate tau-GFP progeny, TgTP6.3 mice were intercrossed with CD1 wild type mice. The first day of vaginal plug was designated as E0.5. Pregnant females were killed by anesthesia and cervical dislocation. The embryos were removed immediately by caesarean surgery.

E14.5 embryos were used for the *in vitro* explant culture experiments. Embryos were collected in the Earle's balanced salt solution (EBSS). At E14.5, *Apc* mutant embryos displayed an obvious open-mouth phenotype, which appeared to be close-mouth in the normal mouse embryos. Therefore the phenotype of the embryos was used to distinguish the mutants from the normal mouse embryos. For the explant co-culture experiments, *Apc* mutant embryos were $Emx1^{Cre/+}Apc^{580S/580S}$, while the control embryos were the phenotypically normal litter mates which were either $Emx1^{Cre/+}Apc^{580S/+}$, $Emx1^{+/+}Apc^{580S/580S}$ or $Emx1^{+/+}Apc^{580S/+}$. The *tau*-GFP positive

embryos were recognized and selected under a dissection fluorescent microscope with a GFP filter.

The thalamic tissues used for explant cultures were taken from *tau*-GFP positive embryos so that thalamic axons could be distinguished from non-GFP cortical axons by using anti-GFP antibodies. The thalamus from E14.5 *tau*-GFP positive embryos was dissected out under a dissection microscope and cut into small explants at a size of about 500 x 500 x 300 µm, using a fine dissection knife. The lateral cortex was dissected out from E14.5 control and mutant brains, respectively, and cut into small explants at a size of about 500 x 500 x 250 µm. The hypothalamus was dissected out from E14.5 control mice and cut into small explants at a size of about 500 x 500 x 300 µm. The explants were submerged in cold EBSS during the dissection, after which they were transferred to serum free culture medium by pipetting and kept at 37°C.

Collagen (10-20 µl) was spread evenly onto the wells of a 4-well culture dish and allowed to set at 37°C. In each well of the culture dish, one *tau*-GFP thalamic explant was placed on top of the collagen adjacent to one cortical explant or hypothalamic explant in a distance ranging from 200 µm to 500 µm. Another 20 µl of collagen was added to submerge the explants and allowed to set at 37°C. Once the collagen was set, 500 µl of serum free culture medium was added into each well of the culture dish and the explants were incubated at 37°C for 3 days to allow the three-dimensional outgrowth of axons.

Explant cultures were fixed in cold 4% PFA in PBS for 1 hour after 3 days of incubation at 37°C. Then the explant cultures were washed in 0.1% Triton-X-100 in PBS (PBSTx-100) for 15 minutes at 4°C, before being blocked in 20% goat serum, 0.1% PBSTx-100 for 1 hour at 4°C. Primary antibody: rabbit GFP (1:3000) (Abcam) was added to the explant cultures and incubated overnight at 4°C. Following washes in 0.1% PBSTx-100 for 5 hours at 4°C, the cultures were incubated overnight at 4°C with secondary antibody: goat anti-rabbit Alexa Fluor 568 (1:200) (Molecular Probes). Following washes in 0.1% PBSTx-100 for 5 hours at 4°C, cultures were

incubated in TO-PRO-3 (1:1000) in PBS for 1 hour at 4°C and then submerged in a 9:1 solution of glycerol: PBS. Once the collagen became quite transparent, the cultures were mounted in Mowiol and images were acquired by using an epifluorescence microscope and digital camera (Leica, Nussloch, Germany).

Figure 1 A shows a typical image of an E14.5 GFP-positive thalamic explant cultured with a cortical explant from the lateral cortex of E14.5 control embryos. Figure 1 B-D demonstrate the procedures to analyse the percentage axon coverage in each image. The thalamic explants were divided into four quadrants (Figure 1 B). The amount of thalamic axonal outgrowth was estimated by surrounding each explant by a line at 60 pixel distance (yellow polygon, 60 pixel distance ≈ 110 µm) from explant border (blue) and calculating the percentage of its circumference that was covered by neurites crossing it (Figure 1 B). This estimate is referred to as 'percentage axon coverage' (Tian et al., 2008).

The percentage axon coverage of thalamic axons in the quadrant that was facing toward the cortical explant was compared to that in the quadrant that was away from the cortical explant (Figure 1 B). Figure 1 C shows a close-up view of a region of the explant featuring the neurite fascicles that were crossing the yellow polygon. In Image J, the colour intensity of every pixel that the yellow polygon came cross in the image was automatically measured by using a plug-in, and the results were shown as a list of data as well as a colour intensity plot (Figure 1 D).

In the colour intensity plot for Image J selection, the X axis represented the circumference of measuring polygon (the yellow circle in B), while the Y axis represented the colour intensity of anything that the measuring polygon came across in the image (Figure 1 D). The blue box highlighted the colour intensity of the region that the measuring polygon (yellow) came across in C. A base line (red) was drawn on the graph to distinguish the axonal signal from the background noise. The way to determine the base line level is: First, draw a line across an area in the background of the image (see the yellow line in the background area in B). Second, get a graph that shows the colour intensity plot of anything that the yellow line came cross in the

image. Third, identify the highest colour intensity in the plot and use it as the base line level.

The data was copied into an excel file. The percentage axon coverage was calculated by summing up every pixel along the measuring polygon in each quadrant with the colour intensity above the base line level and dividing it by the length of the measuring polygon in each quadrant. Student's t-test was used to assess the significance of differences between the percentage axon coverage of thalamic axons in the quadrant that was facing toward the cortical explant and that in the quadrant that was away from the cortical explant ($P<0.05$).

For the comparison of total outgrowth of thalamic axons between different culture groups, the amount of thalamic axonal outgrowth was measured at 60, 100, 140, 180 & 220 pixel distances (yellow polygons, 60 pixel distance ≈ 100 µm) from explant border (blue). The % axon coverage was estimated as described in Figure 2. Since the measuring polygons (yellow) in the quadrant of the thalamic explant facing toward the cortical explant came across the cortical explant in most cases, the % axon coverage in the quadrant towards the cortical explant was excluded. The % axon coverage in the other three quadrants was summed up for each explant. Two Way Repeated Measures ANOVA was used to assess the significance of differences between groups and, where differences were significant ($P<0.05$), Student's t-test were used to assess the differences between pairs of groups.

2.6 Brain slice cultures

E14.5 embryos were used for the *in vitro* brain slice culture experiments. Embryos were collected in ice cold Krebs in a Petri dish. Brains were removed and embedded in LMP agarose in molds. The molds were placed on ice for hardening. 300 µm thick coronal sections were cut using a vibratome. The vibratome well contains ice cold Krebs. Brain sections were collected into small Petri dishes containing sterile filtered Krebs on ice. The sections were handled with thin spatulas. The sections were then transferred in the hood to the membranes in tissue culture dishes containing 1 ml

Figure 1

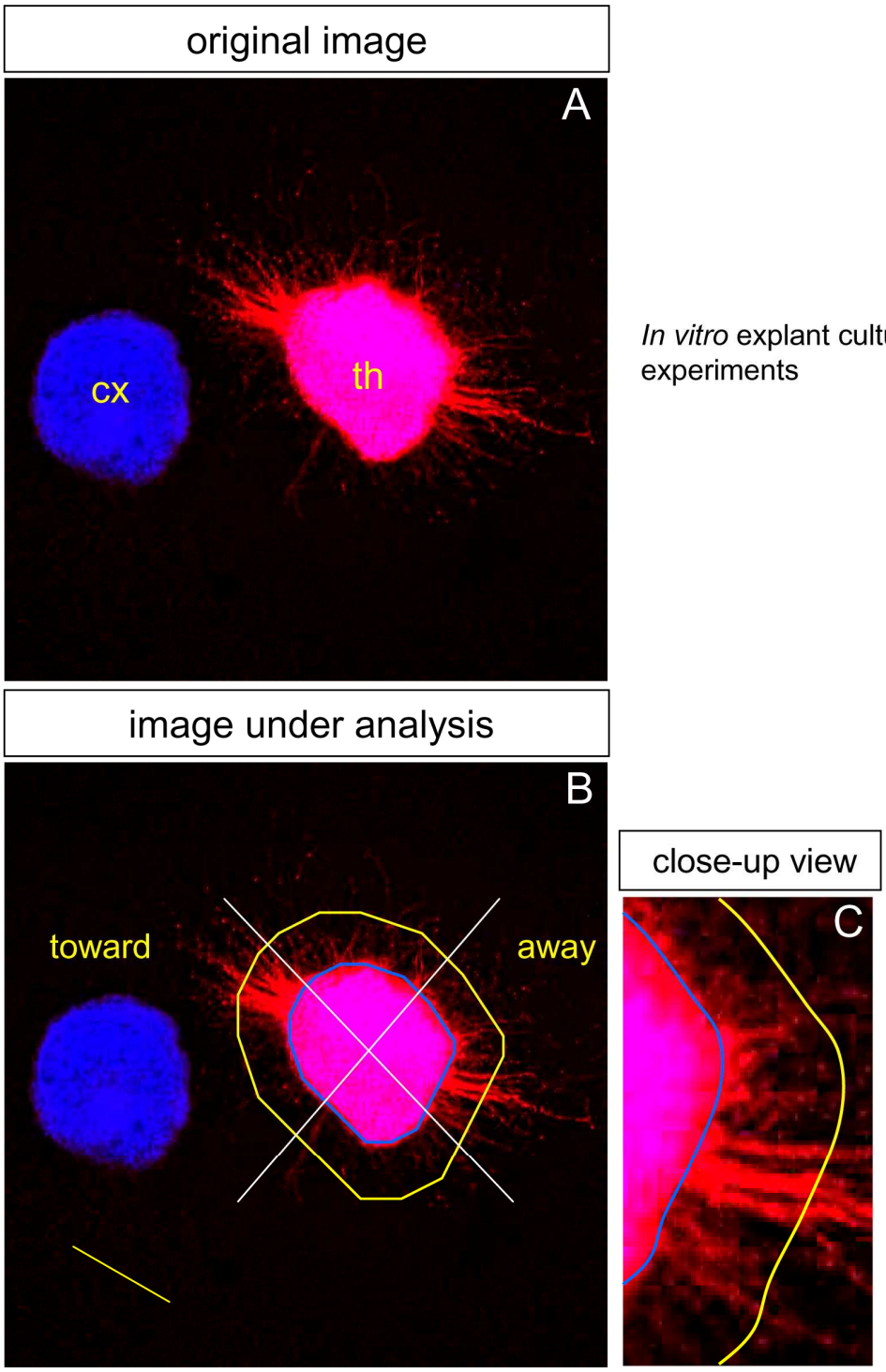

In vitro explant culture experiments

(*Figure 1 continues on the next page*)

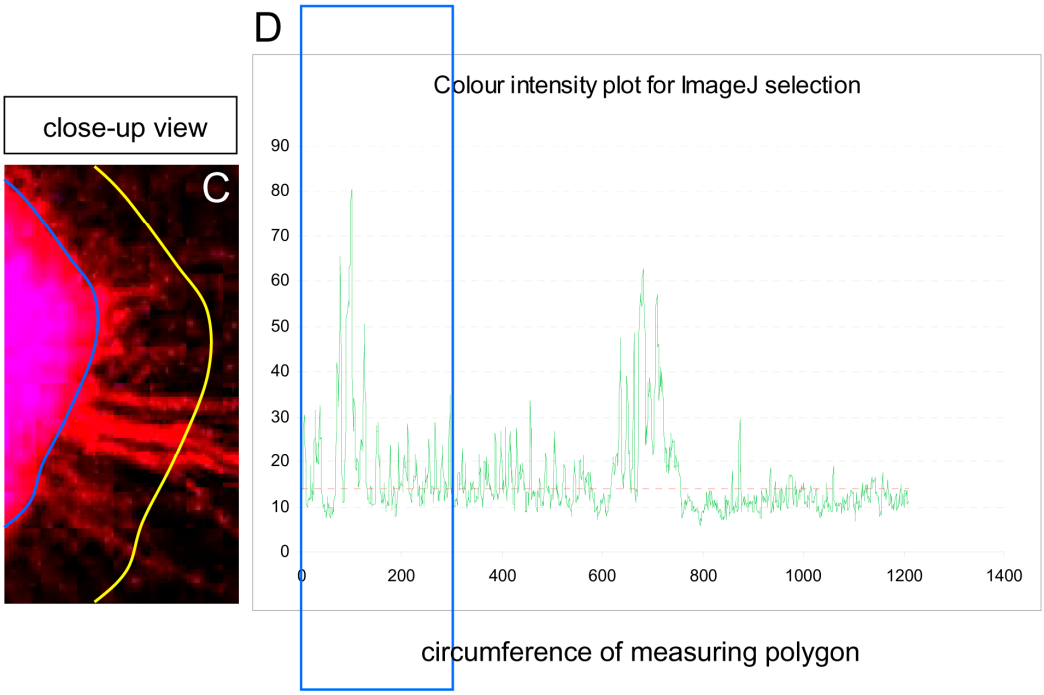

$$\%\ \text{axon coverage} = \frac{\text{sum of all neurite fascicle widths in each quadrant} \times 100}{\text{circumference of measuring polygon in each quadrant}}$$

Figure 1. Measurement of % axon coverage in the explant culture. (A) A typical image of an E14.5 GFP-positive thalamic explant cultured with a cortical explant from the lateral cortex of E14.5 control embryos. Immunohistochemistry was with GFP antibody (red) and nuclei were counterstained with TO-PRO-3 (blue). **(B)** The amount of thalamic axonal outgrowth was measured at 60 pixel distance (yellow polygon, 60 pixel distance ≈ 110 µm) from explant border (blue). The % axon coverage was estimated by calculating the percentage of circumference of the measuring polygon that was covered by neurites crossing it. The thalamic explant was divided into four quadrants. The % axon coverage of thalamic axons in the quadrant that was facing toward the cortical explant was compared to that in the quadrant that was away from the cortical explant. **(C)** A close-up view of a region of the explant featuring the neurite fascicles that were crossing the yellow polygon. **(D)** A graph showing a colour intensity plot for a thalamic explant under analysis. While X axis represented the circumference of measuring polygon (the yellow circle in B), Y axis represented the colour intensity of anything that the measuring polygon came across in the image. The blue box highlighted the colour intensity of the region that the measuring polygon (yellow) came across in C. A base line (red) was drawn on the graph to distinguish the axonal signal from the background noise. The way to determine the base line level is: First, draw a line across an area in the background of the image (see the yellow line in the background area in B). Second, get a graph that shows the colour intensity plot of anything that the yellow line came cross in the image. Third, identify the highest colour intensity in the plot and use it as the base line level. Student's t-test was used to assess the significance of differences between thalamic axons growing towards and away from the cortical explant ($P<0.05$). cx – cortex, an – angle region, th – thalamus, ht – hypothalamus.

Figure 2

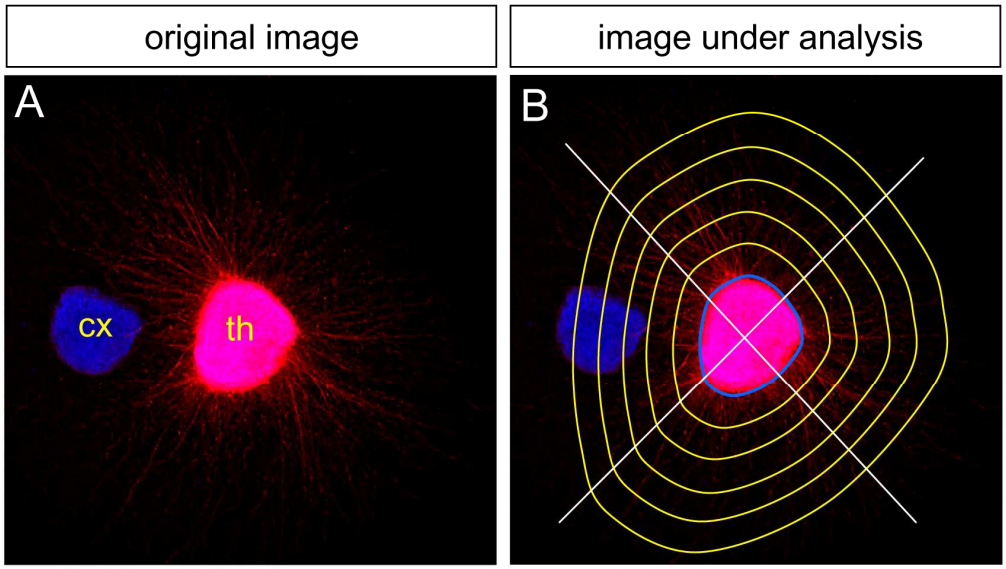

Figure 2. Measurement of the total % axon coverage in the explant culture. (A) A typical image of an E14.5 GFP-positive thalamic explant cultured with a cortical explant from the lateral cortex of E14.5 mutant embryos. Immunohistochemistry was with GFP antibody (red) and nuclei were counterstained with TO-PRO-3 (blue). **(B)** The amount of thalamic axonal outgrowth were measured at 60, 100, 140, 180 & 220 pixel distances (yellow polygons, 60 pixel distance ≈ 100 µm) from explant border (blue). The % axon coverage was estimated as described in Figure 1. Since the measuring polygons (yellow) in the quadrant of the thalamic explant facing toward the cortical explant came across the cortical explant in most cases, the % axon coverage in the quadrant towards the cortical explant was excluded. The % axon coverage in the other three quadrants was summed up for each explant. Two Way Repeated Measures ANOVA was used to assess the significance of differences between groups and, where differences were significant ($P<0.05$), Student's t-test were used to assess the differences between pairs of groups. Th-thalamus, cx-cortex.

MEM medium. The sections were then incubated for 1 h (37°C, 5% CO_2), before being transferred to 1 ml Neurobasal medium. Transplants were cut with fine scissors from the donor slice and transferred to the host slice with fine forceps. The transplants were incubated at 37°C for 3 days to allow the outgrowth of axons.

Transplants were fixed in cold 4% PFA in PBS overnight after 3 days of incubation at 37°C. Then the transplants were rinsed with PBS. Red dyes were placed into the thalamic transplants while green dyes were placed into the cortex. The transplants were then returned to fixative and kept for 2 weeks at room temperature to allow the diffusion of the fluorescence dyes along the axons. The transplants were rinsed with PBS before transferred to 1:1 Glycerol/PBS, and counterstained with TO-PRO 3. Before observations, they were mounted in 1:1 Glycerol/PBS. Images were acquired by using a confocal microscope (Zeiss).

Chapter 3. *Apc* deletion in the cerebral cortex and the defects of CTAs and TCAs

In this chapter I describe the specific inactivation of Apc gene in the cerebral cortex and the defects of reciprocal connections between the cortex and the thalamus. The mechanisms by which the cortex and the thalamus establish reciprocal connections are poorly understood. It has been postulated that CTAs and TCAs meet in the ventral telencephalon, after which they use each other as axonal scaffolds to reach their final targets. This is described as the Handshake hypothesis. To test this hypothesis, I used the *Emx1*-Cre/*Apc*-LoxP mouse to generate a conditional mutant model where CTAs development might be interrupted, and test whether TCAs are able to reach the cerebral cortex in the absence of the guidance from the descending CTAs.

By using immunohistochemistry as well as axonal tract tracing techniques, here I show that neuronal differentiation in the cerebral cortex is disrupted in the conditional *Apc* mutant, and that there are fewer postmitotic neurons (including the projection neurons), which lead to the defects of CTAs outgrowth. In addition, TCAs fail to reach the cerebral cortex. TCAs navigate into the ventral telencephalon normally, but could not pass the pallial-subpallial boundary (PSPB) and enter the cortex. These results reveal the PSPB as a choice point for TCAs, and that TCAs need guidance from the cortex to cross the PSPB. The Apc mutant cortex lacks these guidance factors, which might be the descending CTAs.

3.1 Proof of *Apc* deletion and the upregulation of β-catenin in the cortex

In the current study, the Adenomatous polyposis coli (*Apc*) gene was conditionally inactivated by Cre recombinase driven by the endogenous *Emx1* promoter (*Emx*-Cre) (Ivaniutsin et al., 2009). *Emx1* starts to be expressed in the cerebral cortex from E9.5 (For review see Cecchi and Boncinelli, 2000). The activity of Cre recombinase was confirmed by LacZ staining of embryos carrying *Emx1*-Cre and a floxed-stop R26R

LacZ reporter allele (Figure 1 A) (Iwasato et al., 2000). The staining was restricted to the cerebral cortex and did not include the PSPB.

To examine the deletion of Apc protein in the mutant, Apc immunofluorescence was performed on paraffin sections and vibrotome sections of embryos (Ivaniutsin et al., 2009). My data showed a distinct expression pattern of Apc throughout the cerebral cortex from E11.5 to E14.5 during normal brain development (Figure 1).

At E11.5, Apc showed prominent expression at the ventricular surface of the cortex, with small groups of high expressing cells present at the pial surface (Figure 1 B & C). Radial processes within the cortex also showed Apc staining. In the mutant cortex, the Apc expression level was decreased at E11.5 (Figure 1 D) compared to the control (Figure 1 C). The prominent expression at the ventricular surface of the control cortex was not present in the mutant. A small group of cells showed higher expression of Apc near the pial surface of the mutant cortex. Apc was observed in some radial processes within the mutant cortex (Figure 1 D).

At E12.5 and E13.5, Apc was expressed throughout the ventricular zone of the control cortex especially at the ventricular surface, and showed the highest level of expression in the newly formed cortical neurons (Figure 1 E-H). Radial processes within the control cortex also showed Apc staining. In the mutant cortex, the level of Apc expression was much lower than in the control at E13.5 (compare Figure 1 H & I). No prominent expression of Apc was observed at the ventricular surface of the ventricular zone in the mutant cortex. The Apc highly expressing cortical plate was missing in the mutant cortex. Small groups of cells with Apc staining were detected in the ventricular zone and near the pial surface of the mutant cortex (Figure 1 I). Radial processes with Apc staining were not present in the mutant cortex.

At E14.5, Apc was strongly expressed in the cortical plate and the intermediate zone of the control cortex, with weaker signal in the ventricular zone (Figure 1 J & K). In the mutant, there was a dramatic reduction of Apc staining throughout the cortex compared to the control at E14.5 (compare Figure 1 K & L). Very few cells in the

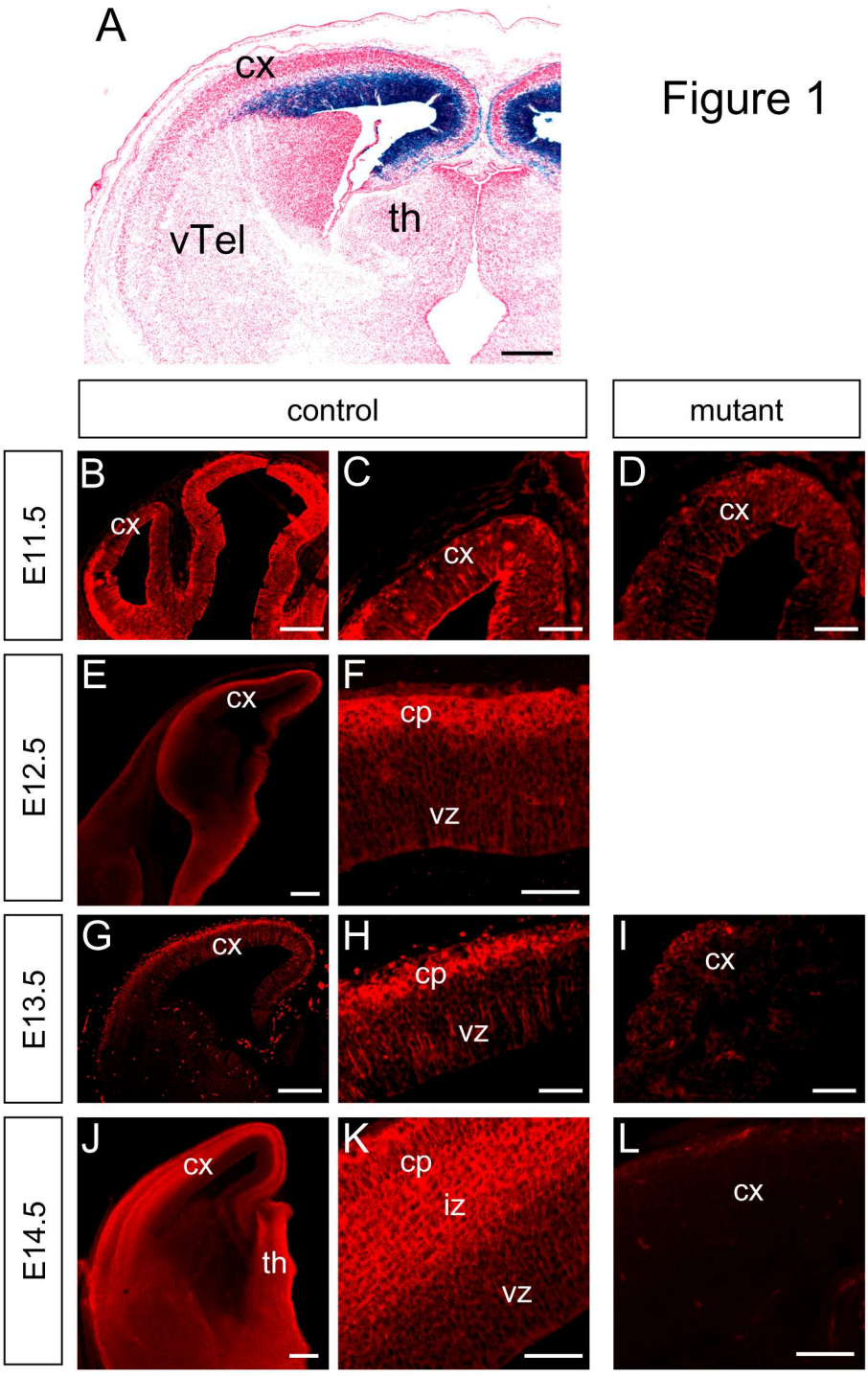
A
cx
vTel
th
control
mutant
E11.5
E12.5
E13.5
E14.5
B
C
D
E
F
G
H
I
J
K
L
cx
cp
vz
iz
th

Figure 1

Figure 1. Expression pattern of *Emx1*-Cre and the proof of Apc deletion in the cortex. (A) Coronal section of Rosa26-LacZ reporter embryo at E15.5. Blue staining showed the region of the cortex where Emx1-cre was active. Cx – cortex, th – thalamus. vTel – ventral telencephalon. All other tissue looked negative. **(B, E, G, J)** Coronal sections of control embryos. **(C, F, H & K)** Higher power magnification of the control cerebral cortex. **(C)** At E11.5, Apc showed prominent expression at the ventricular surface of the control cortex, with small groups of high expressing cells present at the pial surface. Radial process within the cortex also showed Apc staining. **(D)** In the mutant cortex, Apc expression level decreased at E11.5 compared to the control. The prominent expression at the ventricular surface of the control cortex was not present in the mutant. A small group of cells showed higher expression of Apc near the pial surface of the mutant cortex. Apc was observed in some radial process within the mutant cortex. **(F & H)** At E12.5 and E13.5, Apc was expressed throughout the ventricular zone of the control cortex especially at the ventricular surface, and showed highest level of expression in the newly formed cortical neurons. Radial process within the control cortex also showed Apc staining. **(I)** In the mutant cortex, the level of Apc expression was much lower than the control at E13.5. No prominent expression of Apc was observed at the ventricular surface of the ventricular zone in the mutant cortex. The Apc highly expressing cortical plate was missing in the mutant cortex. Small groups of cells with high levels of Apc were detected in the ventricular zone and near the pial surface of the mutant cortex. Radial process with Apc staining was not present in the mutant cortex. **(K)** At E14.5, Apc was strongly expressed in the cortical plate and the intermediate zone of the control cortex, with weaker signal in the ventricular zone. (L) In the mutant, there was a dramatic reduction of Apc staining throughout the cortex compared to the control at E14.5. Very few cells in the mutant cortex remained Apc positive. Therefore Apc immunohistochemistry revealed a gradual decrease of Apc expression in the mutant cortex from E11.5 to E14.5. While Apc expression level in the mutant cortex was slightly lower than the control at E11.5, the loss of Apc was dramatic in the mutant cortex at E14.5 compared to the control. Scale bars: (A) 100 µm; (B, E, G, J) 200 µm; (C, D, F, H, I, K, L) 50 µm.

mutant cortex remained Apc positive. Therefore, Apc immunohistochemistry revealed a gradual decrease of Apc expression in the mutant cortex from E11.5 to E14.5. While the Apc expression level in the mutant cortex was slightly lower than the control at E11.5, the loss of Apc was dramatic in the mutant cortex at E14.5 compared to the control. No Apc depletion was observed in the thalamus or the ventral telencephalon of the mutant compared to the control, indicating that Apc inactivation was restricted to the cerebral cortex (Figure 2 A-D).

Apc is well characterized as a tumor-suppressor that plays an important role in controlling the stability and subcellular localization of β-catenin via the Wnt signalling pathway. In the absence of Apc, β-catenin is stabilised and translocated to the nuclei, binds LEF-1/TCF proteins, and activates Wnt target genes (Sierra et al., 2006). Here β-catenin immunohistochemistry was performed to elucidate the regions of the mutant cortex where Apc was depleted. In the control cortex, β-catenin was highly expressed in the cortical plate and the intermediate zone, and weaker in the ventricular zone of the cortex at E14.5 (Figure 3 E & F). In the mutant, β-catenin staining was dramatically enhanced in the cortex (Figure 3 G & H). No increase in β-catenin staining was observed in the ventral telencephalon or the thalamus, indicating that β-catenin was only up-regulated in the cortex, consistent with the observation that Apc was only deleted in the cortex (Figure 3 C & D, compare with Figure 3 A & B).

3.2 Loss of Apc causes CTA defects in the cortex

3.2.1 The reduction of Map2 positive neurons in the mutant cortex

Apc regulates cell proliferation and neuronal differentiation. Our previous work has shown that the *Apc* mutant exhibits severe disruption in the development of the cerebral cortex, including a reduction in the size of the cortex, the disorganisation of cell types, and changes in the molecular identity of its cells (Ivaniutsin et al., 2009). This prompted me to wonder if the formation of cortical projection neurons is

Figure 2

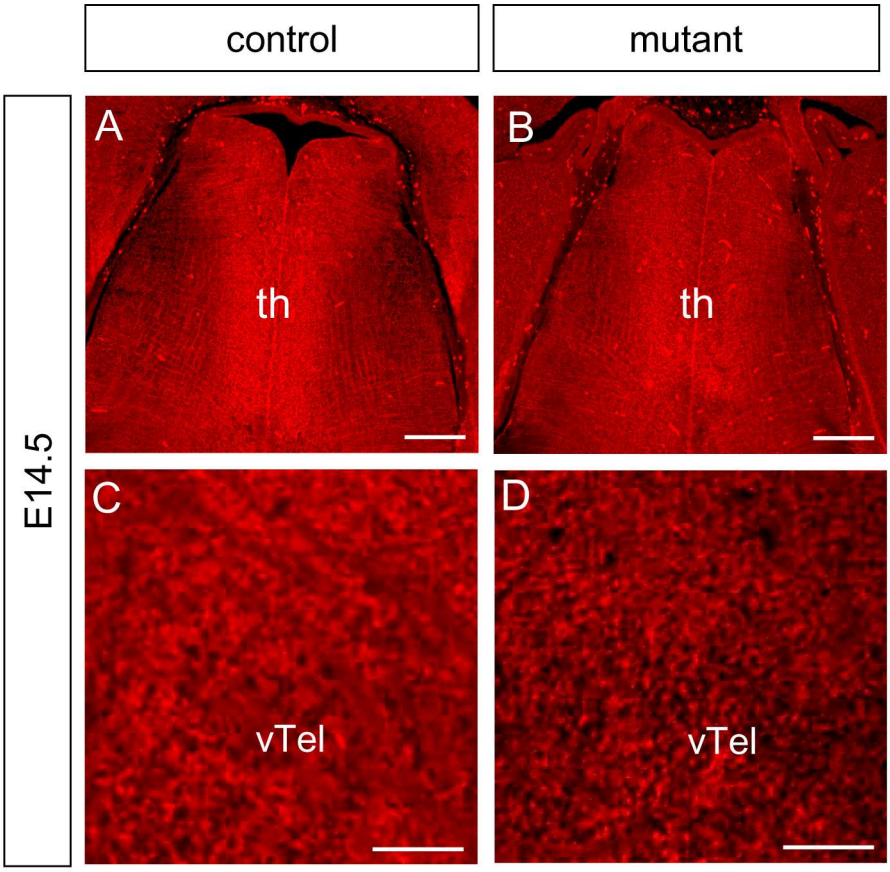

Figure 2. Apc expressions in the subcortical areas were not affected in the *Apc* mutants. (A, B, C & D) No Apc deletion was observed in the thalamus or the ventral telencephalon of the mutant compared to the control, indicating that Apc inactivation was restricted to the cerebral cortex. Scale bars: (A, B) 100 μm; (C, D) 50 μm.

Figure 3

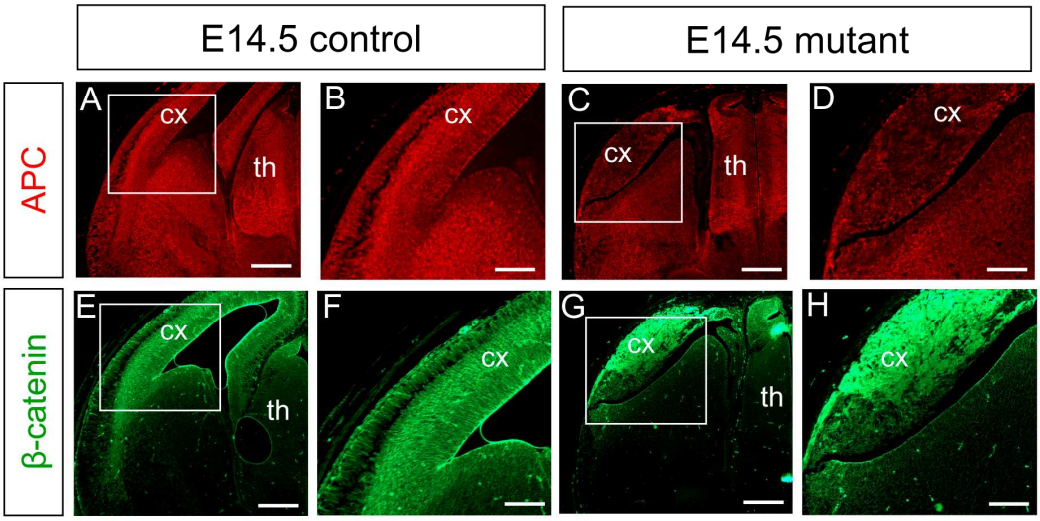

Figure 3. **β-catenin immunohistochemistry was performed to further confirm the inactivation of *Apc*. (C & D)** At E14.5, there was a large reduction of Apc throughout the mutant cortex compared to the control **(A & B). (E & F)** In the control cortex, β-catenin was highly expressed in the cortical plate and the intermediate zone, and weaker in the ventricular zone of the cortex at E14.5. **(G & H)** In the mutant, β-catenin staining was dramatically enhanced in the cortex. No increased β-catenin staining was observed in the ventral telencephalon or the thalamus, indicating that β-catenin was only up-regulated in the cortex, consistent with the above observation that Apc was only deleted in the cortex. Scale bars: (A, C, E, G) 200 μm; (B, D, F, H) 100 μm.

affected in the *Apc* mutant. Cortical projection neurons are differentiated post-mitotic cells which project out axons to connect to the subcortical areas. Here Map2 immunohistochemistry was carried out on paraffin sections of the embryos, as Map2 is a marker for post-mitotic neurons (Liu et al., 2005; Menezes and Luskin, 1994). In the dorsal telencephalon of the control, Map2 was detected through the whole extent of the cortical plate and the intermediate zone at E13.5 (Figure 4 A). One or two layers of cells in the most superficial area of the cortex were strongly labelled with Map2, while in the intermediate zone, the signal was weaker, and some tangentially distributed processes were observed (Figure 4 C).

In the mutant especially more medially, very few cortical cells were Map2 positive at E13.5, and in some regions of the cortical plate, no cells expressed Map2 at all (Figure 4 B). The very heavily labelled cells observed in the preplate (PPL) in the control cortex were not present in the mutant. In the lateral cortex, small groups of Map2 positive cells accumulated near the angle region (Figure 4 D, arrows). In some sections, axon-like fibers were observed around the angle region, descending from the lateral cortex (Figure 4 E). In the *Apc* mutant, the width of the cortex at the angle region was half that in the control embryos, and the ventricular zone was very near the pial surface (compare Figure 4 C & D).

Map2 fluorescence immunohistochemistry was also applied on E13.5 embryos. The control cortex showed a high expression of Map2 along the whole extent of the cortical plate and the intermediate zone, while the mutant cortex showed a dramatic reduction of Map2 positive cells (compare Figure 4 F and G). A small accumulation of Map2 cells as well as axonal-like fibers was observed again near the angle region of the mutant cortex, whereas in the control cortex a number of axons and cells were labelled in the cortical plate and the intermediate zone near the exit of the cortex (compare Figure 4 H and I).

The expression pattern of Map2 in the ventral telencephalon was similar between the mutant and the control, indicating that neuronal differentiation and maturation were not affected in the ventral telencephalon of the mutant (compare Figure 4 A & B, F

& G). Additionally, Map2 showed a similar expression pattern in the thalamus of both the control and the mutant, indicating that neuronal differentiation and maturation were not affected in the mutant thalamus either (compare Figure 4 J & K).

3.2.2 The decrease of Neurofilament staining in the mutant cortex

The large decrease of Map2 staining in the mutant cortex indicates a dramatic reduction of postmitotic neurons, including the projection neurons. The depletion of projection neurons in the mutant cortex would suggest a large reduction of cortical axonal outgrowth. To test whether cortical axonal development is disrupted in the mutant cortex, the expression of Neurofilament (NF) protein was examined. In E13.5 control embryos, cells in the whole tangential extent of the cortical plate expressed a high level of NF (Figure 5 A). Additionally, CTAs projecting from these neurons traversed within the intermediate zone toward the ventral telencephalon (Figure 5 C).

In the mutant, very few cells in the cortical plate were stained with NF (Figure 6 B). Very rarely, some axon-like fibers were detected at the most ventral site of the neocortex, around the angle region, which descended along the lateral edge of the cerebral cortex (Figure 5 D). These axon-like fibers coincide with the Map2 positive axon-like fibers in the lateral cortex (compare Figure 5 D and Figure 4 E). Thus Map2 and NF immunohistochemistry revealed a large reduction of projection neurons as well as cortical axons in the mutant cortex.

3.2.3 GAP43 expression pattern changes in the mutant cortex

GAP43 is another marker for axons. Expressed at high levels in neuronal growth cones during development, GAP43 is considered to play a key role in neurite formation (Aarts 1998; Benowitz 1997). In E13.5 control embryos, cells in the whole extent of the cortical plate were stained with GAP43 (Figure 6 A). The descending cortical axons and their growth cones were observed in the intermediate zone of the cortex (Figure 6 C).

Figure 4

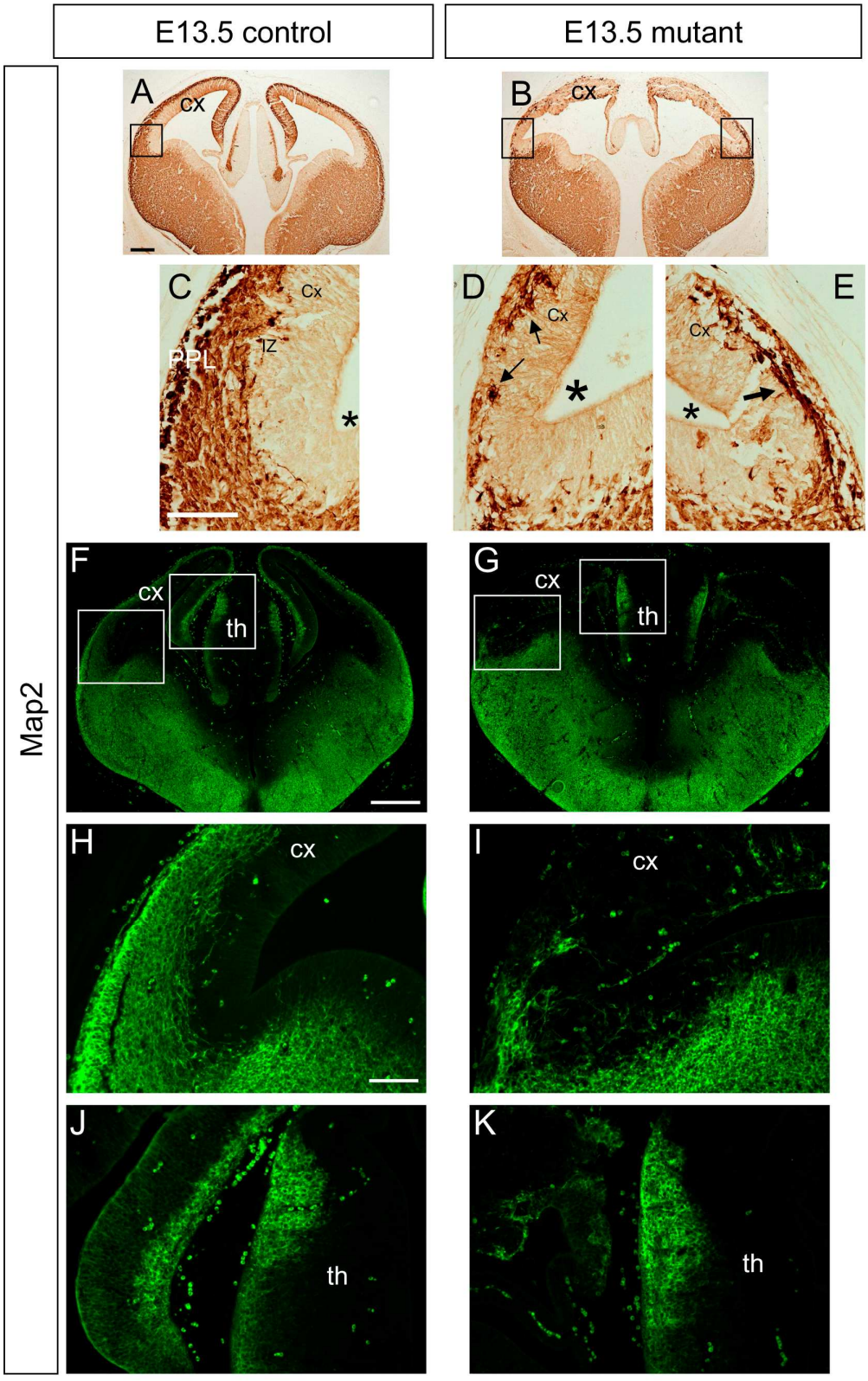
E13.5 control
E13.5 mutant
Map2
A
cx
B
cx
C
Cx
IZ
PPL
*
D
Cx
*
E
Cx
*
F
cx
th
G
cx
th
H
cx
I
cx
J
th
K
th

Figure 4. Map2 expressing cells were largely reduced in the cortex of *Apc* mutants. (A) In the dorsal telencephalon of the control, Map2 was detected through the whole extent of the cortical plate and the intermediate zone at E13.5. **(C)** One or two layers of cells in the most superficial area of the cortical plate were strongly labelled with Map2, while in the intermediate zone, the signal was weaker, and some tangentially distributed process were observed. **(B)** In the mutant, very few cells were Map2 positive, and the very heavily labelled cells observed in the preplate (PPL) in the control cortex were not present in the mutant. **(D)** In the lateral cortex, small groups of Map2 positive cells accumulated near the angle region. **(E)** In some sections, axon-like fibers were observed around the angle region, descending from the lateral cortex. In the *Apc* mutant, the width of the cortex at the angle region was half as that in the control embryos, and that ventricular zone was very near the pial surface (Compare C and D). **(C, D & E)** Higher power magnification of the areas boxed in A & B, respectively. **(F, G)** Map2 fluorescence immunohistochemistry on both control and mutant embryos. The results were similar to those with DAB staining techniques in (A-E). **(H, I, J, K)** Higher power magnification of the areas boxed in F & G, respectively. The expression patterns of Map2 in the ventral telencephalon and the thalamus were similar between the mutant and the control, indicating that neuronal differentiation and maturation were not affected in the ventral telencephalon and the thalamus of the mutant (Compare A & B, F & G, J & K). Scale bars: (A, B) 100 µm; (C, D, E) 100 µm; (F, G) 200 µm; (H, I, J, K) 50 µm.

Figure 5

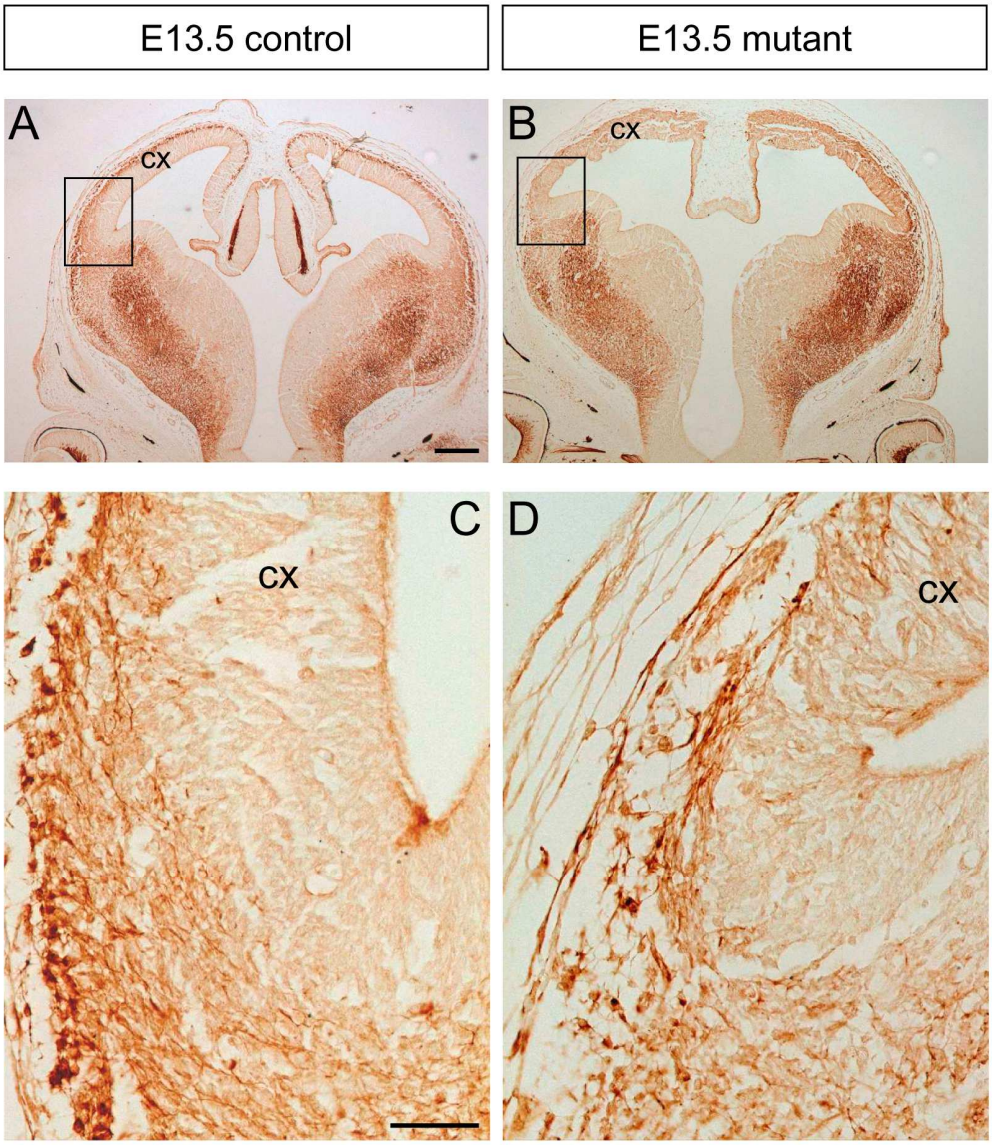

Figure 5. The decrease of Neurofilament staining in the *Apc* mutant cortex. (A) At E13.5 in the control embryos, cells in the whole tangential extent of the cortical plate expressed high level of neurofilament (NF). **(C)** CTAs projected from the NF positive neurons traversed within the intermediate zone toward the ventral telencephalon. **(B)** In the mutant, very few cells in the cortical plate were stained with NF. **(D)** Very rarely, some axon-like fibers were detected at the most ventral site of the neocortex, around the angle region, which descended along the lateral edge of the cerebral cortex. **(C, D)** Higher power magnification of the area boxed in A & B, respectively. Scale bars: (A, B) 200 µm; (C, D) 50 µm.

In the mutant, GAP43 positive cells and fibers were largely reduced in the cortical plate, indicating the disruption of cortical axonal development (Figure 6 B). However, many cells and processes in the ventricular zone were strongly stained with GAP43 (Figure 6 D). The reason for the upregulation of GAP43 in the cortical ventricular zone is unclear. It could be related to the cell proliferation defects in the *Apc* mutant cortex, since GAP43 is a component of the centrosome and has crucial functions in neurogenic cell divisions. It also implies that GAP43 expression might be directly or indirectly regulated by Apc. The expression of Apc in the ventricular zone might suppress the expression of GAP43 in normal mice. In the absence of Apc in the mutant cortex, GAP43 might be upregulated.

3.2.4 Normal CTAs and reciprocal projections from the LGE are absent in the *Apc* mutant

The large reduction of Map2 positive cells in the mutant cortex implies that mature neurons, including projection neurons, are dramatically reduced in the cortex and this would contribute to the defects of cortical axonal outgrowth. Indeed, NF immunohistochemistry showed a dramatic reduction of axonal fibers in the mutant cortex, suggesting that the outgrowth of CTAs is disrupted in the mutant. To further examine the defects of CTAs in the mutant, DiI crystals were placed into the rostral and caudal part of the lateral cortex in E13.5 embryos. By using this tracing technique, any fibers projecting from/to the lateral cortex will be anterogradely/retrogradely labelled.

In E13.5 control embryos, CTAs were projecting from neurons along the whole extent of the cortex (Figure 7 A). CTAs descended within the intermediate zone towards the ventral telencephalon (Figure 7 E, yellow arrows). These axons could be traced back to the strongly labelled neurons in the cortical plate and the subplate (Figure 7 G, a yellow arrow points to an axon whereas a yellow arrowhead points to a cell body). In the lateral cortex, radial glial processes were in an organized pattern, perpendicular to the descending cortical fibers (Figure 7 E). On reaching the exit

Figure 6

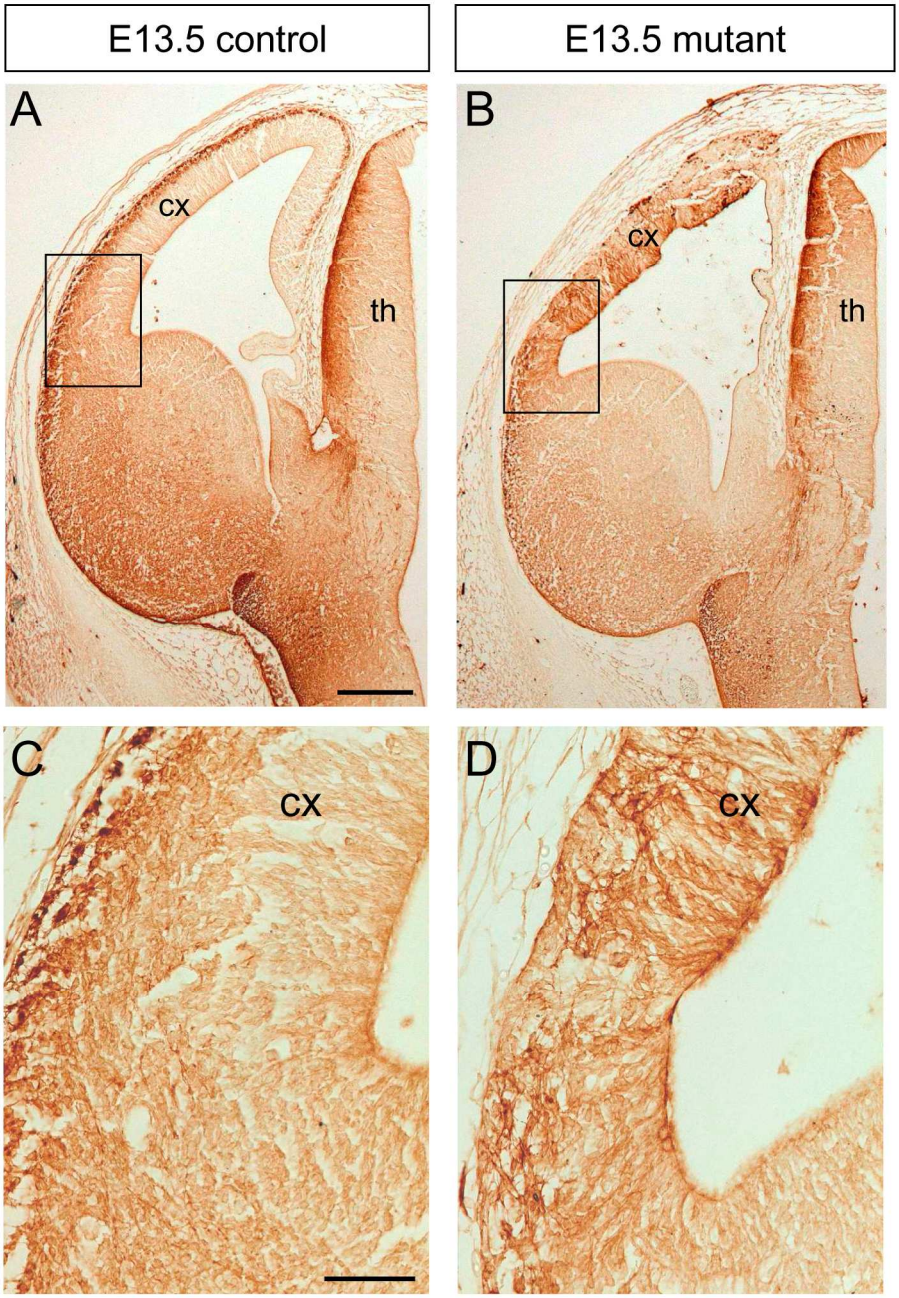

Figure 6. The change of GAP43 expression pattern in the *Apc* mutant cortex. (A) At E13.5 in the control embryos, cells in the whole extent of the cortical plate were stained with GAP43. **(C)** The descending cortical axons and their growth cones were observed in the intermediate zone of the cortex. **(B)** In the mutant, GAP43 positive cells were largely reduced in the cortical plate. **(D)** Many cells and processes in the ventricular zone were strongly stained with GAP43. **(C, D)** Higher power magnification of the area boxed in A & B, respectively. Scale bars: (A, B) 200 µm; (C, D) 50 µm.

from the cortex, CTAs crossed the intermediate zone and turned into the mantle region of the LGE. Most of them were tipped with large and bifurcated growth cones (Figure 7 I, yellow arrow). In the LGE, CTAs were defasciculated, navigating among some retrogradely labelled cells (Figure 7 I, yellow arrowhead). Occasionally, fibers were observed projecting from these round and large cell bodies.

However, CTAs were rarely detected in the lateral cortex of the mutant brain at E13.5, confirming the disruption of CTA outgrowth in the mutant cortex (Figure 7 C & F). In some sections, I observed some radial glia cells in both the medial and the lateral cortex of the mutant, which seem more normal, similar to the control (compare Figure 7 F & H to E & G). However, CTAs were not observed in these areas. Very rarely, some fibers were seen in the medial cortex: these underwent several directional changes (Figure 7 J). These fibers may originate from the cortical projection neurons that have escaped the cre-mediated inactivation of the *Apc* gene or perhaps these neurons are able to survive and project axons without the presence of *Apc*. As mentioned above, cell bodies were often observed in the mantle region of the LGE in the control brain, distributed among CTAs. However, these retrogradely labelled cell bodies were hardly detected in the corresponding regions of the mutant, implying that reciprocal projections from the LGE to the cortex are absent or largely reduced in the mutant (Figure 7 C). In the ventral telencephalon, a group of cells and their fiber-like connections at the lateral edge were stained with DiI (Figure 7 C, yellow arrow), but I did not observe any axons projecting from these cells towards the cortex. Therefore, these cells were probably located in the ventral telencephalon and accidentally picked up DiI from the placement site near the lateral-ventral cortex. This is a problem with DiI labeling techniques. The brain of the mutant is somehow different from the control, which is smaller and has a thinner cortex. It is more difficult to predict the location in the mutant lateral cortex where the DiI should be placed. Here in this particular mutant some ventral telencephalic cells were labelled with DiI, in addition to the radial glial processes in the cortex.

Figure 7

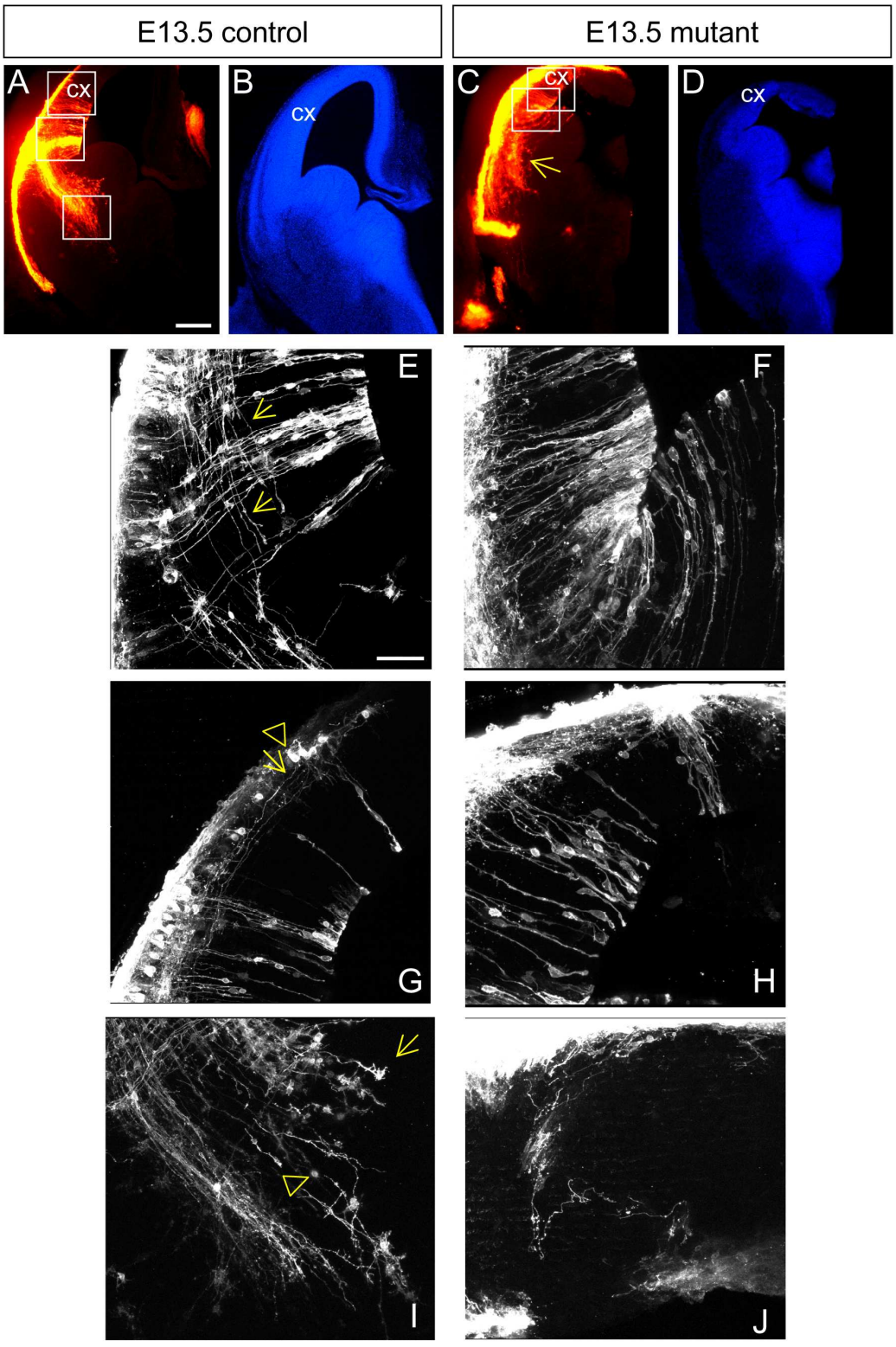

Figure 7. Normal CTAs and LGE projections were absent in the *Apc* mutant. DiI placements in the lateral cortex of the control **(A)** and the mutant **(C)**. **(B and D)** The same sections as observed in A and C, respectively, stained with Hoechst. **(E, G, I)** Higher magnification of the areas boxed in A. **(F, H, J)** Higher magnification of the areas boxed in C. **(E)** In the control**,** CTAs descended within the intermediate zone and left the neocotex at the angle region (yellow arrows). Radial glial processes went across the ventricular zone and the pial surface, with cell bodies along them. **(F)** Radial glial processes were present in the lateral cortex of the mutant, but CTAs were not detected. **(G)** In the control, cortical axons could be traced back to the strongly labelled neurons in the cortical plate and the subplate (a yellow arrow points to an axon whereas a yellow arrowhead points to a cell body). **(H)** In the mutant, projection neurons and CTAs were not observed in the medial cortex. **(I)** In the control, lots of cortical axons turned into the mantle zone of the LGE, some of which were tipped with large and bifurcated growth cones (yellow arrow). CTAs were defasciculated in the LGE, navigating along some retrogradely labelled cells (yellow arrowhead). These retrogragely labelled cells were not observed in the mutant. The yellow arrow in (C) points to the unspecific DiI labelling of some ventral telencephalic cells. **(J)** In the medial cortex of the mutant, some fibers were observed, turning in several directions. Scale bars: (A-D) 200 μm; (E-J) 50 μm.

In order to not mis-interpret the DiI results in the mutant, another DiI placement strategy was used where DiI crystals were placed in the medial part of the cortex at E13.5. In the control, a great number of cortical axons descended within the intermediate zone and made a sharp turn at the exit from the cortex and turned into the mantle region of the ventral telencephalon (Figure 8 A & E, star), which were not observed in the mutant (Figure 8 C & F, star). However, an aberrant axonal tract descended from the mutant cortex towards the lateral part of the ventral telencephalon (Figure 8 F, white arrow), which was not observed in the control (Figure 8 E). This aberrant axonal tract was very tiny and not often detected, suggesting that only very few axons were projecting from the cortex. Also, the tiny cortical axonal tract labelled by DiI coincides with the axon-like fibers detected with Map2 and NF antibodies (Figure 4 E & 5D). Thus, DiI placements in the cortex showed that normal CTAs were absent in the mutant.

Figure 9 illustrates the DiI placement sites and the axons that are labelled in the control and the mutant at E13.5 (Figure 9). In the control, DiI crystals placed in the lateral cortex most likely label the pioneer axons projecting from the early born lateral cortical neurons (Figure 9 A). These axons are travelling in the mantle region of the LGE in the ventral telencephalon at E13.5. In the mutant, DiI crystals placed in the lateral cortex do not label pioneer axons that are navigating through the ventral telencephalon (Figure 9 B). DiI crystals placed in the medial cortex of the control embryos label axons that are descending towards the exit of the cortex and just turn into the ventral telencephalon at E13.5 (Figure 9 C). DiI crystals placed in the medial cortex of the mutant embryos label a small amount of axons that are descending towards the lateral part of the ventral telencephalon rather than turning into the mantle region of the ventral telencephalon (Figure 9 D).

In order to identify whether there were any CTAs descending from the mutant cortex and growing into the ventral telencephalon at later ages, fluorescent dyes were placed in both control and mutant cortex at E16.5 and E18.5. In the control, a large bundle of DiI labelled axons was travelling through the ventral telencephalon at

Figure 8

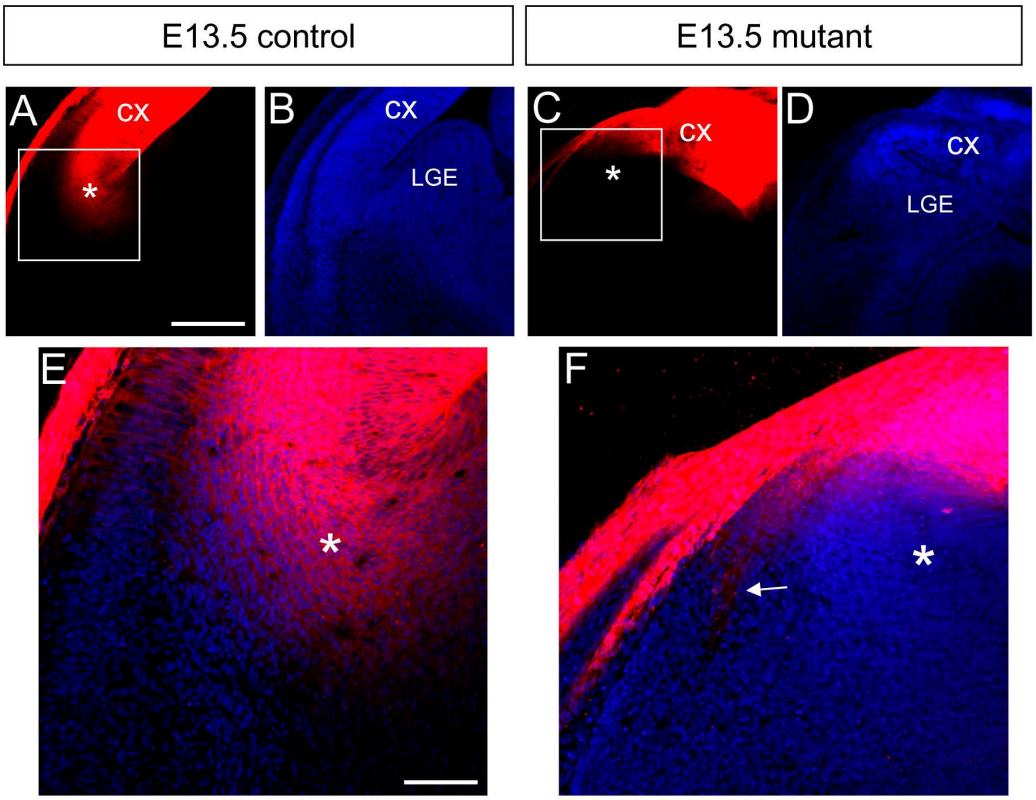

Figure 8. Defects of CTAs projecting from the medial cortex of the *Apc* mutant. DiI crystals were placed in the medial cortex in both control **(A)** and the mutant **(C)**. **(B & D)** The same sections as observed in A & C, respectively, stained with TO-PRO 3. **(A & E)** In the control, a great number of cortical axons descended within the intermediate zone and made a sharp turn at the exit from the cortex and turned into the mantle region of the ventral telencephalon (star), which were not observed in the mutant (**C & F**, star). **(F)** An aberrant axonal tract descended from the mutant cortex towards the lateral part of the ventral telencephalon (white arrow), which was not observed in the control (E). This aberrant axonal tract was very tiny and not often detected, suggesting that only very few axons were projecting from the cortex. Thus, DiI placements in the cortex showed that normal CTAs were absent in the mutant. Scale bars: (A-D) 200 μm; (E, F) 50 μm.

Figure 9

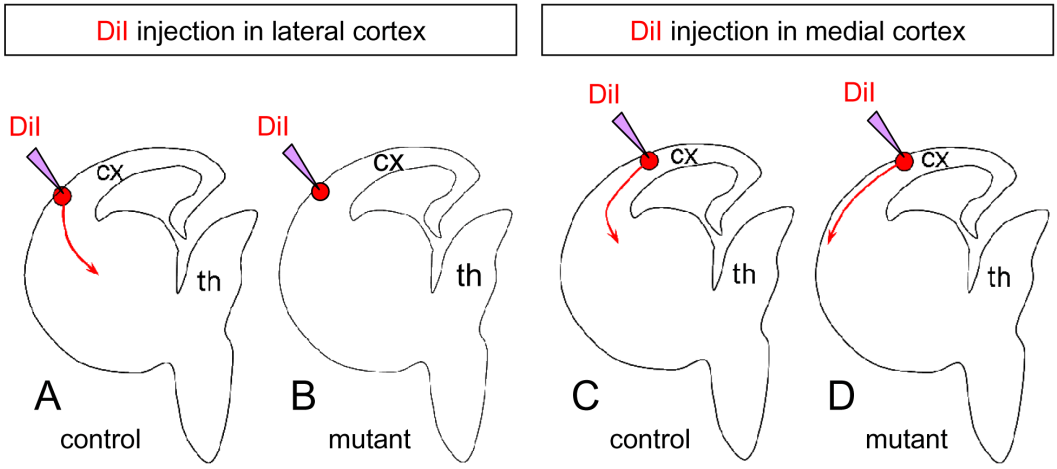

Figure 9. A diagram illustrating the DiI placement sites and the axons that are labelled. (A) In the control, DiI crystals placed in the lateral cortex most likely label the pioneer axons projecting from the early born lateral cortical neurons. These axons are travelling in the mantle region of the LGE in the ventral telencephalon at E13.5. **(B)** In the mutant, DiI crystals placed in the lateral cortex do not label pioneer axons that are navigating through the ventral telencephalon. **(C)** In the control, DiI crystals placed in the medial cortex label axons that are descending towards the exit of the cortex and just turn into the ventral telencephalon at E13.5. **(D)** In the mutant, DiI crystals placed in the medial cortex label a small amount of axons that are descending towards the lateral part of the ventral telencephalon rather than turning into the mantle region of the ventral telencephalon. cx – cortex. th – thalamus.

E16.5 (Figure 10 A & C). However, normal cortical axons were not observed in the mutant cortex (Figure 10 B & D). In some sections, one or two axons were seen descending from the mutant cortex towards the exit of the cortex, bearing a growth cone at the tip of the axon (Figure 10 D, arrow). At E18.5, DiA crystals placed in the control cortex anterogradely labelled axons projecting from the cortex to the thalamus and retrogradely labelled axons projecting from the thalamus to the cortex (Figure 11 A). Cell bodies were observed in the thalamus of the control (Figure 11 A, star) but not in the mutant (Figure 11 B, star**)**. Normal cortical axons were not observed in the mutant cortex (Figure 11 C).

3.3 TCAs fail to enter the cerebral cortex in the *Apc* mutant

In the Handshake hypothesis, CTAs are proposed to be guiding TCAs into the cortex (Allendoerfer and Shatz, 1994; Molnar et al., 1998b; Molnar and Blakemore, 1995). Therefore, it is of interest to determine whether TCAs navigating into the mutant cortex follow a normal route, where normal CTAs are not present. At E15.5, DiI crystal placements in the thalamus of the control brain traced a large bundle of axons that were projecting from the thalamus and navigating through the intermediate zone of the cortex (Figure 12 A). In the mutant, thick bundles of axons were observed traversing the ventral telencephalon but they stopped before entering the cortex, where they seemed to change direction and turn ventrally in the ventral telencephalon (Figure 12 B & C). In order to identify whether there were any TCAs reaching the cerebral cortex of the *Apc* mutant at later ages, DiI crystals were placed into the thalamus of both control and mutant embryos at E18.5. In the control, a large bundle of DiI labelled axons was identified traversing into the cortex at E18.5 (Figure 12 D). Cell bodies were often observed in the control cortex at this age (Figure 12 G, white arrows). In the mutant brain, a vast majority of TCAs turned ventrally in the ventral telencephalon but a small number of axons did enter into the cortex (Figure 12 E & H). Cell bodies were rarely observed in the mutant cortex (Figure 12 H, white arrow), while in the control cell bodies were more frequently

Figure 10

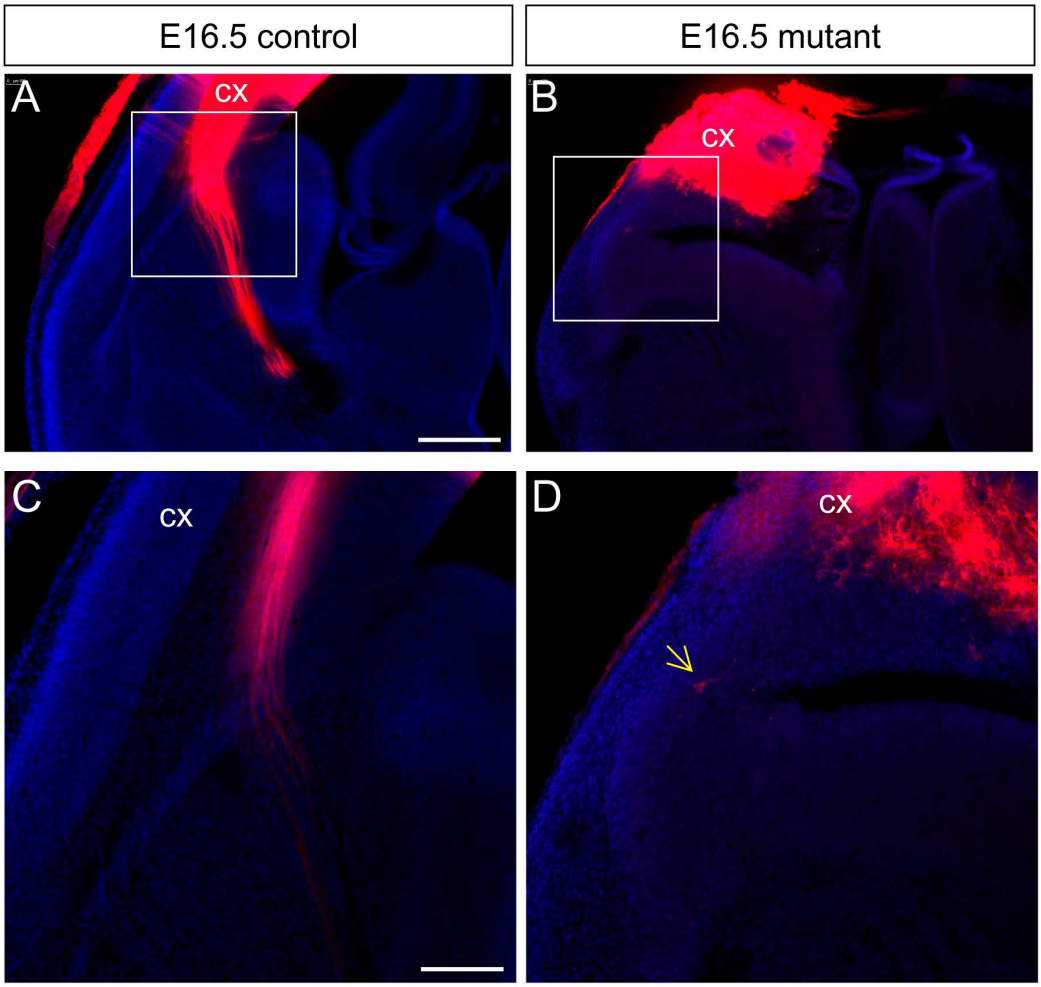

Figure 10. DiI crystals placed in the cortex at E16.5 revealed CTAs defects in *Apc* mutants at later ages. (A, C) In the control, a large bundle of axons was travelling through the ventral telencephalon. **(B, D)** Normal cortical axons were not observed in the mutant cortex. Very rarely, one or two axons were seen descending from the cortex towards the exit of the cortex, bearing a growth cone at the tip of the axon (D, arrow). **(C & D)** Higher magnification of the area boxed in (A & B), respectively. Scale bars: (A, B) 500 µm; (C, D) 200 µm.

Figure 11

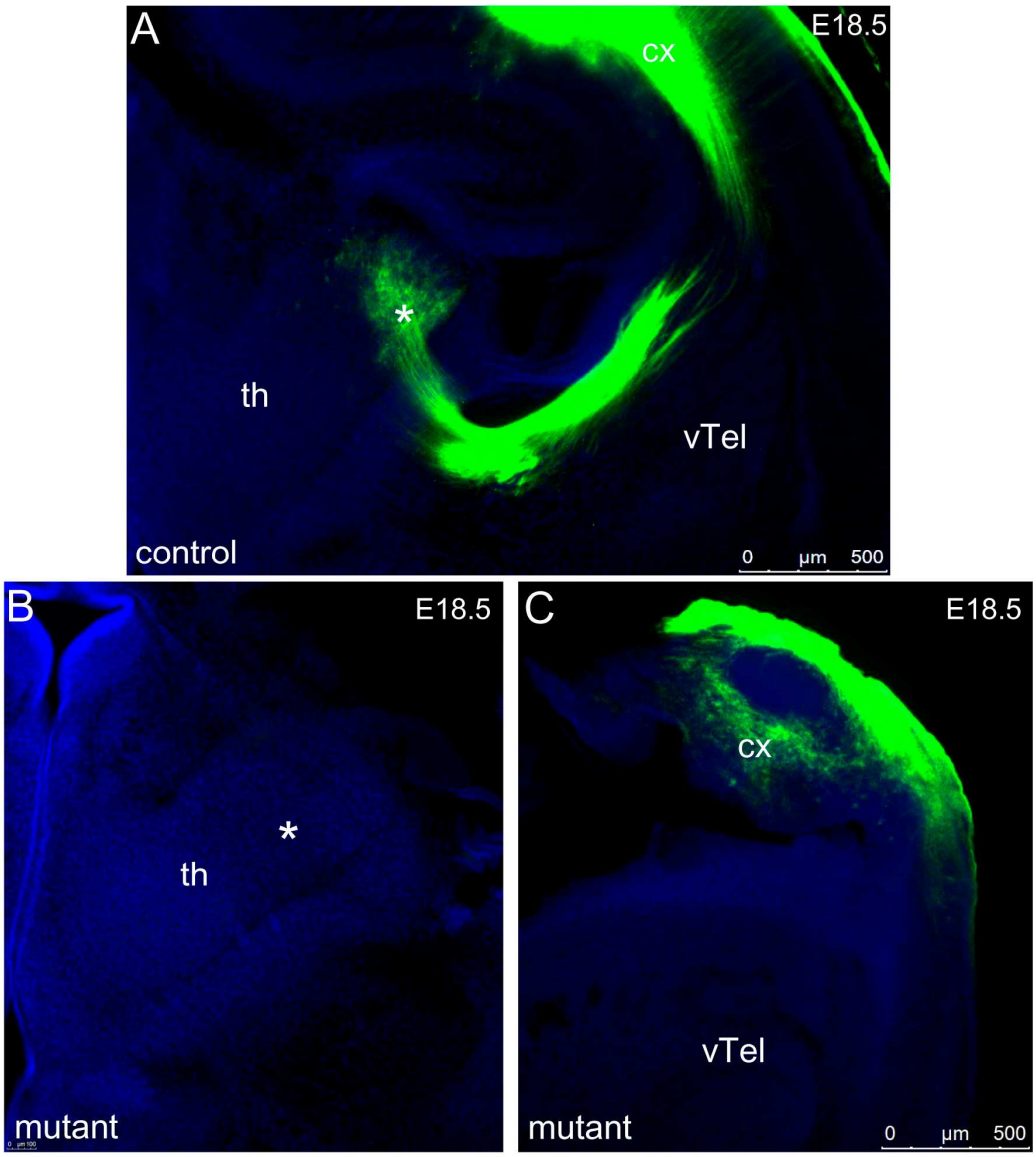

Figure 11. DiA crystals placed in the cortex at E18.5 revealed CTAs defects in *Apc* mutant at later ages. (A) In the control, green dyes placed in the cortex anterogradely labelled axons projecting from the cortex to the thalamus and retrogradely labelled axons projecting from the thalamus to the cortex. Cell bodies were observed in the thalamus of the control (A, star) but not in the mutant **(B**, star**)**. **(C)** Normal cortical axons were not observed in the mutant cortex. Scale bars: (A-C) 500 µm.

Figure 12

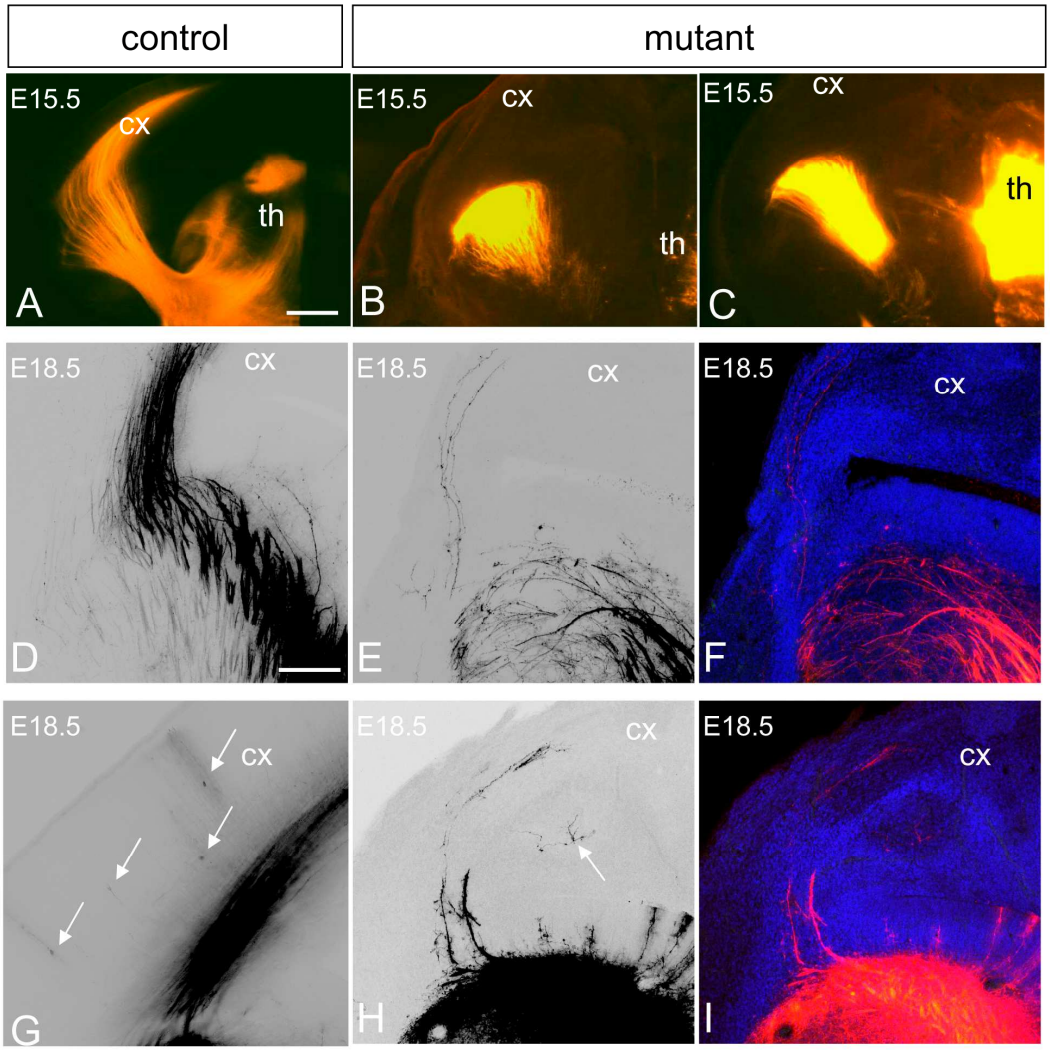

Figure 12. Axon tracing experiments showed that most TCAs failed to reach the cerebral cortex in the *Apc* mutant. (A) At E15.5, DiI crystal placements in the thalamus of the control brain traced a large bundle of axons that were projecting from the thalamus and navigating through the intermediate zone of the cortex. **(B, C)** In the mutant, thick bundles of axons were observed traversing the ventral telencephalon but they stopped before entering the cortex, where they seemed to change direction and turn ventrally in the ventral telencephalon. **(D, G)** At E18.5, DiI placements in the thalamus of the control brain labelled a large bundle of axons which was traversing into the cortex. Cell bodies were often observed in the control cortex at this age (G, white arrows). **(E, H)** In the mutant, a vast majority of TCAs turned ventrally in the ventral telencephalon but a small number of axons did enter into the cortex. Cell bodies were rarely observed in the mutant cortex (H, white arrow). **(F & I)** TOPRO3 staining for the sections in (E & H). cx – cortex, th – thalamus. Scale bars: (A-C) 200 µm; (D-I) 200 µm.

observed (Figure 12 G, white arrows). These axon tracing experiments showed that the vast majority of TCAs failed to reach the cerebral cortex of the mutant embryos.

Topro 3 nuclear staining methods were used in conjugation with dye tract tracing techniques to reveal the anatomical location where TCA defects occur. At E18.5 in the control, a great number of axons showed a distinct about 90 degree turn as they crossed the region with high density of cells between the pallium and the subpallium (Figure 13 A & B, arrow). This high cell density zone is likely to be comprised of the lateral cortical stream (LCS) migrating PSPB neurons which originate from the ventricular progenitors at the PSPB and migrate towards the ventral part of the basal telencephalon (Carney et al., 2006). In the mutant, the region with high cell density was still present in the corresponding area compared to the control, but there were hardly any axons crossing this region from or towards the cortex (Figure 13 C, arrow). Very rarely in some sections of the mutant, one or two axons were observed crossing the high cell density region and turning into the cortex in a 90 degree angle (Figure 13 D-H). In some other sections of the mutant, a lot of axons traversing in the ventral telencephalon were seen running down along the medial side of the high cell density zone towards the basal ventral telencephalon, and a few axons managed to cross the high cell density region from the ventral-lateral edge of the basal telencephalon and ascend towards the cortex (Figure 13 I-K). However, most axons were turning ventrally in the ventral telencephalon without crossing the high cell density zone and entering the cortex.

3.4 TCA defects occur near the PSPB region

DiI tracing experiments showed that most TCAs failed to reach the cerebral cortex of the mutant embryos. Topro 3 nuclei staining further showed that the anatomical location for TCA defects was at the high cell density region between the pallium and the subpallium, which is likely to consist of LCS migrating cells. Since the LCS migrating cells are derived from the PSPB (Carney et al., 2006; Carney et al., 2009), and the PSPB has been suggested to be a territory that TCAs have to cross before

Figure 13

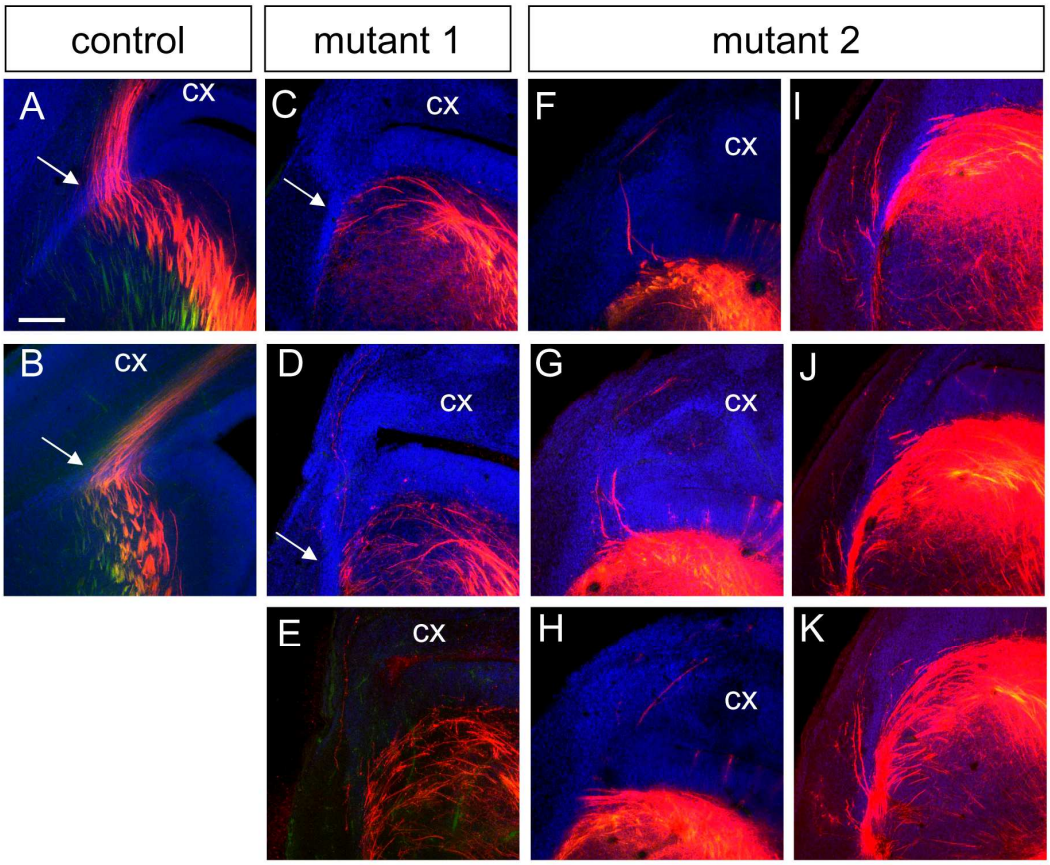

Figure 13. Dyes placed in the thalamus at E18.5 revealed TCAs defects in *Apc* mutant at later stages. Nuclei were counter stained with topro 3. **(A, B)** In the control, a great number of axons showed a distinct about 90 degree turn as they crossed the region with high density of cells between the pallium and the subpallium (arrow). **(C-K)** Showing two mutant forebrain sections in a rostral to caudal axis. The region with high cell density was still present in the corresponding area compared to the control, but there were hardly any axons crossing this region from or towards the cortex (C, arrow). Very rarely in some sections of the mutant, one or two axons were observed crossing the high cell density region and turning into the cortex in a 90 degree angle (D-H). In some other sections of the mutant, thick bundles of axons traversing in the ventral telencephalon were seen running down along the medial side of the high cell density zone towards the basal ventral telencephalon, and a few axons managed to cross the high cell density region from the ventral-lateral edge of the basal telencephalon and ascend towards the cortex (I-K). However, most axons were turning ventrally in the ventral telencephalon without crossing the high cell density zone and entering the cortex. Scale bars: (A-K) 200 µm.

they reach the cortex (Molnar et al., 1998a; Molnar and Butler, 2002; Molnar and Cordery, 1999), it is of interest to examine the location of the TCA defects in the mutant in relation to the place where the PSPB is located.

During the early stage of brain development, a distinct RC2 positive radial glial processes is observed extending from the PSPB to the ventrolateral telencephalic pial surface (Carney et al., 2006; Carney et al., 2009; Chapouton et al., 2001). Here double immunofluorescence for RC2 and the axonal marker L1 was performed on brain sections from both control and mutant embryos. At E15.5 in controls, a great number of axons passed the PSPB and navigated within the intermediate zone of the cerebral cortex (Figure 14 A & C). In the mutant, TCAs traversed through the ventral telencephalon but stopped proximal to the PSPB, indicating that these fibers failed to cross the PSPB and to reach the cortex at E15.5 (Figure 14 B & D). Although no descending axons were observed crossing the PSPB in the mutant, a high level of L1 staining was detected in the mutant cortex (Figure 14 B). To further investigate the L1 labelled tissue in the mutant cortex, high power magnification images were taken at the cortical region. While in the control cortex, L1 clearly labelled axonal fibers navigating within the intermediate zone, in the mutant cortex L1 labelled clusters of cells and tissue, which did not mimic normal axons (Figure 14, compare E and F). In addition, RC2 positive radial glia in the control cortex could be clearly distinguished from each other, extending from the ventricular surface towards the pial surface perpendicular to L1 positive axonal fibers (Figure 14 E). In the mutant, most RC2 labelled radial glia extended from the ventricular surface but lost their connection with the pial surface. They were also mixed together and bent in different directions in the ventricular zone (Figure 14 F).

Next, RC2 & L1 double immunohistochemistry was performed on brain sections of E18.5 embryos in order to further examine the location of TCA defects in the mutant verses the PSPB region at a later age. In the control embryos, a large number of L1 positive axons were identified within the intermediate zone of the cerebral cortex (Figure 15 A & B). A thick bundle of L1 positive axons was also observed close to

the lateral side of the RC2 positive radial glial fascicles at the PSPB (Figure 15 A & B). In the ventral telencephalon, L1 positive axons fasciculated into small bundles and spread in a fan-shape before crossing the RC2 positive radial glia fascicles at the PSPB (Figure 15 A & B). In the mutant, a large number of L1 positive axons were observed in the ventral telencephalon (Figure 15 C & D). Bundles of fasciculated axons were heading towards the RC2 positive radial glia fascicles at the PSPB, but instead of spreading in a fan-shape and crossing the PSPB, the L1 positive axons in the mutant made a sharp turn ventrally towards the basal telencephalon once they reached the PSPB (Figure 15 C & D). These L1 positive axons were navigating ventrally along the RC2 positive radial glia at the PSPB and closely apposed to the RC2 stained radial glial processes (Figure 15 C & D).

These data showed that TCA guidance defects occur before TCAs reach the anatomical defects in the cortex, suggesting that TCA defects are not due to the anatomical structural change of the cortex, but may be due to the change of some guidance factors from the cortex. Moreover, these results reveal the PSPB as a critical choice point for TCAs and indicate that the cortex is very important for guiding TCAs into their final targets. The *Apc* mutant cortex lacks these guidance cues for TCAs.

3.5 Loss of cerebral cortical Apc does not alter TCA topography

The results above showed that TCAs fail to get through the PSPB and enter the cortex following the loss of Apc in the cortex. To determine whether the topography of TCAs is altered in the mutant, I applied DiI and DiA placements in the rostral and caudal part of the thalamus, respectively, to trace a subpopulation of thalamic axons. In both the control and the mutant embryos, DiI-labelled TCAs from rostral thalamus navigated dorsally while DiA-labelled caudal TCAs traversed ventrally in the ventral telencephalon at E14.5 (Figure 16 A-I). Thus the topography of TCAs seemed to be similar between the control and the mutant, implying that TCA topography during early development is not affected by the loss of Apc in the cortex.

Figure 14

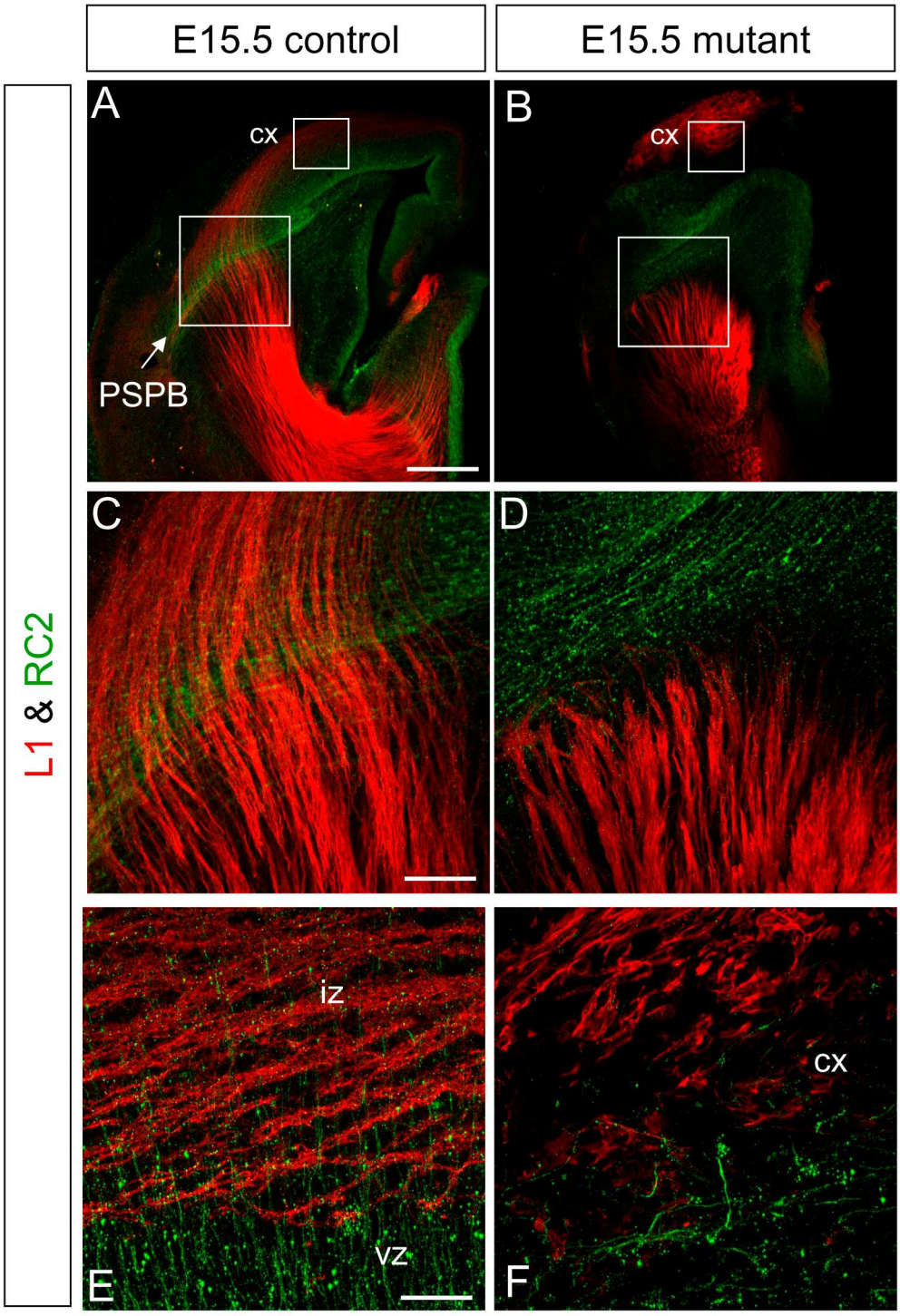

Figure 14. TCA defects occurred near the PSPB. (A, C) At E15.5, a great number of axons passed the PSPB and navigated within the intermediate zone (iz) of the cerebral cortex in the control mice. **(B, D)** In the mutant, TCAs traversed through the ventral telencephalon but stopped proximal to the PSPB, indicating that these fibers failed to cross the PSPB and reach the cortex at E15.5. **(C-F)** Higher magnification of the areas boxed in A & B, respectively. In the control cortex L1 clearly labelled axonal fibers navigating within the intermediate zone, while in the mutant cortex L1 labelled clusters of cells and tissue that did not mimic normal axons (Compare E and F). In addition, RC2 positive radial glia in the control cortex could be clearly distinguished from each other, extending from the ventricular surface towards the pial surface perpendicular to L1 positive axonal fibers (E). In the mutant, most RC2 labelled radial glia extended from the ventricular surface but lost their connection with the pial surface, and they were mixed together and bent in different directions in the ventricular zone (F). Scale bars: (A, B) 200 μm; (C, D) 50 μm; (E, F) 25 μm.

Figure 15

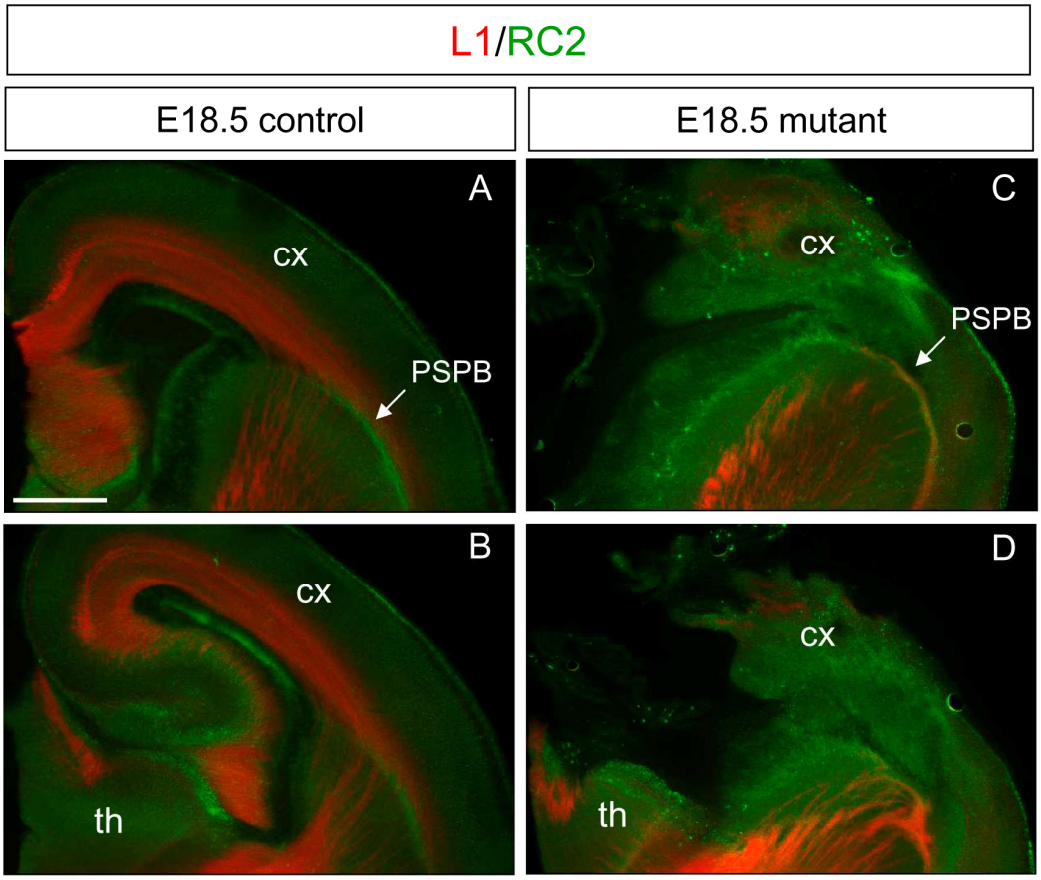

Figure 15. TCAs in the *Apc* mutants failed to cross the PSPB at E18.5. (A,B) In control embryos, a large number of L1 positive axons were identified within the intermediate zone of the cerebral cortex. A thick bundle of L1 positive axons was also observed close to the lateral side of the RC2 positive radial glial fascicles at the PSPB. In the ventral telencephalon, L1 positive axons fasciculated into small bundles and spread in a fan-shape before crossing the RC2 positive radial glia fascicles at the PSPB. **(C,D)** In mutant embryos, a large number of L1 positive axons were traversing in the ventral telencephalon. Bundles of fasciculated axons were heading towards the RC2 positive radial glia fascicles at the PSPB, but instead of spreading in a fan-shape and crossing the PSPB, the L1 positive axons in the mutant made a sharp turn ventrally towards the basal telencephalon once they reached the PSPB. These L1 positive axons were navigating ventrally along the RC2 positive radial glia at the PSPB and closely apposed to the RC2 stained radial glia processes. Scale bars: 500 μm.

Figure 16

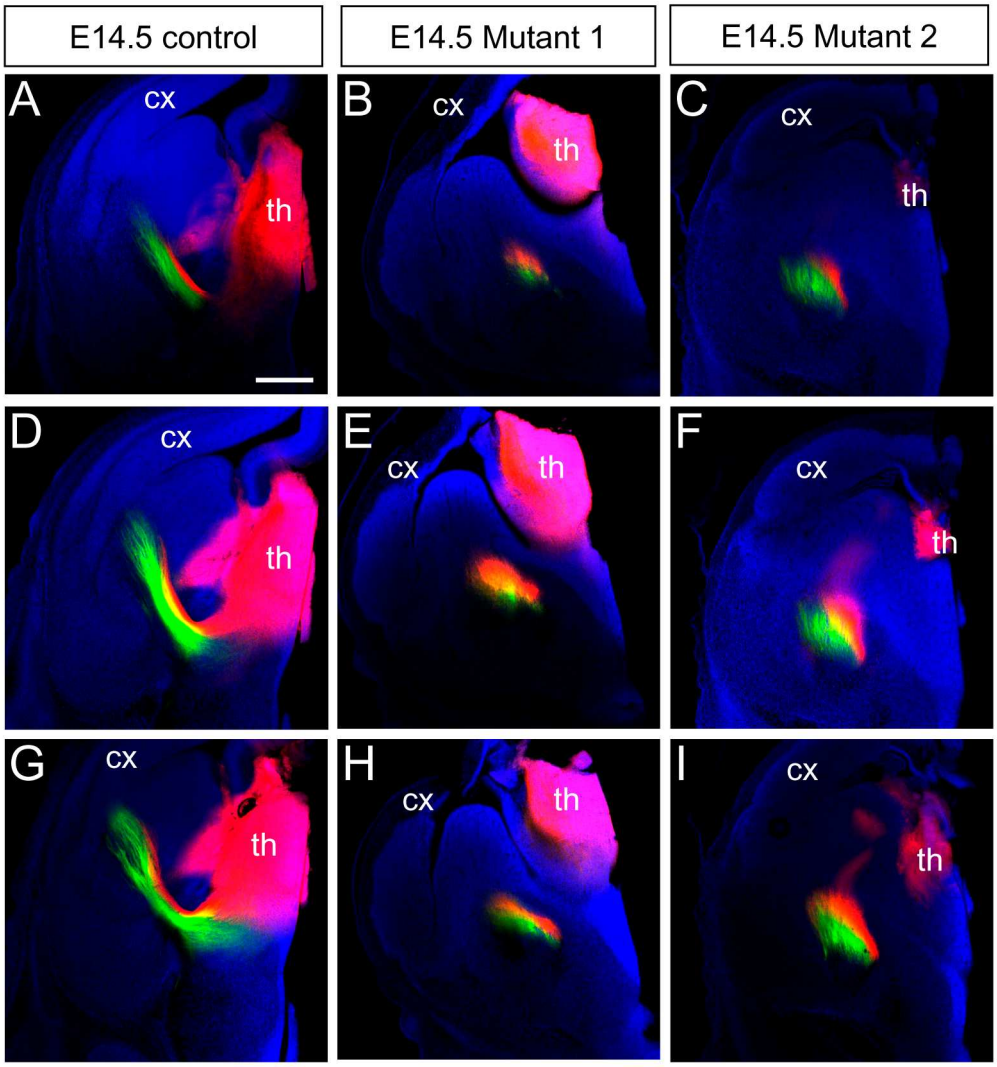

Figure 16. Loss of cerebral cortical Apc does not alter TCA topography. The topography of TCAs seems similar between the control **(A, D & G)** and mutant 1 **(B, E & H)** and mutant 2 **(C, F & I)** at E14.5. DiI was placed in rostral thalamus whereas DiA was placed in caudal thalamus. In both the control and the mutant embryos, DiI labelled TCAs (red) were navigating more dorsally compared to the DiA labelled TCAs (green) in the ventral telencephalon. Cx – cortex, th – thalamus. Scale bars: 200 μm.

3.6 The cellular and molecular patterns of the PSPB are similar between the control and the mutant

The above results showed that TCAs in the *Apc* mutant failed to cross the PSPB and enter the cerebral cortex. Since Emx1 is not expressed in the ventral pallium (VP), the deletion of *Apc* by Emx1-Cre is not expected to occur in the PSPB region. Thus it is less likely that the failure of TCAs to reach the cerebral cortex in the mutant is due to the defects of the PSPB. In order to verify that the characteristics of the PSPB in the *Apc* mutant are not changed, I examined further the cellular and molecular patterns of the PSPB.

At E13.5, the PSPB in the control embryos was characterized by the fascicles of RC2 positive radial glial processes (Figure 17 A, white bracket). In the mutant embryos, the fascicles of RC2 positive radial glial processes were still present at the PSPB (Figure 17 B, white bracket). Next, I compared the pattern of the radial glia processes in the cerebral cortex between the control and the mutant. In the control embryos, radial glial processes were present throughout the cortex at E13.5, extending from the ventricular surface of the ventricular zone to the pial surface, perpendicular to the pial edge of the cortex (Figure 17 A, C & E). Individual radial glia were parallel to each other and were clearly distinguishable from each other. In the mutant, RC2 staining was prominent in the ventricular zone but was fainter in the cortical plate at E13.5 (Figure 17 B, D & F). Individual radial glia were mixed together and harder to distinguish individually. Some of them bent in different directions and did not show a perpendicular pattern towards the pial surface. Moreover, most radial glia processes initiated from the ventricular surface of the ventricular zone but stopped near the cortical plate area and failed to connect to the pial surface of the cortex (Figure 17 D & F). Taken together, the observation that the radial glial processes lost their typical features in the mutant cerebral cortex but not at the PSPB indicates that the radial glial cell defects caused by *Apc* deletion were restricted to the cortex, but were not at the PSPB.

Gsh2 is a homeobox containing gene that expresses in the ventricular zone of the LGE, and the expression stops at the boundary between the pallium and subpallium (Carney et al. 2009). Therefore Gsh2 would be another useful marker to define the PSPB, other than the RC2 positive radial glial fascicles. Here my data showed that the pattern of Gsh2 expression at the PSPB was similar between the control and mutant embryos at E13.5 (Figure 17 A & B, white arrow indicating the lateral edge of the LGE). Therefore, RC2 and Gsh2 double immunofluorescence implies that the cellular and molecular pattern of the PSPB is not affected by the loss of Apc in the dorsal telencephalon.

3.7 Intermediate zone (IZ) cells are missing or largely reduced in the lateral cortex of the *Apc* mutant

The above results demonstrate that most TCAs fail to cross the PSPB and reach the cortex when *Apc* is inactivated in the cortex. The PSPB is not affected in the mutant and the expression pattern of genes that defines the PSPB (i.e. Gsh2) is similar between the control and the mutant. Normal CTAs are absent from the cortex. Since CTAs and TCAs navigate within the intermediate zone in the cortex, and that CTAs have been suggested to have close contact with calbindin-positive intermediate zone (IZ) cells and regulate the tangential migration of these IZ cells (Metin et al., 2000), it is of interest to determine whether the trajectory of migrating cortical interneurons is affected in the *Apc* mutant. From Calbindin immunostaining, I observed two subpopulations of calbindin-positive cells migrating into the cortex from the LGE (Figure 18 A). One of them advanced within the IZ while the other was at the edge of lateral cortex (Figure 18 B, arrows). They sent long processes towards the cortex.

Both populations of calbindin-expressing cells were not detected in the lateral cortex of the *Apc* mutant (Figure 18 D). Nevertheless, in some sections of the mutant, calbindin cells appeared as if they were attempting to enter the neocortex, with long process (Figure 18 E). The observation of calbindin positive cells attempting to enter the cortex at the lateral edge of the mutant cortex coincide with the detection of

Figure 17

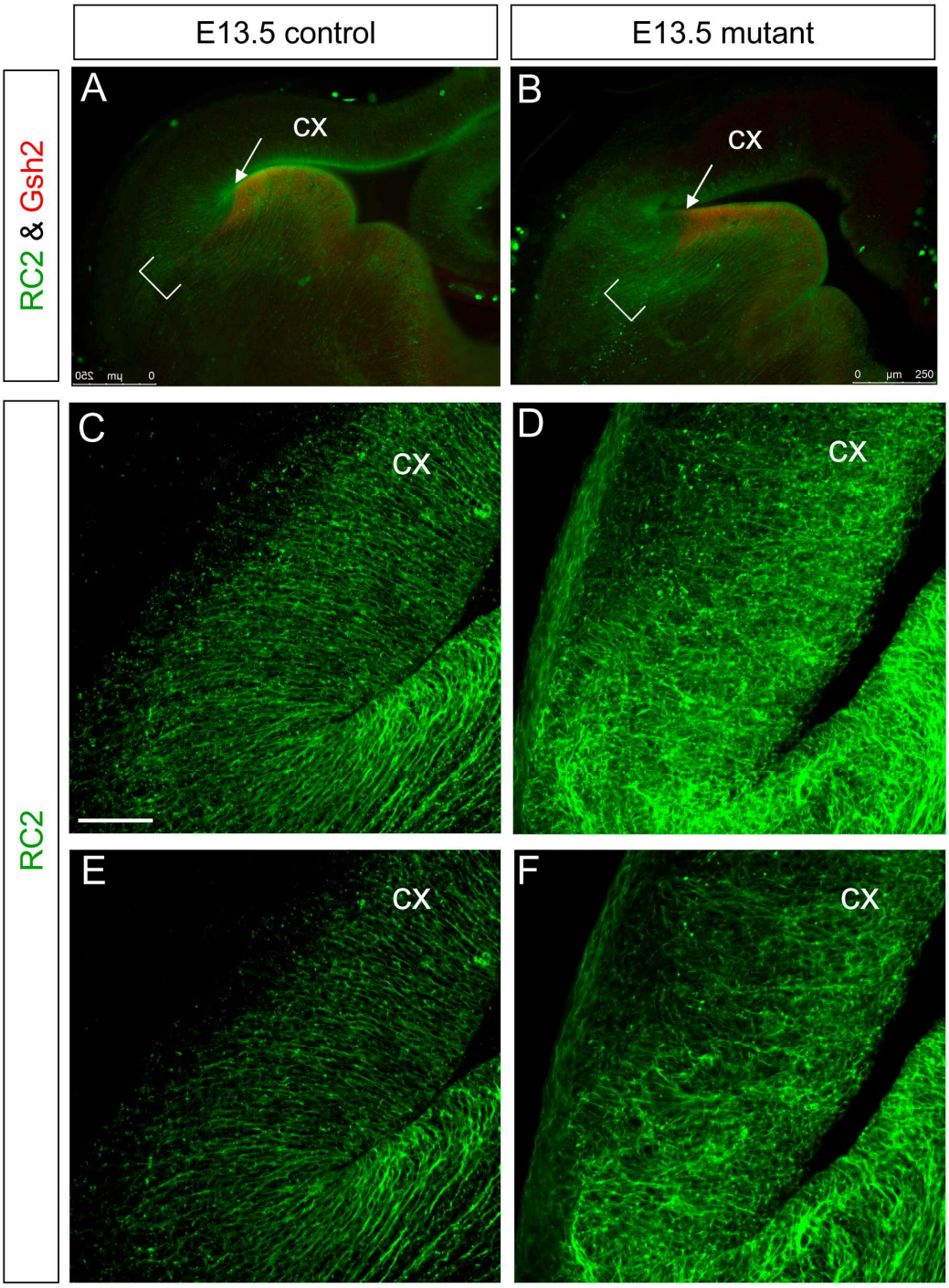
E13.5 control
E13.5 mutant
RC2 & Gsh2
RC2
A
B
C
D
E
F
cx
cx
cx
cx
cx
cx
0 µm 250

Figure 17. Disruption of RC2 positive radial glial cells in the *Apc* mutant cortex. (A, C, E) In the control embryos, radial glial processes were present throughout the cortex at E13.5, extending from the ventricular surface of the ventricular zone to the pial surface, perpendicular to the pial edge of the cortex. Individual radial glia were parallel to each other and could be clearly distinguishable from each other. **(B, D, F)** In the mutant, RC2 staining was prominent in the ventricular zone but was fainter in the cortical plate at E13.5. Individual radial glia were mixed together and harder to individually distinguish. Some of them bent in different directions and did not show a perpendicular pattern towards the pial surface. Moreover, most radial glia processes initiated from the ventricular surface but stopped near the cortical plate area and failed to connect the pial surface. While radial glial processes lost their typical features in the mutant cerebral cortex, the radial glial fascicles seemed preserved at the PSPB in the mutant embryos. At E13.5, the PSPB in the control embryos was characterized by the fascicles of RC2 positive radial glial processes (A, white bracket). In the mutant embryos, the fascicles of RC2 positive radial glial processes were present at the PSPB (B, white bracket). Additionally, Gsh2 showed similar expression pattern at the PSPB between the control and mutant embryos at E13.5 (A & B, white arrow). Scale bars: (A, B) 250 μm; (C-F) 50 μm.

axonal-like fibers in the lateral cortex of the mutant in the adjacent sections shown by Map2 as well as Neurofilament staining (Compare Figure 18 E with Figure 4 E and Figure 5 D). Where there were no axonal-like fibers present at the exit of the mutant cortex, the calbindin positive cells that were attempting to enter the cortex were not observed either (Compare Figure 18 D with Figure 4 D). The expression pattern of calbindin in the ventral telencephalon was similar between the control and the mutant, further confirming that the ventral telencephalon is not affected in the *Apc* mutant (Compare Figure 18 A and C).

Figure 18

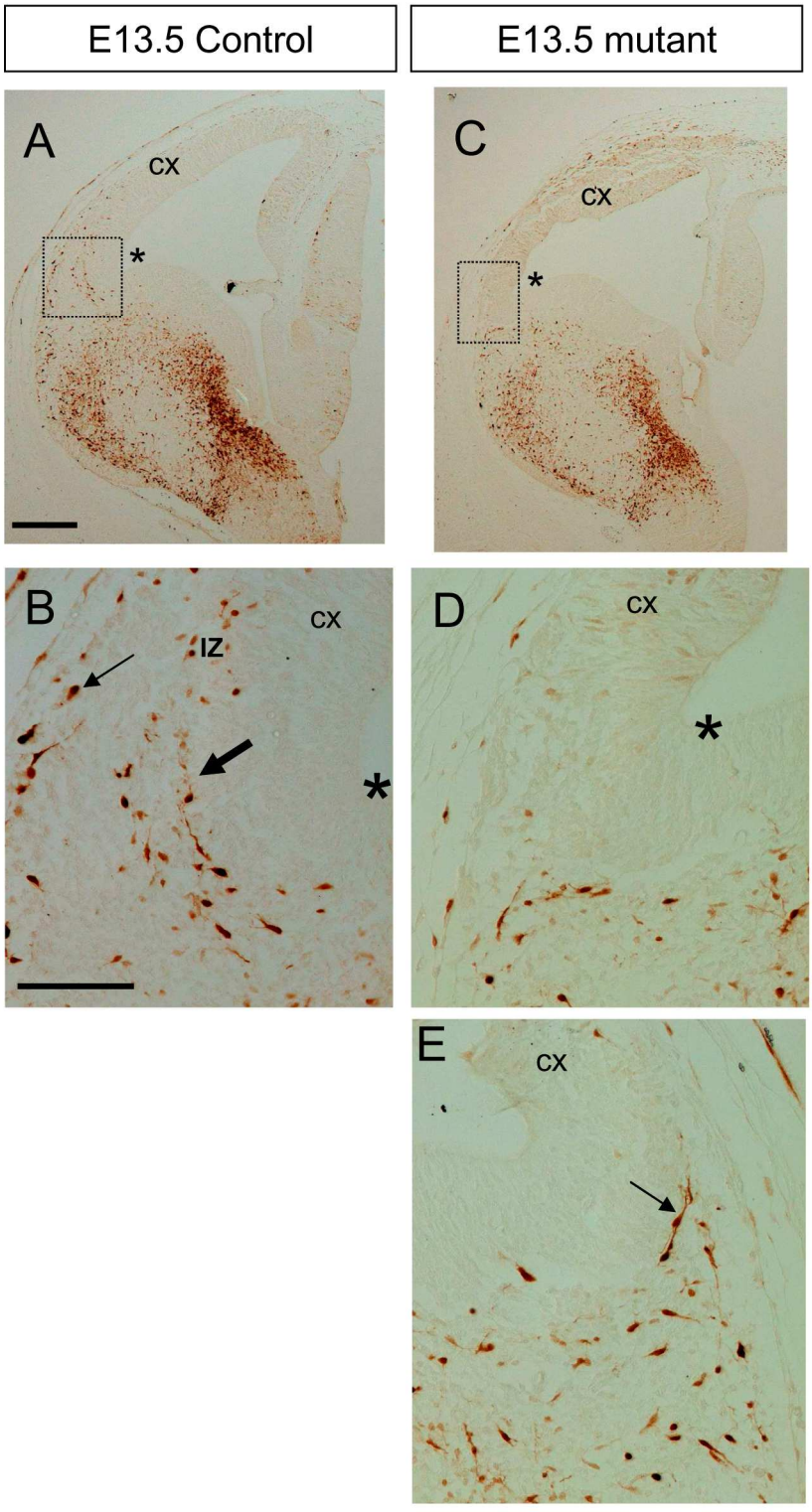

Figure 18. Large reduction of intermediate zone (IZ) cells in the lateral cortex of the *Apc* mutant. Coronal sections of E13.5 control **(A)** and mutant **(C)** mouse embryos showing Calbindin immunostaining in the forebrain. The star indicates the ventricular angle. **(B, D, E)** Higher magnifications of the areas boxed in (A, C), respectively. **(B)** In the neocortex of the control, a stream of calbindin-positive cells is present within the lower half of the intermediate zone (IZ, thick arrow), some of which are sending processes. A few calbindin-expressing cells are seen at the edge of lateral cortex (thin arrow). **(D)** Both populations of calbindin-positive cells are not observed in the mutant. **(E)** Some calbindin positive cells send process toward the cortex in the mutant (arrow). Scale bars: (A, C) 200 µm; (B, D, E) 100 µm.

3.8 Discussion

This chapter introduced an animal model in which the *Apc* gene is specifically knocked out in the cerebral cortex, driven by the Emx1-Cre expression. Since the cellular features such as RC2-positive radial glial processes and gene expression such as Gsh2 in the mutant showed that the diencephalon as well as the ventral telencephalon and the PSPB are not affected by the loss of Apc in the cortex, this animal model is useful to address how important the cortex is in guiding TCAs into their final targets.

3.8.1 The PSPB is not directly affected by the deletion of *Apc* in the mutant cortex

The blue staining on the coronal section of E15.5 Rosa26-LacZ reporter mouse embryo showed the region where Emx1-Cre is active (Figure 1 A). The section was counterstained with Nuclear Fast Red, which labelled a cell dense stream that is LacZ-negative at the PSPB. Apparently Emx1 Cre expression was restricted in the cerebral cortex and displayed a distinct pattern at the PSPB along the lateral edge of the cell dense steam. Since *Apc* is inactivated specifically in the cortex driven by the Emx1-Cre expression, it is very likely that the possible disruption of gene expression and cell differentiation will be restricted to the cerebral cortical area that is dorsal to the PSPB, while the PSPB itself and the subcortical region that is ventral to the PSPB should not be affected, in theory. In fact, the ventral telencephalic based transcription factor Gsh2 showed similar expression pattern at the PSPB between the control and the mutant brain indicates that the ventral telencephalic tissue that is ventral to the PSPB is not affected in the *Apc* mutant.

3.8.2 The PSPB is a choice point for TCAs

The PSPB is suggested to be a molecular barrier for dorsal and ventral cell types. What's more, PSPB is also suggested to be a barrier for CTAs and TCAs. Pax6-LacZ

mutants show that both CTAs and TCAs fail to cross the PSPB. However, the mechanisms by which CTAs and TCAs cross the PSPB might be different. CTAs might not need the guidance from TCAs to cross the PSPB, although once CTAs meet with TCAs in the ventral telencephalon, CTAs might need the scaffold of TCAs to reach the thalamus. In *Tbr1*$^{-/-}$ mutants, CTAs cross the PSPB and meet with TCAs in the ventral telencephalon. Thus CTAs cross the PSPB through the guidance of other factors, e.g. reciprocal projections from LGE towards the cortex. In the Apc mutant, TCAs navigate into the ventral telencephalon normally but fail to cross the PSPB and enter the cortex. This suggests that guidance factors from the cortex are needed for TCAs to cross the PSPB, which are absent in the *Apc* mutant.

There are a few possibilities what these guidance factors might be. They could be the descending CTAs or secreted molecules from the cortex. They could also be the interneurons migrating from the ventral telencephalon into the dorsal telencephalon and generating a permissive corridor in the intermediate zone (IZ) of the cortex. It is well known that CTAs descend within the IZ and then cross the PSPB to traverse in the mantle zone of the LGE. Therefore CTAs are strong candidates for guiding TCAs to cross the PSPB. In the *Apc* mutant, TCAs arrive at the PSPB without the presence of CTAs, indicating that TCAs navigate through the ventral telencephalon by the aid of other guidance cues, e.g. the corridor cells formed by cells migrating from the LGE to the MGE. But the meeting with CTAs in the ventral telencephalon may be necessary for TCAs to establish intimate relation with corresponding CTAs and prepare to cross the PSPB. In the *Apc* mutant, CTAs are absent, which may be the main reason that TCAs fail to cross the PSPB. However, it remains to be clarified which CTA subtypes play the major role in the guidance of TCAs, since all the CTA subtypes such as those derive from the subplate and true cortical plate cells fail to grow out of the mutant cortex. In the control brains, DiI-labelled corticofugal axons descend into the ventral telencephalon at around E13.5, but the DiI labelling strategy used here does not allow the distinction between different CTA subtypes, because the DiI is likely to label a mix of subplate and cortical plate axons. To further investigate the roles of different CTA subtypes in the guidance of TCAs, future work sees the potential use of subplate specific Cre lines to inactivate Apc in subplate cells.

In conclusion, TCAs fail to cross the PSPB and enter the cortex in the *Apc* mutant. In the lateral cortex of the mutant, I observed the absence of normal CTAs, cortical plate, marginal zone and IZ migrating cells. One or several of these missing cues from the cortex might be critical candidates for guiding TCAs to pass the PSPB and enter the cortex. In the next chapter, I will describe the experiments that I did to examine the expression of some potential attractive molecules for TCAs in mutant embryos, i.e. Ig-Nrg1. I will also introduce the *in vitro* explant culture experiments, which show that the mutant cortex does not secrete long-range chemorepellent molecules to repel or inhibit thalamic axonal extension. In contrast, the angle region of the mutant cortex still has the ability to promote thalamic axonal outgrowth. Thus it is less likely that the secreted molecules from the cortex are sufficient in the guidance of TCAs. The guidance factors for TCAs are likely to function through cell-cell contact mediated mechanisms. TCAs may need the direct contact with cortical axons and use them as an axonal scaffold to navigate into the cerebral cortex.

Chapter 4. *In vitro* evidence that CTAs are important for guiding TCAs into the cerebral cortex

In Chapter 3, I described the defects of TCAs in the *Emx1*-Cre/*Apc*-LoxP conditional mutant mice, where TCAs failed to cross the PSPB and enter the cerebral cortex. Normal CTAs were absent in the conditional mutants. Therefore one possible explanation for the TCA defects in the conditional mutant is that the mutant cerebral cortex lacks CTAs which serve as an axonal scaffold to guide TCAs into the cortex.

One other possibility is that the cortex of the *Emx1*-Cre/*Apc*-LoxP conditional mutant lacks secreted attractive molecules which are important to direct the TCAs into the cortex. To test this, I examined the expression pattern of the secreted isoform of Neuregulin-1 (Ig-Nrg1), which was proposed to be a strong candidate to direct TCAs into the cerebral cortex (Lopez-Bendito et al., 2006). Here I show that Ig-Nrg1 is still present in the ventricular angle of the conditional mutant cortex. Thus the failure of TCAs to enter the cerebral cortex in the conditional mutants is less likely to be ascribed to the lack of attractive molecules secreted by the cortex.

However, another possibility is that the *Emx1*-Cre/*Apc*-LoxP conditional mutant cortex becomes very repulsive to TCAs due to an increase of repulsive molecules secreted by the cortex. To test this, I used *in vitro* explant culture experiments where thalamic explants were co-cultured with cortical explants taken from both the control and the conditional mutant cortex. The amount of axonal outgrowth from the thalamic explants was measured and compared between different culture groups. The results show that thalamic axons do not grow away from the cortical explants of the conditional mutants, indicating that the failure of TCAs to enter the cortex of the conditional mutants is not due to an increase of repulsive cues secreted by the mutant cortex that repel TCAs and prevent them from navigating into the cortex. The angle region of the conditional mutant cortex is capable of promoting the overall outgrowth of thalamic axons, suggesting that the mutant cortex still has growth promoting effect on thalamic axons. Thus the failure of TCAs to enter the cortex of the conditional mutant might be ascribed to the loss of descending CTAs in the cortex.

To test this further, *in vitro* brain slice culture experiments were performed where mutant cortex was replaced with control cortex, and the results show that descending cortical axons regenerate from the control cortex and rescue thalamic axon growth into the cortex. These results indicate that descending cortical axons are important in directing thalamic axons into the cerebral cortex.

4.1 *In vivo* evidence that the mutant cortex is still attractive to TCAs

Recently, it has been suggested that Neuregulin-1 (Ig-Nrg1) plays long-range roles in attracting thalamic axons towards the cortex (Lopez-Bendito et al., 2006). In the *Emx1*-Cre/*Apc*-LoxP conditional mutant, Ig-Nrg1 could be lost due to the deletion of Apc in the cortex, and this might subsequently cause the TCA defects in this mutant. To assess the expression pattern of *Ig-Nrg1* in the conditional mutant cortex, in situ hybridization was performed on E13.5 brains. *Ig-Nrg1* was highly expressed in the ventricular angle of the cerebral cortex of both the conditional mutant and the control embryos, with a decreasing gradient towards dorsal-medial cortex as well as through the ventricular zone of the ganglionic eminence (Figure 1 A & B, arrow). The presence of Ig-Nrg1 in the angle region of the conditional mutant cortex shows that TCA defects in the *Emx1*-Cre/*Apc*-LoxP conditional mutants are not caused by loss of Ig-Nrg1. It also indicates that Ig-Nrg1 is not sufficient for the extension of TCAs in the conditional mutant, and that additional factors are needed to guide these axons into the cortex.

4.2 *In vitro* evidence that the conditional mutant cortex neither repels nor inhibits thalamic axonal outgrowth

Another possibility for the TCA defects in the *Emx1*-Cre/*Apc*-LoxP conditional mutant is that the mutant cortex becomes very repulsive to TCAs due to an increase of repulsive molecules secreted by the cortex. Apc is well characterized as a tumor-suppressor that plays an important role in controlling the stability and subcellular localization of β-catenin, and subsequently affects the Wnt signaling pathway. In the

Figure 1

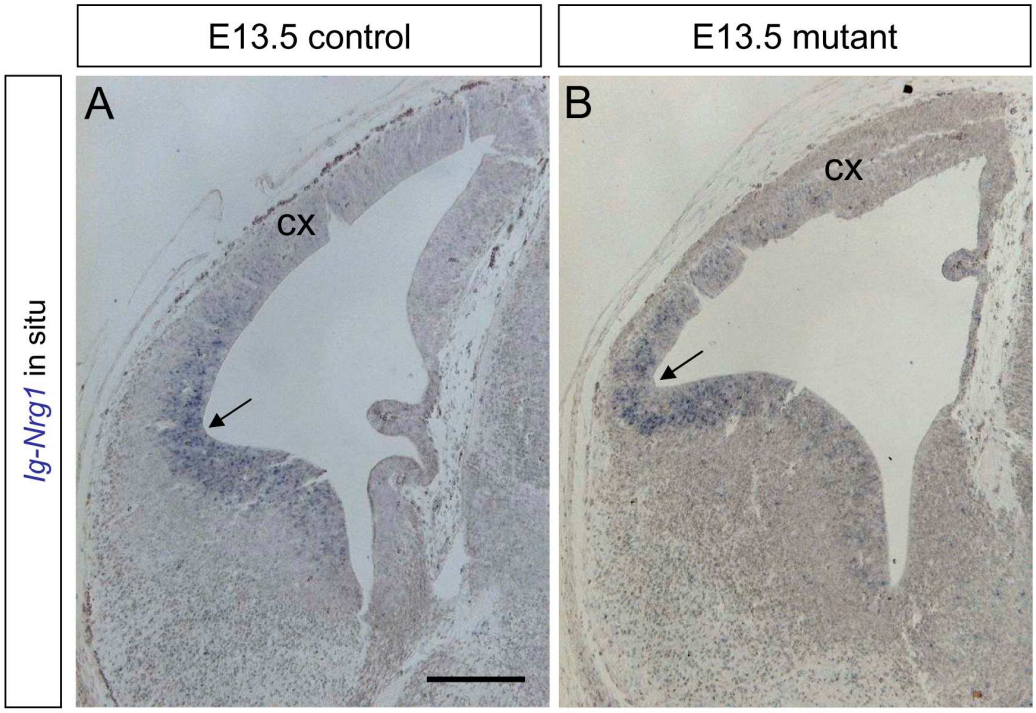

Figure 1. The presence of attractive molecules for axonal guidance in the cortex of the *Apc* mutant. (A, B) *Ig-Nrg1* (Neuregulin-1), a gene that was suggested to play long-range roles in attracting thalamic axons towards the cortex was present in the angle region of both the control and the conditional mutant (arrow), which indicates that Ig-Nrg1 does not account for the TCA defects in the conditional mutant. It also implies that Ig-Nrg1 is not sufficient for the extension of TCAs in the conditional mutant, and that additional factors are needed to guide these axons into the cortex. cx-cortex. Scale bar: (A & B) 200 µm.

absence of Apc, β-catenin expression is enhanced in the nucleus, where it binds to LEF-1/TCF proteins and activates the transcription of Wnt target genes (Sierra et al., 2006). It is possible that the change of Wnt/β-catenin signalling due to the absence of Apc in the cerebral cortex of the conditional mutant would affect the expression of repulsive molecules in the cortex. The angle region is located at the entrance of the cerebral cortex, and it contains an activity that is essential for the normal navigation of TCAs since the ablation of angle region in the brain slice culture causes failure of TCAs to grow towards the cortex (Lopez-Bendito et al., 2006). Thus I wanted to test whether the angle region of the *Emx1*-Cre/*Apc*-LoxP conditional mutant cortex was secreting repulsive molecules which prevented TCAs from entering the cortex. Additionally, the lateral part of the conditional mutant cortex, which is dorsal to the angle region, could also be secreting repulsive molecules that would repel TCAs away from the cortex.

To test these hypotheses, I used *in vitro* explant culture experiments where thalamic explants were co-cultured with cortical explants taken from the lateral cortex or the ventricular angle region of E14.5 control or conditional mutant cortex. The thalamic explants used for explant cultures were taken from GFP+ embryos so that thalamic axons could be distinguished from non-GFP cortical axons by using anti-GFP antibodies. In previous explant culture assays the explants were positioned within a short distance, i.e. 150-300 µm (Braisted et al., 2000; Braisted et al., 2009; Braisted et al., 1999), or 200-400 µm (Bonnin et al., 2007), or 500 µm apart from each other (Lopez-Bendito et al., 2006). Here I positioned the explants at 200-500 µm apart. By culturing thalamic explants with cortical explants within a short distance, I would be able to detect if the conditional mutant cortex is secreting repulsive molecules which repel thalamic axons away from the cortical explants. Previous explant culture experiments have demonstrated that the hypothalamus is repulsive to thalamic axons (Bagri et al., 2002; Braisted et al., 2009). Here I also cultured thalamic explant with hypothalamic explant and used it as a positive control to test the sensitivity of the current explant culture assay in detecting repulsive effects.

4.2.1 Phenotype of explant cultures

By observing the phenotype of the explant cultures, there seemed to be variations among different groups of explant cultures in the direction of thalamic axonal outgrowth, as well as in the length and density of thalamic axons (Figure 2). However, there were some trends from visual inspection. Firstly, there appeared to be more thalamic axonal outgrowth when thalamic explants were co-cultured with angle regions from either control or conditional mutant cerebral cortex (Figure 2 J-O), compared to thalamic explants cultured alone (Figure 2 A-C). These results imply that the angle region of the cortex might have a growth promoting effect on thalamic axons. Secondly, explants of angle region seemed to stimulate more thalamic axonal outgrowth than explants of lateral cortex (compare Figure 2 J-L with D-F). This observation implies that the angle region of the cortex might be more capable of promoting the outgrowth of thalamic axons, compared to the lateral cortex. Thirdly, thalamic explants co-cultured with the conditional mutant cortex seemed to produce more thalamic axonal outgrowth (Figure 2 G-I), compared to thalamic explants cultured alone (Figure 2 A-C). This observation implies that the conditional mutant cortex might be capable of promoting thalamic axonal outgrowth.

Since there was variation in the amount of thalamic axonal outgrowth in different co-culture groups, a statistical analysis of quantitative data was needed. Previous studies have shown that molecules secreted by the hypothalamus are repulsive to thalamic axons (Braisted et al., 2009). Therefore the data from thalamic explants co-cultured with hypothalamic explants in the present study was used as a positive control for the repulsive effects of diffusible molecules on the direction of thalamic axonal outgrowth (Figure 2 P-T).

4.2.2 Statistical analysis of axon phenotype

Figure 3 illustrates a schematic diagram of the possible outcome in the *in vitro* explant culture experiments where thalamic explants were cultured alone or with other explants. If the thalamic explant is cultured alone, thalamic axonal outgrowth

Figure 2

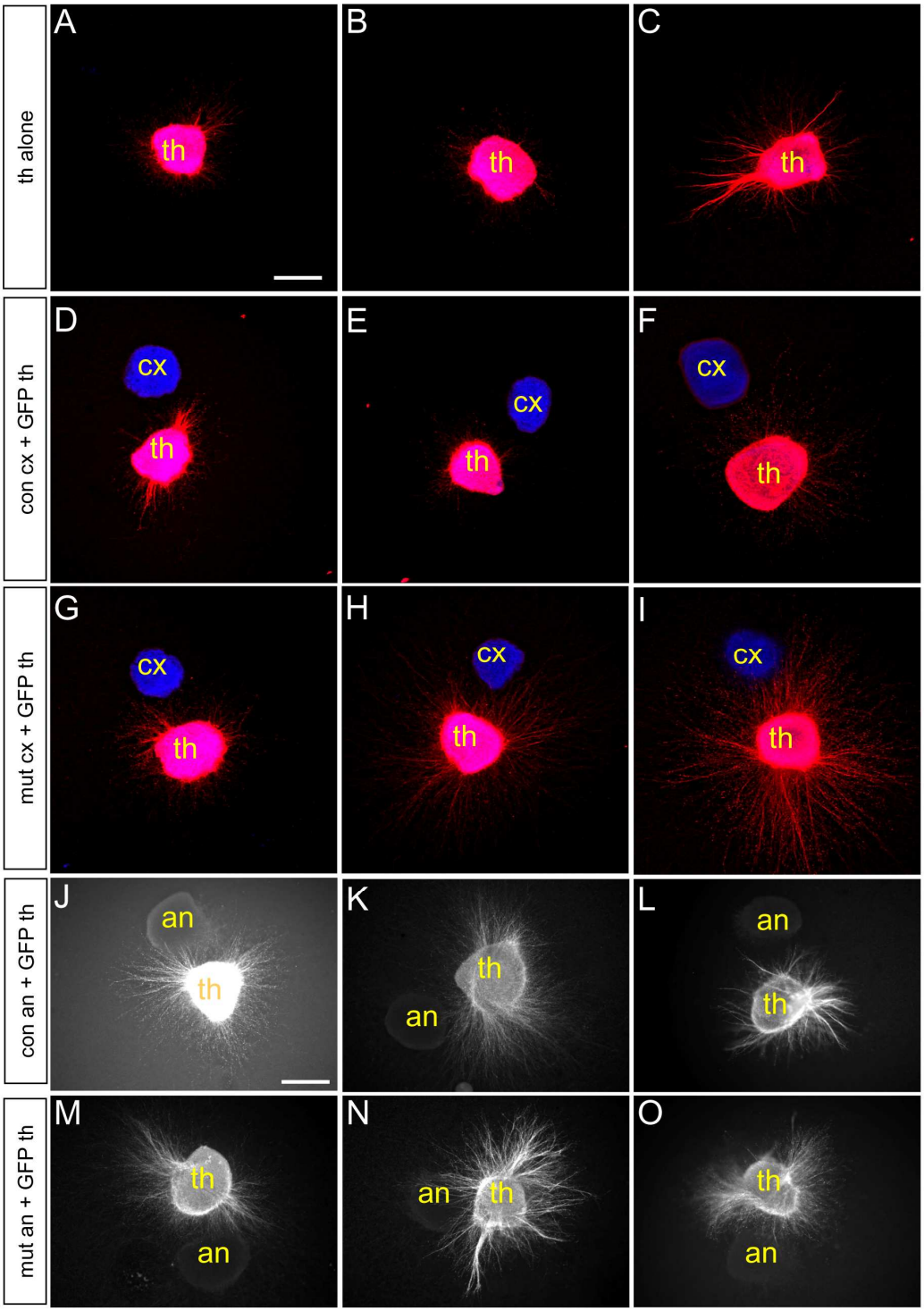

(Figure 2 continues on the next page)

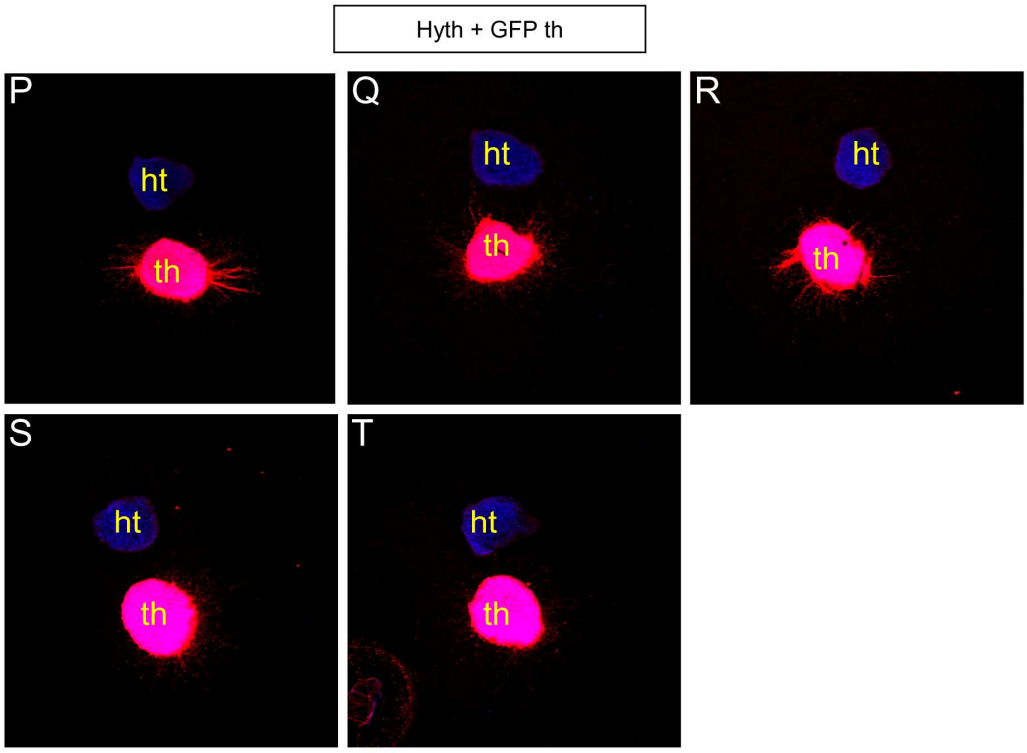

Figure 2. Examples of E14.5 explant cultures from different culture groups. Immunohistochemistry was with GFP antibody (red) and nuclei were counterstained with TO-PRO-3 (blue). **(A-I, P-T)** Confocal images. **(J-O)** Digital images with grey scale. **(A-C)** GFP+ thalamic explants cultured alone. **(D-F)** GFP+ thalamic explants cultured with explants from the control lateral cortex. **(G-I)** GFP+ thalamic explants cultured with explants from the mutant lateral cortex. **(J-L)** GFP+ thalamic explants cultured with explants from the angle region of the control cortex. **(M-O)** GFP+ thalamic explants cultured with explants from the angle region of the conditional mutant cortex. **(P-T)** GFP+ thalamic explants cultured with hypothalamic explants from control embryos. an-angle region; th-thalamus; cx-cortex; ht-hypothalamus; con-control; mut-mutant. Scale bars: (A-I, P-T) 200 µm; (J-O) 250 µm.

would have no bias in different directions (Figure 3 A). If the cortical explant is secreting repulsive molecules that diffuse in a gradient and exert a repulsive effect based on their concentration, the amount of thalamic axonal outgrowth would be higher in the region that is facing away from the cortical explant than that in the region that is facing toward the cortical explant (Figure 3 B). On the other hand, if the cortical explant is secreting attractive molecules that diffuse in a gradient and exert an attractive effect based on their concentration, the amount of thalamic axonal outgrowth would be higher in the region that is facing toward the cortical explant than that in the region that is facing away from the cortical explant (Figure 3 C).

However, if the molecules secreted by the cortical explant exert a growth inhibiting effect irrespective of their concentration or above a maximum effect threshold, thalamic axons would not particularly grow away from the cortical explant, but the total amount of thalamic axonal outgrowth would be low (Figure 3 D). On the other hand, if the molecules secreted by the cortical explant exert a growth promoting effect irrespective of their concentration, thalamic axons would not particularly grow toward the cortical explant, but the total amount of thalamic axonal outgrowth would be high (Figure 3 E). If the cortical explant does not secrete repulsive/attractive or growth inhibiting/promoting molecules, the total amount of thalamic axonal outgrowth would be similar to thalamic explants cultured alone, and also there would be no significant difference in the amount of thalamic axonal outgrowth in any direction (Figure 3 F).

Here different approaches were used to analyse the repulsive/attractive and growth inhibiting/promoting aspects of the secreted molecules from the cortical explant, respectively.

4.2.2.1 Mutant cortex does not repel thalamic axons *in vitro*

In order to be able to examine the effect of diffusible molecules on the direction of thalamic axons quantitatively, the amount of thalamic axonal outgrowth was

Figure 3

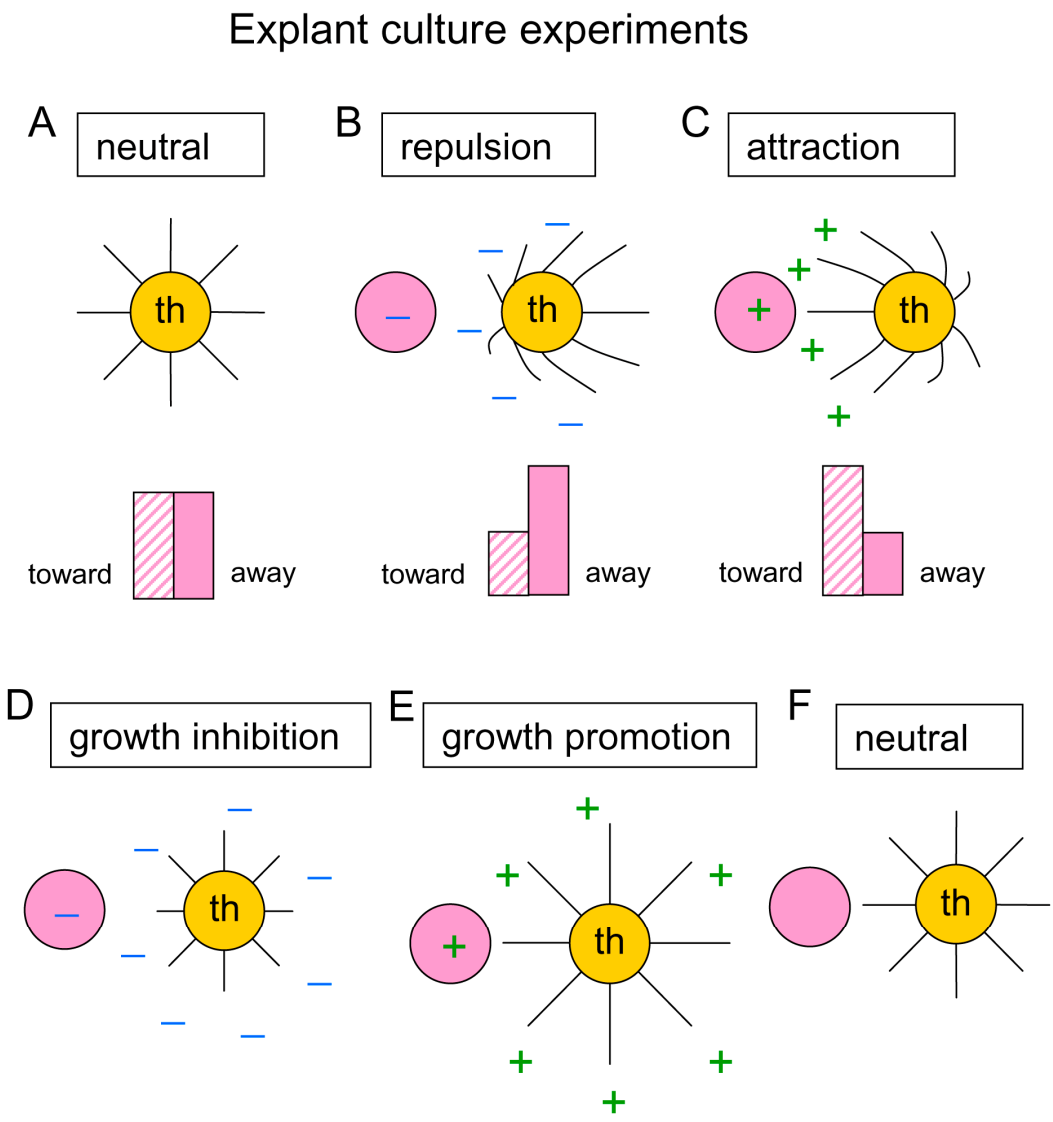

Figure 3. Schematic diagram of the possible outcome in the *in vitro* explant culture experiments where thalamic explants were cultured alone or with other explants. (A) Thalamic explant cultured alone. **(B)** Thalamic explant cultured with another explant that secretes repulsive molecules. **(C)** Thalamic explant cultured with another explant that secretes attractive molecules. **(D)** Thalamic explant cultured with another explant that secretes growth inhibiting molecules. **(E)** Thalamic explant cultured with another explant that secretes growth promoting molecules. **(F)** Thalamic explant cultured with another explant that does not secrete repulsive/attractive or growth inhibiting/promoting molecules. th-thalamus.

measured at 60 pixel distance (60 pixel distance ≈ 110 µm) from the explant border (see Figure 1 in Chapter 2 Materials and Methods for explant cultures). Each thalamic explant was divided into four quadrants. Student's t-test was used to assess the significance of differences between the percentage axon coverage of thalamic axons in the quadrant that was facing toward the cortical explant and that in the quadrant that was facing away from the cortical explant (% axon coverage toward vs. % axon coverage away).

My data showed that when thalamic explants were co-cultured with cortical explants from the lateral cortex or the angle region of both the control and the conditional mutant embryos at E14.5 (Figure 4 A), there were no significant differences in the percentage axon coverage between thalamic axons growing from the quadrant that was facing toward the cortical explants and that from the quadrant that was facing away from the cortical explants (first four sets of bars in Figure 4 B; numbers of cultures are 10-18). There were significantly more thalamic axons growing away than towards the hypothalamic explants (fifth set of bars in Figure 4 B; 5 cultures; Student's t-test, $p<0.05$), which is consistent with the published finding that the hypothalamus repels thalamic axons (Bagri et al., 2002; Braisted et al., 2009), and confirms the sensitivity of the explant culture assay in the present study. These data indicate that the molecules secreted by the cortical explants from the conditional mutant cortex at E14.5 do not direct thalamic axons to grow away from the cortical explants.

4.2.2.2 Mutant cortex does not inhibit thalamic axonal outgrowth *in vitro*

For detecting the growth inhibiting/promoting effects of the molecules secreted by the cortical explants on thalamic axons, I compared the total percentage axon coverage of thalamic axons from E14.5 GFP-positive thalamic explants, when thalamic explants were cultured alone or co-cultured with cortical explants taken

Figure 4

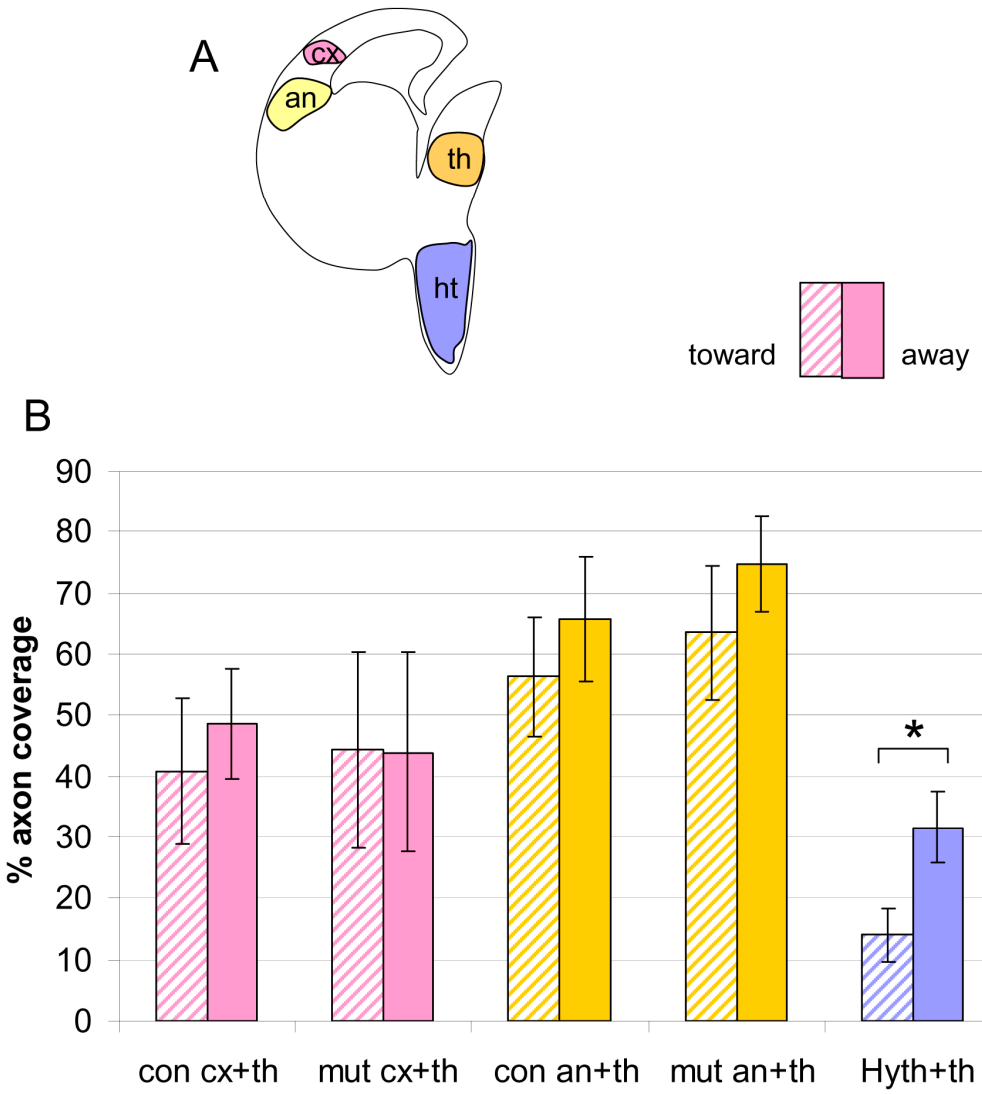

Figure 4. The conditional mutant cortex is not more repulsive to thalamic axons compared to the control cortex. (A) A diagram showing that the explants were taken from the region in the thalamus (th), hypothalamus (ht), the angle region of the cortex (an) and the lateral cortex (cx). **(B)** Mean % axon coverage (±s.e.m.) 60 pixel distance (≈110 µm) from the border of thalamic explants. Student's t-test revealed no significant differences in the direction of thalamic axonal outgrowth in terms of growing towards or away from the cortical explants of either the control or the conditional mutant cortex (P<0.05). There were significantly more thalamic axons growing away than towards the hypothalamic explants, which is consistent with the published finding that the hypothalamus repels thalamic axons. cx – cortex; an – angle region; th – thalamus; ht (Hyth) – hypothalamus; con – control; mut – mutant.

from the lateral cortex or the angle region of either the control or the conditional mutant E14.5 embryos.

The percentage axon coverage was measured at 60, 100, 140, 180 & 220 pixel distances (60 pixel distance ≈ 110 μm) from each explant border (see Figure 2 in Chapter 2 Materials and Methods for explant cultures). Each thalamic explant was divided into four quadrants. Since the measuring polygons (yellow) in the quadrant of the thalamic explant facing toward the cortical explant came across the cortical explant in most cases, the percentage axon coverage in the quadrant towards the cortical explant was excluded. The percentage axon coverage in the other three quadrants was summed up for each explant (Table 1). Two Way Repeated Measures ANOVA was used to assess the significance of differences between groups.

The analysis of total percentage axon coverage by Two Way Repeated Measures ANOVA indicates that there were significant differences in the total outgrowth of thalamic axons in different co-culture groups ($P<0.05$). To isolate which group(s) differ from the others a multiple comparison procedure was used (Table 2).

(1) No significant differences in 'thalamus with or without control lateral cortex'

When the differences in the total outgrowth of thalamic axons were compaired between pairs of co-culture groups, no significant differences were detected in the total outgrowth of thalamic axons between thalamic explants cultured alone and thalamic explants co-cultured with cortical explants from the control lateral cortex (Figure 5 and Table 2, th alone vs. con cx + th). These data indicate that the cortical explants from the control lateral cortex neither inhibit nor promote thalamic axonal outgrowth.

(2) There were significant differences in 'thalamus with or without mutant lateral cortex'

Table 1

% axon percentage table for explant culture

Distance / Culture groups (n)	Means ± S.E.M				
	60 pixels	100 pixels	140 pixels	180 pixels	220 pixels
Th alone (18)	162.947±24.336	80.373±17.765	46.85±11.541	23.404±5.866	7.529±2.479
Con cx+th (10)	126.957±20.000	81.681±19.122	35.527±10.853	20.457±7.680	13.205±5.723
Mut cx+th (10)	159.942±42.584	122.965±38.683	99.708±36.252	65.146±28.195	50.116±24.565
Con an+th (15)	196.615±26.109	155.216±22.857	109.404±20.931	59.903±16.645	34.311±10.718
Mut an+th (13)	217.609±21.429	183.759±26.470	136.035±28.810	87.468±28.842	66.145±26.276

- Th alone: thalamic explant cultured alone
- Con cx + th: control lateral cortical explant cultured with thalamic explant
- Mut cx + th : mutant lateral cortical explant cultured with thalamic explant
- Con an + th : control angle region cultured with thalamic explant
- Mut an + th : mutant angle region cultured with thalamic explant

$$\% \text{ axon coverage} = \frac{\text{sum of all neurite fascicle widths in each quadrant} \times 100}{\text{circumference of measuring polygon in each quadrant}}$$

Table 1. A data table for the mean of total % axon coverage (±s.e.m.) at 60, 100, 140, 180 and 220 pixel distances (60 pixel distance ≈ 110 µm) from the border of thalamic explants.

Table 2

Distance / Culture groups	Student's t-test (P<0.05)				
	60 pixels	100 pixels	140 pixels	180 pixels	220 pixels
th alone vs. con cx+th	0.327	0.963	0.524	0.765	0.301
th alone vs. mut cx+th	0.948	0.263	0.099	0.071	0.028 *
th alone vs. con an+th	0.359	0.013 *	0.010 *	0.034 *	0.013 *
th alone vs. mut an+th	0.130	0.002 *	0.003 *	0.017 *	0.014 *
con cx+th vs. con an+th	0.066	0.032 *	0.013 *	0.079	0.145

Table 2. A table showing the P values for the comparison of total % axon coverage between different culture groups using Student ' s t-test, with significant differences highlighted with a star.

Figure 5

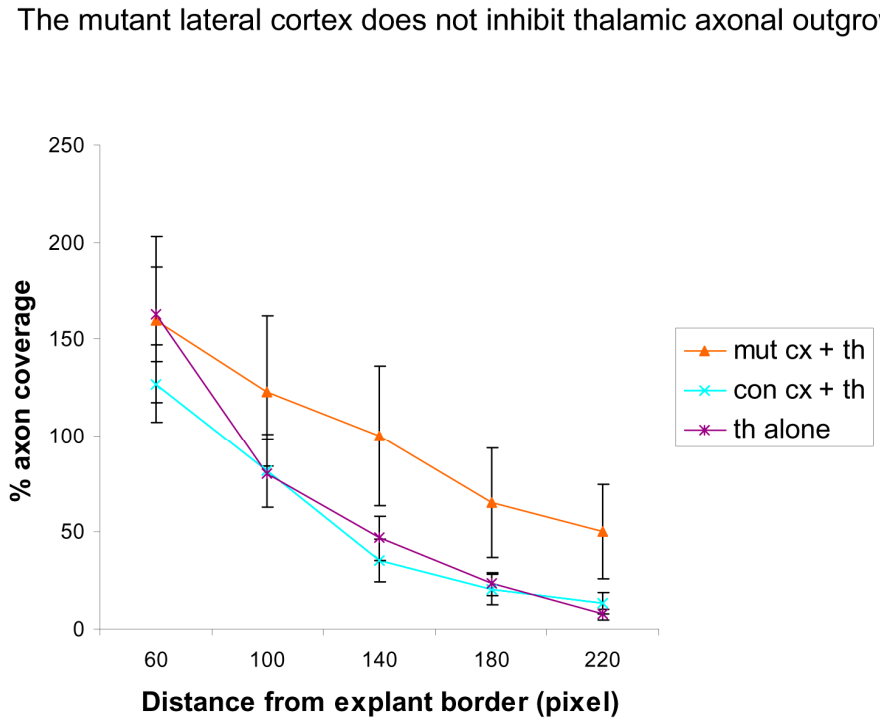

- mut cx + th : mutant lateral cortical explant cultured with thalamic explant
- con cx + th : control lateral cortical explant cultured with thalamic explant
- th alone : thalamic explant cultured alone

Figure 5. The *Apc* mutant lateral cortex does not inhibit thalamic axonal outgrowth. A diagram showing the mean % axon coverage (± s.e.m.) 60, 100, 140, 180 & 220 pixel distances (60 pixel distance ≈ 100 µm) from the border of thalamic explants. The data points within the same culture group were lined up to show the trend. Results were from thalamic explants cultured alone or with explants from the lateral cortex of either control or conditional mutants.

When the comparison was made between thalamic explants cultured alone and thalamic explants co-cultured with cortical explants from the conditional mutant lateral cortex (th alone vs. mut cx + th), no significant differences were detected in the total thalamic axonal outgrowth at 60, 100, 140 and 180 pixel distances (Figure 5 and Table 2).

Nevertheless, a significant difference was detected at 220 pixel distance, with P value = 0.028 for the comparison between 'th alone' and 'mut cx + th'. These data indicate that the initial outgrowth of thalamic axons was similar between these two culture groups, but thalamic axons grew slightly longer when thalamic explants were cultured with cortical explants from the conditional mutant lateral cortex than thalamic explants cultured alone. Thus a significant difference was detected when the percentage axon coverage was measured at a distance further than 180 pixels from the explant border. These results suggest that the conditional mutant cortex actually slightly promotes thalamic axon growth.

(3) There were significant differences in 'thalamus with or without control angle region'

Significant differences in the total outgrowth of thalamic axons were found between thalamic explants cultured alone and thalamic explants co-cultured with cortical explants from the angle region of the control cortex (Figure 6 and Table 2, th alone vs. con an + th). The P value for the comparison between 'th alone' and 'con an + th' at 60 pixel distance was 0.359, indicating that the density of thalamic axonal outgrowth was initially not distinguishable between these two culture groups.

However, the P values for the comparison between 'th alone' and 'con an + th' at 100, 140, 180 and 220 pixel distances were 0.013, 0.010, 0.034 and 0.013, respectively, indicating that thalamic axons grew much longer and the amount was much larger when thalamic explants were cultured with cortical explants from the angle region of the control cortex than thalamic explants cultured alone. These data

imply that the diffusible molecules from the angle region of the control cortex have a growth promoting effect on thalamic axonal outgrowth.

(4) There were significant differences in 'thalamus with or without mutant angle region'

Significant differences were also found between thalamic explants cultured alone and thalamic explants co-cultured with cortical explants from the angle region of the conditional mutant cortex (Figure 6 and Table 2, th alone vs. mut an + th). The P value for the comparison between 'th alone' and 'mut an + th' at 60 pixel distance was 0.130, indicating that the density of thalamic axonal outgrowth was initially not distinguishable between these two culture groups.

However, the P values for the comparison between 'th alone' and 'mut an + th' at 100, 140, 180 and 220 pixel distances were 0.002, 0.003, 0.017 and 0.014, respectively, indicating that thalamic axons grew much longer and the amount was much larger when thalamic explants were cultured with cortical explants from the angle region of the conditional mutant cortex than thalamic explants cultured alone. These data also imply that the diffusible molecules from the angle region of the conditional mutant cortex have a growth promoting effect on thalamic axonal outgrowth.

(5) There were significant differences in 'thalamus with control lateral cortex or control angle region'

Significant differences were also detected in the total outgrowth of thalamic axons between thalamic explants co-cultured with cortical explants from the control lateral cortex and thalamic explants co-cultured with cortical explants from the angle region of the control cortex (Table 2, con cx + th vs. con an + th). Significant differences were detected at 100 and 140 pixel distances, with P values = 0.032 and 0.013 for the comparison between 'con cx + th' and 'con an + th', respectively.

Figure 6

The mutant angle region does not inhibit thalamic axonal outgrowth

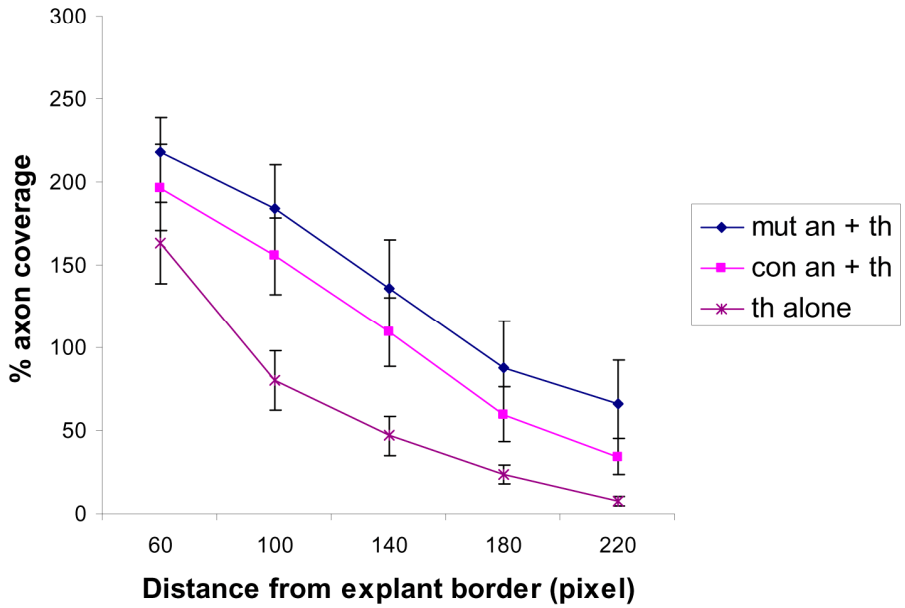

- mut an + th : mutant angle region cultured with thalamic explant
- con an + th : control angle region cultured with thalamic explant
- th alone : thalamic explant cultured alone

Figure 6. The *Apc* mutant angle region does not inhibit thalamic axonal outgrowth. A diagram showing the mean % axon coverage (± s.e.m.) 60, 100, 140, 180 & 220 pixel distances (60 pixel distance ≈ 100 μm) from the border of thalamic explants. The data points within the same culture group were lined up to show the trend. Results were from thalamic explants cultured alone or with explants from the angle region of either control or conditional mutant cortex.

These data indicate that there were significantly greater amounts of thalamic axonal outgrowth when thalamic explants were co-cultured with cortical explants from the angle region of the control cortex than thalamic explants co-cultured with cortical explants from the control lateral cortex. It also implies that the diffusible molecules from the angle region of the control cortex have a greater growth promoting effect on thalamic axonal outgrowth than the control lateral cortex does.

Taken together, the *in vitro* explant culture experiments show that the conditional mutant cortex actually slightly promotes thalamic axonal outgrowth, and that the angle region of the conditional mutants is capable of promoting the overall outgrowth of thalamic axons. These results indicate that the failure of TCAs in reaching the cortex is not due to the increase of repulsive cues or the decrease of growth promoting molecules secreted by the conditional mutant cortex. It implies that the loss of descending CTAs in the conditional mutants might be responsible for the failure of TCAs to cross the PSPB.

4.3 TCAs were rescued into the cortex after replacing a mutant cortex with a control cortex

To test whether descending cortical axons are able to rescue the failure of thalamic axons from the conditional mutants to cross the PSPB and enter the cortex, a series of *in vitro* brain slice culture experiments were performed where mutant cortex was replaced with control cortex that is capable of reintroducing cortical axons (in collaboration with Dario Magnani, who demonstrated the techniques of *in vitro* transplant culture to me and performed certain amounts of transplant culture to contribute to the N number for this transplantation experiment).

Before attempting a rescue, I first tested whether the thalamus of the conditional mutant is able to generate axons and whether the ventral telencephalon of the conditional mutant allows axons to traverse it in the present culture system. E14.5 thalamic explants from either control or conditional mutants were transplanted to the

diencephalic-telencephalic border of control slices, from where they all generated axons that intermingled with the descending cortical axons and grew into the cortex (Figure 7 A, B, E & F; n= 7 out of 9 cultures for control and 5 out of 6 cultures for conditional mutant thalamic explants).

When thalamic explant was transplanted to telencephalic slices from conditional mutants, thalamic axons traversed the ventral telencephalon, but did not enter the cortex (Figure 7 C & G; n= 9), mimicking the failure observed *in vivo* in conditional mutants. When thalamic explant from conditional mutants was transplanted to telencephalic slices from conditional mutants whose cortex was replaced by control cortex, thalamic axons grew into the cortex in close association with descending cortical axons derived from the control cortex (Figure 7 D & H; n= 4 out of 5 cultures). Arrow pointed to an example of a thalamic axon that navigated into the cortex through a bundle of the descending cortical axons (Figure 7 D & H). These results show that a normal cortex and its descending cortical axons are important in directing TCAs into the cortex.

4.4 Descending cortical axons affect the fasciculation of thalamic axons

When thalamic transplant was transplanted to telencephalic slices from conditional mutants, a large numbers of thalamic axons navigated into the ventral telencephalon, but these thalamic fibers were not fasciculated (Figure 7 C & G). However, when the mutant cortex was replaced by a control cortex, thalamic axons were fasciculated into discrete bundles of axons, and these thalamic axons tend to make contacts with the descending cortical axons from the control cortex (Figure 7 A, B & D). A possible explanation is that small bundles of cortical axons open a tract permissive for thalamic axons and guide distinct bundles of thalamic axons into the cortex. Additionally, the descending cortical axons may release some molecules which can affect the direction of thalamic axons. Thalamic axons might be attracted by the molecules secreted by the cortical axons and fasciculated into tight bundles of axons to head towards the same source of attractants from the cortical axons.

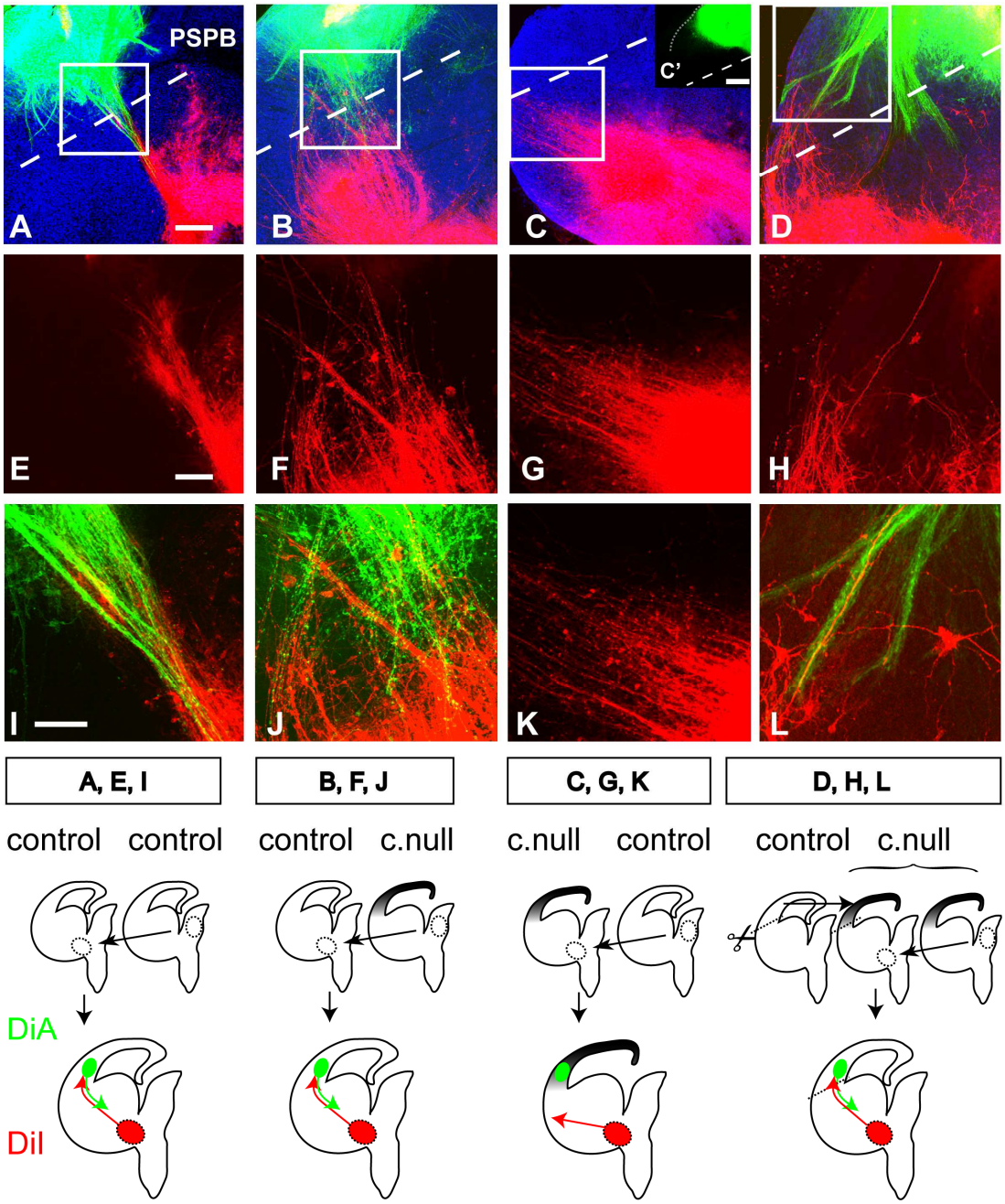
PSPB
A
B
C
C'
D
E
F
G
H
I
J
K
L
A, E, I
B, F, J
C, G, K
D, H, L
control control
control c.null
c.null control
control c.null
DiA
DiI

Figure 7. TCAs were rescued into the cortex after replacing a mutant cortex with a control cortex. (A, B, E, F) E14.5 thalamic explants from either control or conditional mutants were transplanted to the diencephalic-telencephalic border of control slices, from where they all generated axons that intermingled with the descending cortical axons and grew into the cortex (n= 7 out of 9 cultures for control and 5 out of 6 cultures for conditional mutant thalamic explants). **(C & G)** When thalamic explant was transplanted to telencephalic slices from conditional mutants, thalamic axons traversed the ventral telencephalon, but did not enter the cortex (n= 9), mimicking the failure observed *in vivo* in conditional mutants. **(D & H)** When thalamic explant from conditional mutants was transplanted to telencephalic slices from conditional mutants whose cortex was replaced by control cortex, thalamic axons grew into the cortex in close association with descending cortical axons derived from the control cortex (n= 4 out of 5 cultures). **(I-L)** Higher magnification images from the boxed areas in A-D. Nuclei were counterstained with TO-PRO-3 iodide. The diagrams underneath each column of photographs summarize the experimental paradigms and their outcomes. Scale bars: A-D, 50μm; E-L, 25μm. These results show that a normal cortex and its descending cortical axons are important in directing TCAs into the cortex.

4.5 Discussion

4.5.1 Conditional mutant cortex neither repels nor inhibits thalamic outgrowth *in vitro*

In the current study, my *in vitro* explant culture experiments show that the conditional mutant cortex neither repels nor inhibits thalamic axonal outgrowth, indicating that the failure of TCAs in reaching the cortex is not due to the change of repulsive cues secreted by the mutant cortex. Instead, the *in vitro* explant culture experiments reveal a growth promoting effect of the diffusible molecules from the angle region of both the control and the conditional mutant cortex on the outgrowth of thalamic axons. Ig-Nrg1 may be the major component of the growth promoting molecules from the angle region of both the control and the conditional mutant cortex. However, additional guidance cues are needed to regulate the direction of TCAs, which are likely to function through cell-cell contact mediated mechanisms. The *Emx1*-Cre/*Apc*-LoxP conditional mutant cortex lacks these guidance factors, which might be the cortical axons.

4.5.2 Conditional mutant cortex lacks guidance cues for TCAs

In the brain slice culture experiments where thalamic explant was transplanted to telencephalic slices from conditional mutants, a large number of thalamic axons navigated into the ventral telencephalon, but failed to enter the cortex. These results indicate that the ventral telencephalon of the conditional mutant is penetrable by thalamic axons, and that thalamic axons are growing robustly. The failure of thalamic axons entering the cortex implies that the guidance factors for directing thalamic axons are absent in the conditional mutant cortex.

4.5.3 Descending cortical axons can rescue the failure of thalamic axons from mutants to enter the cortex

By replacing the conditional mutant cortex with a control cortex, cortical axons were reproduced and descended into the ventral telencephalon from the conditional mutant. Thalamic axons formed discrete bundles and associated intimately with small bundles of descending cortical axons, following them into the cortex. These bundled thalamic axons were not observed when thalamic explants were cultured with mutant slices where cortical axons were absent. Taken together, these observations show that a normal cortex with descending cortical axons is capable of guiding thalamic axons into the cortex, and support the hypothesis that the 'hand shake' between TCAs and CTAs is important for TCAs to reach the cerebral cortex.

In conclusion, my data show that guidance factors from the cortex are needed for TCAs to cross the PSPB, which are absent in the *Emx1*-Cre/*Apc*-LoxP conditional mutant. TCAs may need the direct contact with cortical axons and use them as an axonal scaffold to navigate into the cerebral cortex, in addition to the growth promoting effect from Ig-Nrg1.

Chapter 5. Inactivation of *Apc* in the thalamus and the development of CTAs and TCAs

In this chapter I describe the conditional inactivation of *Apc* gene in the thalamus and its effect on the development of reciprocal connections between the cortex and the thalamus. As mentioned in the general introduction in Chapter 1, CTAs and TCAs are proposed to use each other as axonal scaffolds to reach their final targets, described as the Handshake hypothesis. To test this hypothesis, I used the *RORα*-Cre/*Apc*-LoxP mouse to generate a conditional mutant model where TCAs development might be interrupted, and test whether CTAs are able to reach the thalamus in the absence of the guidance from the descending TCAs.

By using YFP reporter mouse here I show that *RORα*-Cre is mainly expressed in the primary sensory nuclei of the thalamus, including dorsal lateral geniculate (dLG), ventroposterior (VP), and medial geniculate (MG). *Apc* deletion is most obvious in the dLG of *RORα*-Cre/*Apc*-LoxP conditional mutant thalamus, consistent with the high expression of *RORα* in this region. Examinations of the axonal tracts do not show dramatic defects of CTAs and TCAs in the *RORα*-Cre/*Apc*-LoxP conditional mutants. These results indicate that deletion of *Apc* in postmitotic neurons in the thalamus may not affect axonal development between the cortex and the thalamus.

5.1 The expression pattern of *RORα*-Cre

In the current study, *Apc* was conditionally inactivated in the thalamus by Cre recombinase driven by the endogenous *RORα* promoter (*RORα*-Cre). *RORα* starts to be expressed in the thalamus from E11.5 (Nakagawa and O'Leary, 2003). The activity of Cre recombinase was confirmed by GFP immunofluorescence on embryos carrying *RORα*-Cre and a floxed-stop YFP reporter allele (Figure 1). At E14.5, *RORα*-Cre was expressed in the mantle region of the thalamus, while the proliferative zone of the thalamus was negative for YFP+ cells (Figure 1 A). YFP+ thalamic axons descended from the thalamus and traversed through the ventral telencephalon to enter the cerebral cortex (Figure 1 A, arrows). At E18.5, YFP+ cells

Figure1

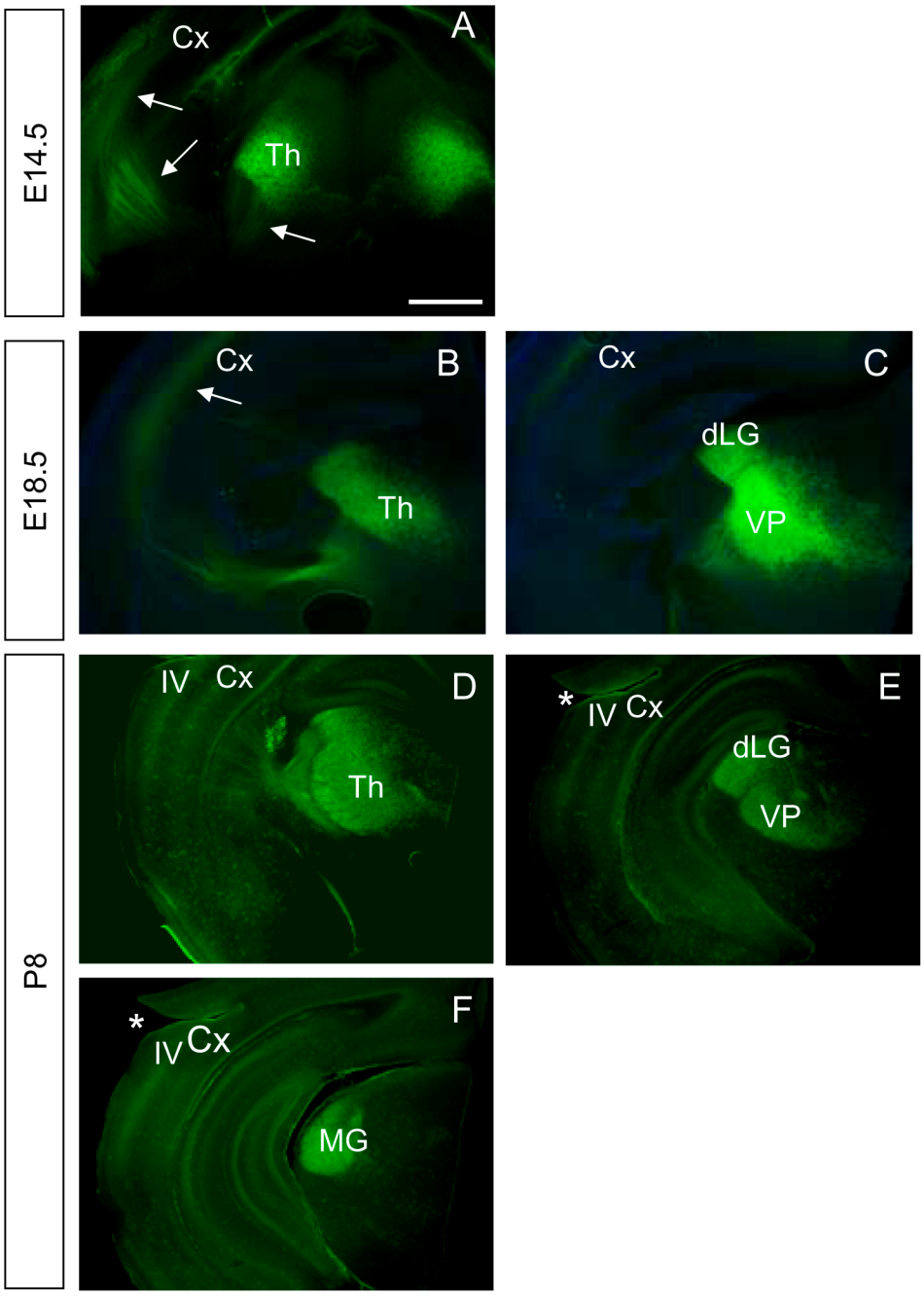
E14.5
A
Cx
Th
E18.5
B
Cx
Th
C
Cx
dLG
VP
P8
D
IV
Cx
Th
E
*
IV
Cx
dLG
VP
F
*
IV
Cx
MG

Figure 1. The expression pattern of *RORα* –Cre. GFP immunofluorescence showing the expression of *RORα* -Cre recombinase in mice carrying *RORα* Cre and a floxed-stop YFP reporter allele. **(A)** At E14.5, *RORα* -Cre was expressed in the mantle region of the thalamus, while the proliferative zone of the thalamus was negative for YFP+ cells. YFP+ thalamic axons descended from the thalamus and traversed through the ventral telencephalon to enter the cerebral cortex (arrows). **(B & C)** At E18.5, YFP+ cells were detected in the thalamus from rostral (B) to caudal (C) sections. YFP+ thalamic axons navigated within the intermediate zone of the cerebral cortex (arrow). **(D, E & F)** At P8, YFP+ cells were observed in the primary sensory nuclei of the thalamus, including the dLG, VP, and MG. YFP+ thalamic axons targeted in the cerebral cortex and formed arbors in layer IV of the cortex. Artifacts were labeled by stars. Th-thalamus, Cx-cortex, dLG-dorsal lateral geniculate, VP-ventroposterior, MG-medial geniculate. Scale bars: (A-F) 500 μm.

were detected in the thalamic cells from rostral to caudal sections (Figure 1 B & C, respectively). YFP+ thalamic axons navigated within the intermediate zone of the cerebral cortex. At P8, YFP+ cells were observed in the primary sensory nuclei of the thalamus, including dorsal lateral geniculate (dLG), ventroposterior (VP), and medial geniculate (MG) (Figure 1 D, E & F). YFP+ thalamic axons targeted in the cerebral cortex and formed arbors in layer IV of the cortex.

5.2 Proof of Apc deletion in the thalamus of the conditional mutant

To examine the deletion of Apc protein in the conditional mutant, Apc immunofluorescence was performed on paraffin sections and cryostat sections of embryos (Figure 2). In P0 control mice, Apc protein was evenly expressed in the thalamus (Figure 2 A & C). In the *RORα*-Cre/*Apc*-LoxP conditional mutant, Apc expression level was reduced in the lateral region of the thalamus, where the presumptive dLG is located (Figure 2 B & D). In the heterozygotes (Figure 2 E), a large number of YFP+ cells were observed in the dLG and the VP of the thalamus, whereas in the *RORα*-Cre/*Apc*-LoxP conditional mutant (Figure 2 F), YFP+ cells were more sparsely distributed in the dLG and VP, and the cell density was lower, compared to the heterozygotes. In the heterozygotes (Figure 2 G), Apc was expressed in both dLG and VP, whereas in the *RORα*-Cre/*Apc*-LoxP conditional mutant (Figure 2 H), APC was hardly detected in dLG. By P14, Apc expression was evenly distributed in the thalamus of the heterozygous mice (Figure 2 I). In the *RORα*-Cre/*Apc*-LoxP conditional mutant, Apc expression was reduced in the dLG and in the region ventral to the VP (Figure 2 J).

5.3 *Apc* deletion in the thalamus and the development of CTAs and TCAs

At E14.5, the growth patterns of L1-positive axonal tracts were similar between the control and the *RORα*-Cre/*Apc*-LoxP conditional mutant (Figure 3 A & B, respectively), with L1-labelled fibers navigating between the thalamus and the

Figure 2

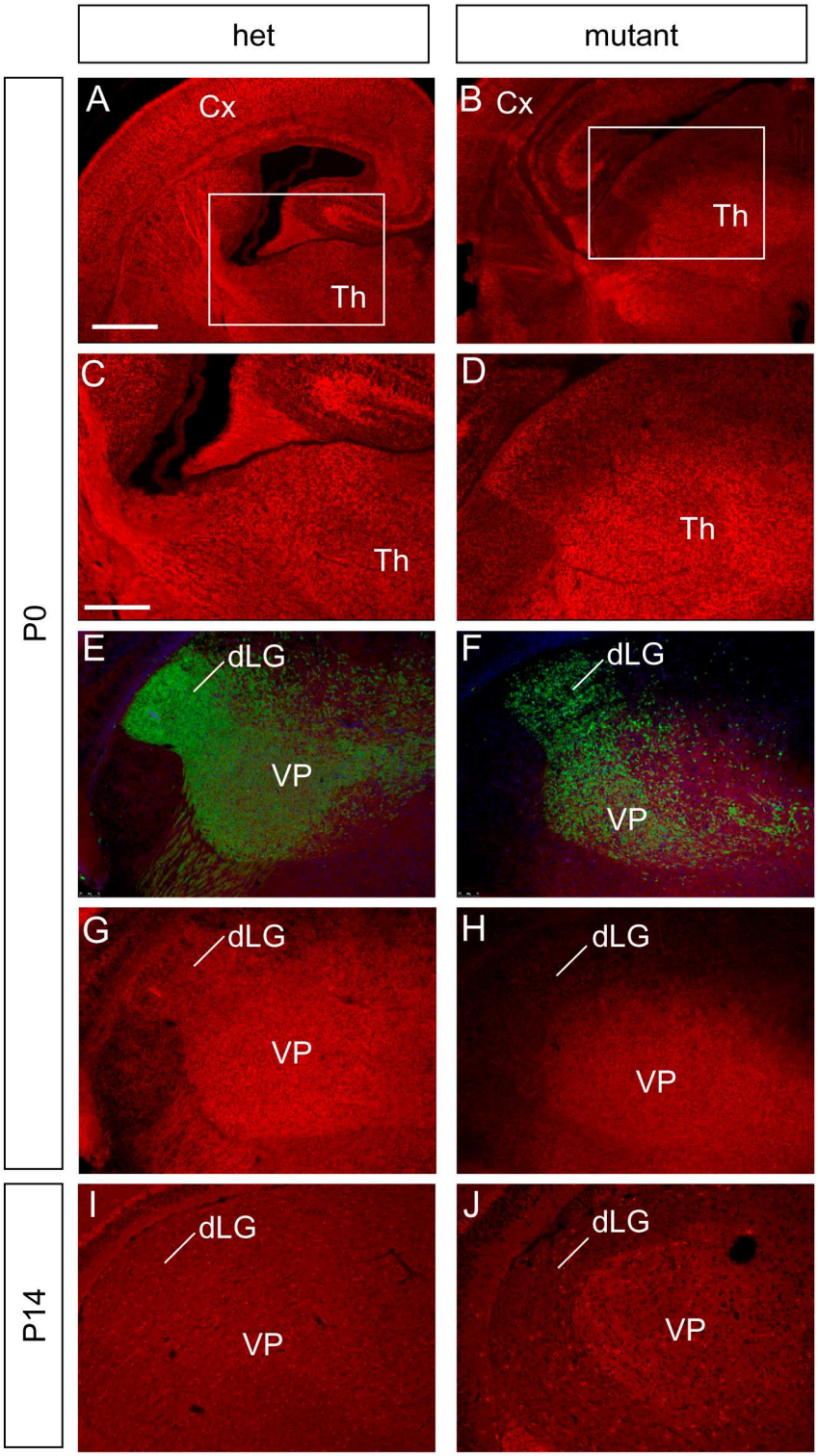
het
mutant
P0
P14
A
Cx
Th
B
Cx
Th
C
Th
D
Th
E
dLG
VP
F
dLG
VP
G
dLG
VP
H
dLG
VP
I
dLG
VP
J
dLG
VP

Figure 2. Proof of Apc deletion in the thalamus of the conditional mutant. (A) APC protein was evenly expressed in the thalamus of P0 control mice. **(B)** In the mutant, APC expression level was reduced in the lateral region of the thalamus, where the presumptive dLG is located. **(C & D)** Higher magnification images of the boxed areas in (A) and (B), respectively. **(E & F)** GFP (green) and APC (red) immunofluorescence on coronal sections of P0 control and mutant mice, respectively. Nuclei were stained with TO-PRO-3 (blue). In the control (E), a large number of YFP+ cells were observed in the dLG and the VP of the thalamus, whereas in the mutant (F), YFP+ cells were more sparsely distributed in the dLG and VP, and the cell density is lower, compared to the control. **(G & H)** The same sections of (E) and (F), respectively, showing the red channel. In the control (G), APC was expressed in both dLG and VP, whereas in the mutant (H), APC was hardly detected in dLG. **(I & J)** By P14, APC expression was evenly distributed in the thalamus of control mice (I), whereas in the mutant (J), APC repression was reduced in the dLG and in the region ventral to the VP. (A-D) Wax sections. (E-J) Cryostat sections. Th-thalamus, Cx-cortex, dLG-dorsal lateral geniculate, VP-ventroposterior, MG-medial geniculate. Scale bars: (A, B) 500 μm; (C-J) 250 μm.

Figure 3

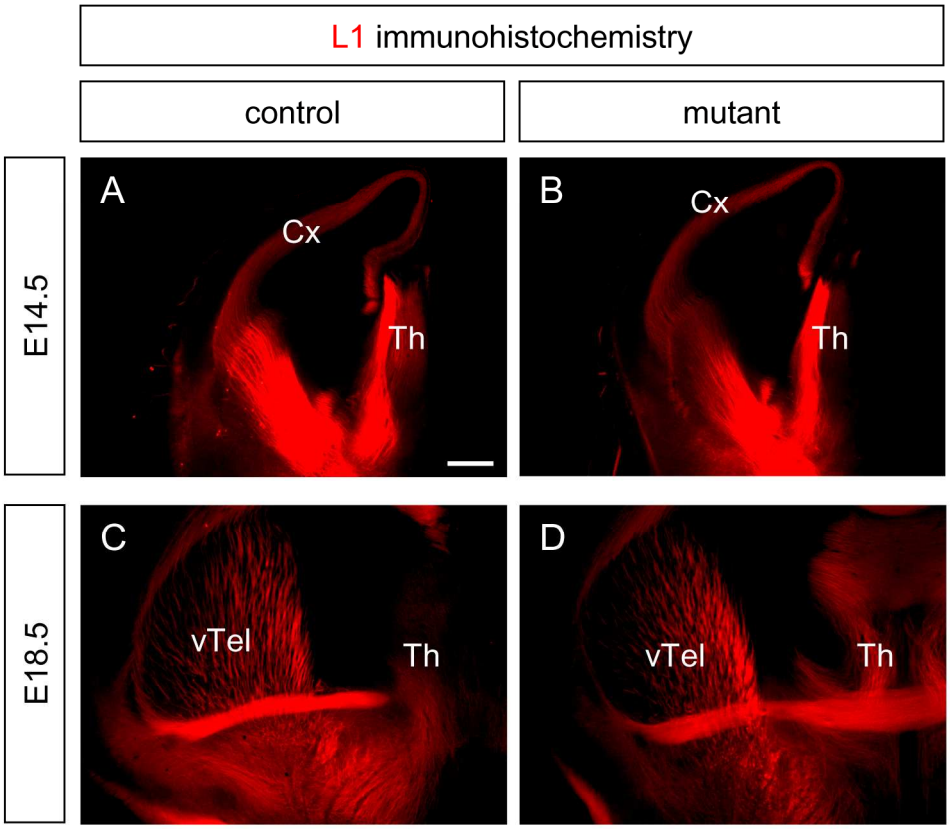

Figure 3. Axonal developmental defects were not observed in the *Apc* conditional mutant. (A & B) At E14.5, the growth patterns of L1-positive axonal tracts were similar between the control (A) and the mutant (B), with L1-labelled fibers navigating between the thalamus and the cerebral cortex. **(C & D)** At E18.5, the growth patterns of L1-positive axonal tracts were similar between the control (C) and the mutant (D), with large number of L1-labelled axons growing through the ventral telencephalon. Th-thalamus, Cx-cortex, vTel-ventral telencephalon. Scale bars: (A-D) 150 μm.

cerebral cortex. At E18.5, the growth patterns of L1-positive axonal tracts were similar between the control and the *RORα*-Cre/*Apc*-LoxP conditional mutant (Figure 3 C & D), with large number of L1-labelled axons growing through the ventral telencephalon. In P14 control mice, barrels were observed in layer IV of the cerebral cortex (Figure 4 A & C, arrow points to one of the barrels). In P13 *RORα*-Cre/*Apc*-LoxP conditional mutant mice, barrels were also detected in the cerebral cortex (Figure 4 B & D, arrow points to one of the barrels).

5.4 *Apc* deletion and cell death in the thalamus of the conditional mutant

As mentioned above, YFP+ cells were more sparsely distributed in the dLG and VP of the *RORα*-Cre/*Apc*-LoxP conditional mutant thalamus, and the cell density was lower, compared to the heterozygotes. Since *RORα* is expressed in thalamic cells that have exited cell cycle and become postmitotic neurons, the reduction of YFP+ cells in *RORα*-Cre/*Apc*-LoxP conditional mutant thalamus would not be due to the proliferative defects in cells that lack *Apc*. In *Emx1*-Cre/*Apc*-LoxP conditional mutant where *Apc* is specifically inactivated in the cerebral cortex, an increase of cell death is observed in the cortex (Ivaniutsin et al., 2009). Therefore I wondered if the deletion of *Apc* in the thalamus could lead to an increase of cell death in *RORα*-Cre/*Apc*-LoxP conditional mutant thalamus, which causes a reduction of YFP+ cells.

Here Caspase 3 immunohistochemistry was carried out on paraffin sections of the embryos, as Caspase 3 is a marker for cells undergoing apoptosis. At E18.5, the *RORα*-Cre/*Apc*-LoxP conditional mutant showed slightly more Caspase 3-positive cells in the thalamus (Figure 5 C & E, arrows), compared to the control (Figure 5 B & D, arrows). In the medial part of the thalamus adjacent to the ventricle of *RORα*-Cre/*Apc*-LoxP conditional mutants, a large number of Caspase 3-lablled cells were observed, with pieces of cell debris scattered around (Figure 5 C, arrows). This was not observed in the control, where only a small number of Caspase 3-positive cells were detected (Figure 5 B, arrow). In the lateral thalamus of the *RORα*-Cre/*Apc*-

Figure 4

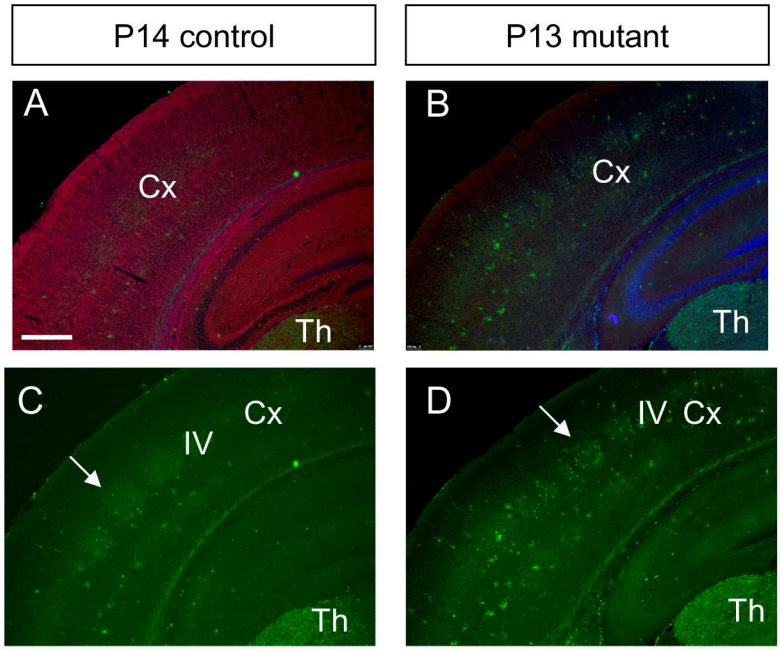

Figure 4. Barrels were formed in the cortex of the Apc conditional mutant. (A & B) APC (red) and GFP (green) immunohistochemistry on coronal sections. Nuclei were counter stained with TOPRO 3 (blue). **(C & D)** The same sections as observed in (A) and (B), respectively, showing the green channel. In P14 control mice, barrels were observed in layer IV of the cerebral cortex (arrow, C). In P13 mutant mice, barrels were also detected in the cerebral cortex (arrow, D). Scale bars: (A-D) 200 µm.

Figure 5

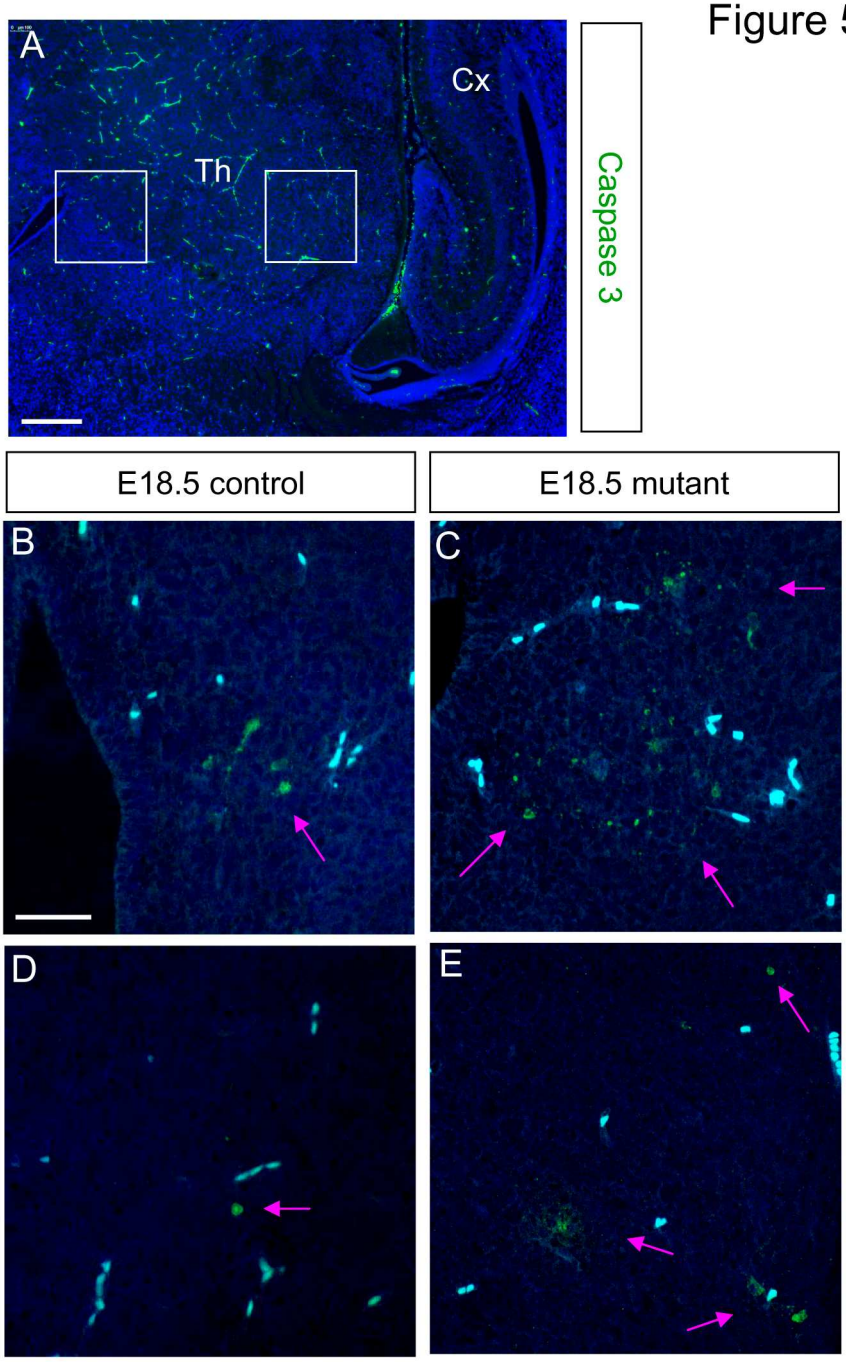

Figure 5. A slight increase of apoptosis in the *Apc* conditional mutant. **(B & C)** High power images showing the medial part of the thalamus in control and mutant E18.5 embryos, respectively (boxed area on the left in **A**). The mutant showed more Caspase 3-positive (green) cells in the medial region of the thalamus (C, arrows), compared to the control (B, arrow). **(D & E)** High power images showing the lateral part of the thalamus in control and mutant E18.5 embryos, respectively (boxed area on the right in A). The mutant showed more Caspase 3-positive cells in the lateral region of the thalamus (E, arrows), compared to the control (D, arrow). These results might indicate that there are more cells undergoing apoptosis in the thalamus of the mutant, compared to the control. Scale bars: (A) 250 μm; (B-E) 50 μm.

LoxP conditional mutants (Figure 5 E, arrows), an increase of Caspase 3-labelled cells was detected, but not as dramatic as seen in the medial thalamus of the *RORα*-Cre/*Apc*-LoxP conditional mutants. In the mutant lateral thalamus, a cloud-like structure was stained by Caspase 3 (Figure 5 E, on the left), which might be the debris from apoptotic cells. This was hardly observed in the control, where only a small number of Caspase 3-positive cells were detected (Figure 5 D, arrow).

Taken together, these preliminary data seemed to show a slight increase of Caspase 3-positive cells in the thalamus of *RORα*-Cre/*Apc*-LoxP conditional mutant, compared to the control, although the difference is not dramatic. However, apoptosis is a tightly regulated process that happens rapidly. Hence even a small change of the apoptotic rate may reflect the difference of cellular activity between the mutant and the control. Thus further quantitative work needs to be done to clarify whether there is a significant increase of apoptotic cells in the thalamus of *RORα*-Cre/*Apc*-LoxP conditional mutants.

5.5 Discussion

In the current study *Apc* is conditionally inactivated in the primary sensory nuclei of the thalamus where *RORα* is expressed. There are no dramatic defects of CTAs and TCAs in this conditional mutant, indicating that deletion of *Apc* in postmitotic neurons in the thalamus may not affect axonal development between the thalamus and cortex. However, when *Apc* is specifically inactivated in the cerebral cortex driven by *Emx1*-Cre expression, there are severe defects of CTAs and TCAs, as mentioned in Chapter 3. It is intriguing to compare *RORα*-Cre/*Apc*-LoxP conditional mutants with *Emx1*-Cre/*Apc*-LoxP conditional mutants, as these two conditional mutants might reveal different aspects of *Apc* in the development of the forebrain and its axonal tracts.

Comparison between *RORα*-Cre/*Apc*-LoxP and *Emx1*-Cre/*Apc*-LoxP conditional mutant models

Firstly, *Apc* is inactivated in different cell types in these two conditional mutants. In *Emx1*-Cre/*Apc*-LoxP conditional mutants, *Apc* is deleted in cerebral cortical progenitor cells that express *Emx1*, whereas in *RORα*-Cre/*Apc*-LoxP conditional mutants *Apc* is inactivated in thalamic postmitotic neurons that express *RORα*. It has been shown that loss of *Apc* in progenitor cells leads to severe defects in the development of the cerebral cortex, such as causing disruption in the anatomic structure, cell type specification, neuronal differentiation and axonal growth, etc (Ivaniutsin et al., 2009; Yokota et al., 2009). Thus *Apc* has important functions in progenitor cells, and that loss of *Apc* in the cerebral cortical progenitors will lead to severe defects in axonal outgrowth and targeting. However, it is unclear what functions *Apc* might have in the postmitotic cells in the thalamus. In the current study, it is the first attempt to delete *Apc* in postmitotic neurons in the thalamus and study its effect on axonal development. The results show that deletion of *Apc* in the primary sensory nuclei of the thalamus driven by *RORα*-Cre expression neither affect the anatomic structure of the thalamus, nor cause dramatic defects in CTAs and

TCAs development, although minor axonal defects can not be ruled out at the moment. Additionally, barrels are formed in P13 *RORα*-Cre/*Apc*-LoxP conditional mutants, indicating that TCAs are able to target the somatosensory cortex. However, there is a large reduction of Apc in the dLG area, which raises the question of whether axons projecting from and/or towards the dLG are normal in *RORα*-Cre/*Apc*-LoxP conditional mutants. Further experiments through DiI placements into the visual cortex or the dLG may help to answer whether thalamic axons derived from the dLG are able to target the visual cortex normally and vice versa. Since *RORα*-Cre/*Apc*-LoxP conditional mutants survive to adult hood, further behaviour experiments such as visual tasks can be used to test whether the visual system develops normally in *RORα*-Cre/*Apc*-LoxP conditional mutants.

Secondly, Apc protein may be more stable in postmitotic cells than in progenitor cells. In *Emx1*-Cre/*Apc*-LoxP conditional mutants, Apc expression is largely reduced in the cerebral cortex soon after the Cre-induced inactivation of *Apc* occurs, whereas in *RORα*-Cre/*Apc*-LoxP conditional mutants Apc expression seems to be preserved in the VP region of the thalamus. It is conceivable that Apc is stabilized in the cytoskeleton structure of postmitotic cells in the VP region and so its expression still maintains at postnatal ages. It would be interesting to isolate YFP+ cells from the *RORα*-Cre/*Apc*-LoxP conditional mutant thalamus through FACS techniques and do PCR to confirm the deletion of *Apc* gene in these cells, as this will prove that the presence of Apc in the VP of the *RORα*-Cre/*Apc*-LoxP conditional mutant thalamus is due to the stable characteristics of this protein in postmitotic cells in the thalamus rather than cells exempt *Apc* gene deletion. Nevertheless, Apc is largely reduced in the dLG of the thalamus, probably due to the extremely high expression of *RORα* in this region (Figure 6 A).

When *Apc* is deleted in the cerebral cortex of *Emx1*-Cre/*Apc*-LoxP conditional mutants, a dramatic increase of cell death is observed, indicating that *Apc* is important in regulating cell number in the cortex (Ivaniutsin et al., 2009). In the *RORα*-Cre/*Apc*-LoxP conditional mutant, YFP reporter mice show a lower density of YFP+ cells in the primary sensory nuclei of the thalamus, which implies cell

Figure 6

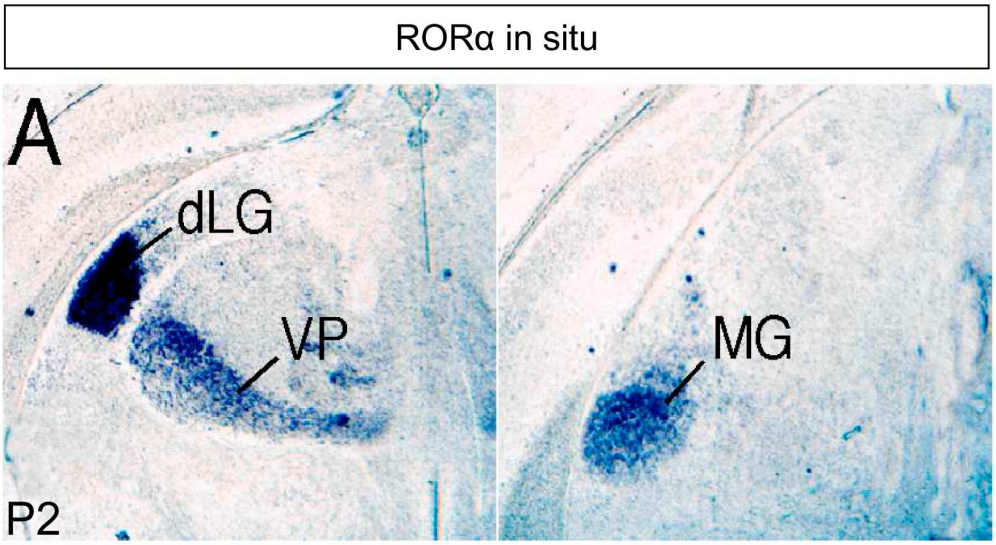

(From B. Hamilton)

Figure 6. Expression pattern of *RORα* in the thalamus. (A) *RORα* in situ hybridization on P2 wildtype mouse (from B. Hamilton). *RORα* is strongly expressed in the dLG, whereas it exhibits a high dorsolateral to low ventromedial graded expression in the VP and a high lateral to low medial gradient in the MG.

autonomous defects in RORα-expressing cells where *Apc* is inactivated. Loss of *Apc* in thalamic cells of *RORα*-Cre/*Apc*-LoxP conditional mutants may cause cell death, since Caspase 3 immunohistochemisty reveals an increase of apoptosis in the *RORα*-Cre/*Apc*-LoxP conditional mutants. However, further work needs to be done to quantify cell numbers in the dLG, VP and MG of the *RORα*-Cre/*Apc*-LoxP conditional mutants, and compare to the control.

In *Emx1*-Cre/*Apc*-LoxP conditional mutants, loss of Apc leads to an increase of β-catenin/Wnt signaling in the cerebral cortex. Since β-catenin/Wnt signaling is robust in the thalamus during early brain development, an increase of β-catenin/Wnt signaling in the thalamus of *RORα*-Cre/*Apc*-LoxP conditional mutant due to *Apc* inactivation may not have a dramatic impact on the patterning of the thalamus. Further study can be done to check whether there is a change in the expression pattern of β-catenin/Wnt signals in the *RORα*-Cre/*Apc*-LoxP conditional mutant.

In summary, conditional deletion of *Apc* in the primary sensory nuclei of the thalamus driven by *RORα*-Cre expression does not show severe defects of CTAs and TCAs, which indicates that *Apc* does not play an important role in axonal growth after thalamic cells become mature postmitotic neurons. However, further experiments through DiI/DiA placements in the dLG, VP and MG areas of *RORα*-Cre/*Apc*-LoxP conditional mutants may help to detect whether there are any topographic defects of CTAs and TCAs during development.

Chapter 6. Final discussion and future perspectives

6.1 CTAs are important for guiding TCAs into the cerebral cortex

Previously identified mutants with CTA defects usually display reciprocal TCA defects, which implies that the intermingling of TCAs and CTAs is important for both sets of axons to reach their targets (Hevner et al., 2002; Jones et al., 2002). It is proposed that not only the intimate association between CTAs and TCAs, but also the recognition and bidirectional signaling between CTAs and TCAs are important for them to guide each other to the final targets (Hevner et al., 2002). For instance, in *Tbr1*$^{-/-}$ mutants CTAs and TCAs meet and intermingle in the basal telencephalon, but they fail to reach the thalamus and cortex, respectively. Since *Tbr1* is expressed in the cortex but not in the thalamus, it could be that the expression of bidirectional signaling molecules is impaired in CTAs, so that CTAs and TCAs intermingle but lose the ability to signal to each other (Hevner et al., 2002).

In *Emx1*-Cre/*Apc*-LoxP conditional mutants, CTAs are absent, whereas TCAs grow into the ventral telencephalon but fail to cross the PSPB and reach the cortex. Instead, TCAs navigate along the ventrally-directed LCS cells towards the ventral part of the basal telencephalon. However, a replacement of the mutant cortex by a control cortex in the *in vitro* brain slice culture experiments is able to rescue TCAs into the control cortex, indicating that a normal cortex is capable of producing guidance cues to direct TCAs into the cortex. Also in the brain slice culture experiments, TCAs show intimate association with the descending CTAs from the control cortex, which indicates attraction between CTAs and TCAs. These results show that CTAs may play important roles in regulating the direction of TCAs, and support the hypothesis that the 'hand shake' between the TCAs and CTAs provides guidance for TCAs to reach the cerebral cortex.

In *Emx1*-Cre/*Apc*-LoxP conditional mutants, *Emx1* starts to be expressed at about E9.5, therefore driving the deletion of *Apc* from an early age during development. The defect of CTAs caused by this conditional deletion of *Apc* is dramatic, with no

normal CTAs generated in the cerebral cortex, which may also be the reason for the almost complete absence of the ascending TCAs in the cortical region. However, it would be interesting to see if deleting *Apc* in the cerebral cortex at later ages could allow the growth of a subset of CTAs, which in turn could guide a subpopulation of corresponding TCAs into the cortex. Recent years have seen the use of inducible-Cre models, where target genes can be deleted at an age after tamoxifen is given to the animal models. By using tamoxifen-induced *Emx1*-Cre/*Apc*-LoxP mouse models to inactivate *Apc* at later ages, i.g. E10.5, E11.5 or E12.5, we may be able to detect a small amount of projection neurons that escape from cortical deletion of *Apc*, and subsequently produce normal CTAs that can pass the PSPB into the ventral telencephalon and guide a subset of TCAs into the cortex.

In *Nestin*-Cre/*Apc*-LoxP mutants, *Apc* deletion occurs in Nestin expressing neural progenitors from around E10 (Yokota et al., 2009). The loss of Apc leads to severe developmental defects of the cerebral cortex, including the disruption of radial glial polarity and scaffolding, the reduction of cortical precursor proliferation, the defects of cortical neuron migration and positioning. In addition, *Nestin*-Cre/*Apc*-LoxP mutants exhibit disruption of both CTA and TCA development. CTAs swirl around and do not orient or fasciculate toward their appropriate targets, while TCAs do not orient or fasciculate properly and are misrouted in the developing cerebral cortex. However, Nestin is widely expressed in the developing radial glia in the CNS, and the deletion of Apc driven by the *Nestin*-Cre transgene not only causes severe defects of cerebral cortex, but also affects the subcortical area, e.g. the size of the lateral ventricles is increased and the ventral telencephalon is thinner, with a shape that is very different compared to wild type. Also the thalamus in the mutant is smaller and the structure is abnormal. Thus the defects of CTAs and TCAs in *Nestin*-Cre/*Apc*-LoxP mutants might be due to the disruption of projection neurons in the cortex and thalamus, and/or the change of guidance cues in the cortex, ventral telencephalon and diencephalon. In *hGFAP*-Cre/*Apc*-LoxP mutants where Apc deletion occurs in the hGFAP expressing radial glial progenitors in the dorsal telencephalon from E13.5, the radial glial scaffold is disrupted in the dorsal telencephalon but not in the ventral telencephalon, where radial glia extend long polarized processes as in controls

(Yokota et al., 2009). However, the development of CTAs and TCAs in *hGFAP*-Cre/*Apc*-LoxP mutants has not been reported.

The handshake hypothesis proposes that the pioneer cortical efferents from the subplate cells provide axonal scaffolds for the ascending thalamic fibers to reach the cortex. To further investigate the roles of subplate axons in the guidance of thalamic afferents, future work sees the potential use of subplate specific Cre lines to inactivate Apc in subplate cells. Additionally, there is potential use of *Nex1*-Cre, which is active in differentiating neurons. By deleting important genes such as *Apc* in *Nex1* expressing subplate and cortical plate cells, the outgrowth and development of cortical efferents might be disrupted and we can test whether thalamic axons are able to reach the cortex without the guidance from the corticofugal axons.

The observations of the growth pattern of the thalamic axons in *reeler* mutant mice have shed light on the guiding role of subplate axons on thalamic axonal navigation. Unlike wildtype mice where the preplate layer would be split by the cortical plate into the marginal zone and the subplate, in *reeler* mice the cortical plate accumulate below the preplate, and the preplate axons run down through the cortical plate into the intermediate zone. In normal mice, most thalamic afferents wait for a couple of days in the subplate before invading the cortical plate. In *reeler* mutant mice, thalamic fibers appear to penetrate the cortical plate as soon as they arrive, following preplate axons up to the superficially located preplate (the superplate layer), where they wait for 2-3 days before plugging down to terminate deep in the cortical plate (Molnar et al., 1998b). Thus, *reeler* mutant mice provide strong evidence that thalamic axons follow the scaffold of preplate axons towards their cell bodies.

In *Dlx5/6*-Cre/*Celsr3*-LoxP conditional mutant mice where *Celsr3* is deleted *Dlx5/6* expressing cells in the ventral region of the telencephalon and diencephalon, both CTAs and TCAs show defects in the ventral telencephalon, with CTAs terminating and forming an abnormal mass in the dorsal striatum and TCAs aberrantly invading the pallidum and amygdala (Zhou et al., 2008). However, the initial outgrowth of CTAs and TCAs are not affected in this mutant, indicating that the environment of

the ventral telencephalon has influence on the trajectory of CTAs and TCAs through the ventral telencephalon but not on their outgrowth.

In *Foxg1*-Cre/*Celsr3*-LoxP conditional mutant mice where *Celsr3* is inactivated in the telencephalon driven by *Foxg1*-Cre, TCAs either run aberrantly along the edge of the basal telencephalon or cross the midline ventrally (Zhou et al., 2008). In the ventral telencephalon, the expression of *Foxg1* is broader than *Dlx5/6*, and the environment of the ventral telencephalon in the *Foxg1*/*Celsr3* mutants appear to be more hostile to TCAs than the *Dlx5/6*/*Celsr3* mutants, since TCAs reach the amygdala region in the later mutant but are pushed to the edge of the basal telencephalon in the former one. These observations indicate that *Celsr3* is important in maintaining/ensuring the permissive characteristics of the ventral telencephalic cells for axonal pathfinding.

In *Emx1*-Cre/*Celsr3*-LoxP conditional mutant mice where *Celsr3* is inactivated in the cerebral cortex driven by *Emx1*-Cre, both CTAs and TCAs develop normally and reach their targets (Zhou et al., 2008), unlike the dramatic axonal defects observed in the *Emx1*-Cre/*Apc*-LoxP conditional mutant mice. These data indicate that different genes have different functions in the same type of cells. While *Apc* plays a crucial role in the development of the cortex and its cortical efferents, *Celsr3* does not have a great impact on the outgrowth of corticofugal axons. However, the presence of *Celsr3* in the ventral telencephalon is essential for the normal development of both CTAs and TCAs, raising an interesting implication that the same gene might have different functions in different tissues.

6.2 The PSPB is a choice point for TCAs

Located at the boundary between the dorsal and ventral telencephalon, the PSPB plays important roles in regulating the gene expression between the cortical and subcortical regions on either side of the PSPB. Additionally, the PSPB has functions in restricting cell migration between the dorsal and ventral telencephalon, and thus

helps to maintain the different cell lineages in the pallium and subpallium. Interestingly, cells derived from the PSPB itself will migrate and populate other regions in the telencephalon. For instance, progenitors from the PSPB provide a source for the lateral cortical stream (LCS), a population of neurons that migrate ventrally towards the basal telencephalon.

The LCS is comprised of a mix of Pax6-positive pallial-derived and Dlx2-positive subpallial-derived neural progenitor cells, which are appearing to migrate along the RC2+ radial glial fascicles extending from the PSPB ventricular zone to the ventrolateral telencephalic pial surface (Carney et al., 2006). Thus the LCS appears to be an extension of the PSPB across the whole lateral border of the striatum. In the *Emx1*-Cre/*Apc*-LoxP conditional mutants, TCAs stop proximal to the medial side of the PSPB and turn ventrally along the RC2+ radial glial fascicles at the PSPB. It is unclear what features of the PSPB make it non-permissive for TCAs. One possibility is that the dynamic movement of the LCS migratory cells generates a barrier between the cortical and striatal region and forms a territory for TCAs to cross before they can reach the cerebral cortex. At E11.5, a few Pax6+ cells are detected along the putative route of the LCS (Carney et al., 2006). At E13.5, more Pax6+ cells are leaving the PSPB ventricular zone with Dlx2+ cells and migrating along the LCS to the developing piriform cortex. By E15.5, Pax6+ and Dlx2+ cell migration along the LCS are highly prominent, which target in the developing basolateral complex of the amygdala. By E18.5, Pax6+ and Dlx2+ cells continue to migrate along the LCS to the basal telencephalon. To pass through the PSPB, TCAs may need guidance from the environment.

The developmental time points of CTAs indicate that they could be an important guidance factor for TCAs to cross the PSPB. A small amount of CTAs descend from the cerebral cortex and start to cross the PSPB into the ventral telencephalon at around E12, an age when cells from the PSPB start to migrate along the putative route of the LCS. It is conceivable that the early CTAs that have passed the PSPB could provide a potential scaffold for the later born CTAs as well as TCAs to cross the PSPB (Figure 1). From E13.5 to E14.5, numerous CTAs cross the PSPB and

enter the ventral telencephalon, but appear to pause in the neostriatum for 24-48 hrs (Bloom et al., 2007). It is speculated that this pause in the neostriatum provides the time for CTAs and the corresponding TCAs to form intimate association and match up with each other (Jacobs et al., 2007).

The spectacular comb-shape pattern of CTAs and TCAs at the PSPB appears to reveal the physical force generated by the ventrally-directed LCS cells (Figure 2 A). Perhaps the migratory LCS cells encounter CTAs and TCAs on their way towards the basal telencephalon, and they push CTAs and TCAs tangentially in a dorsal to ventral direction, which cause CTAs and TCAs to bend and make a unique curve specifically along the LCS route (Figure 2 B). In *Emx1*-Cre/*Apc*-LoxP conditional mutants where the descending CTAs are absent, the ascending TCAs fail to cross the PSPB, but follow the LCS cells ventrally towards the basal telencephalon instead. This suggests that LCS cells are capable of directing TCAs ventrally. It is proposed

Figure 1

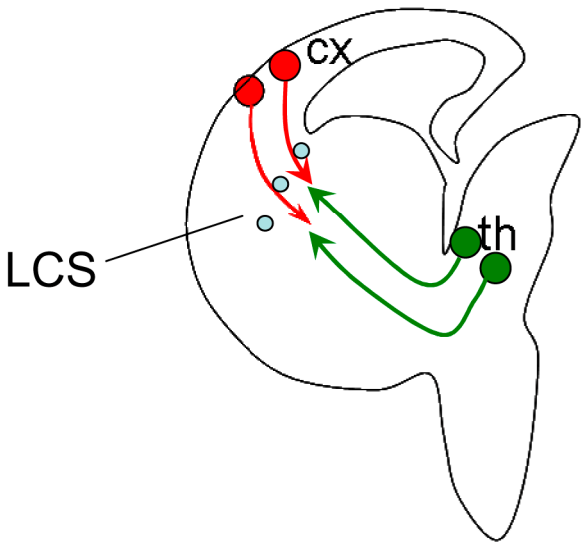

Figure1. Relations between CTAs, TCAs and the LCS. It is conceivable that the early CTAs that have passed the LCS migratory cells at the PSPB could provide a potential scaffold for the TCAs to overcome the ventrally-directed force generated by the LCS cells and cross the PSPB into the cortex.

Figure 2

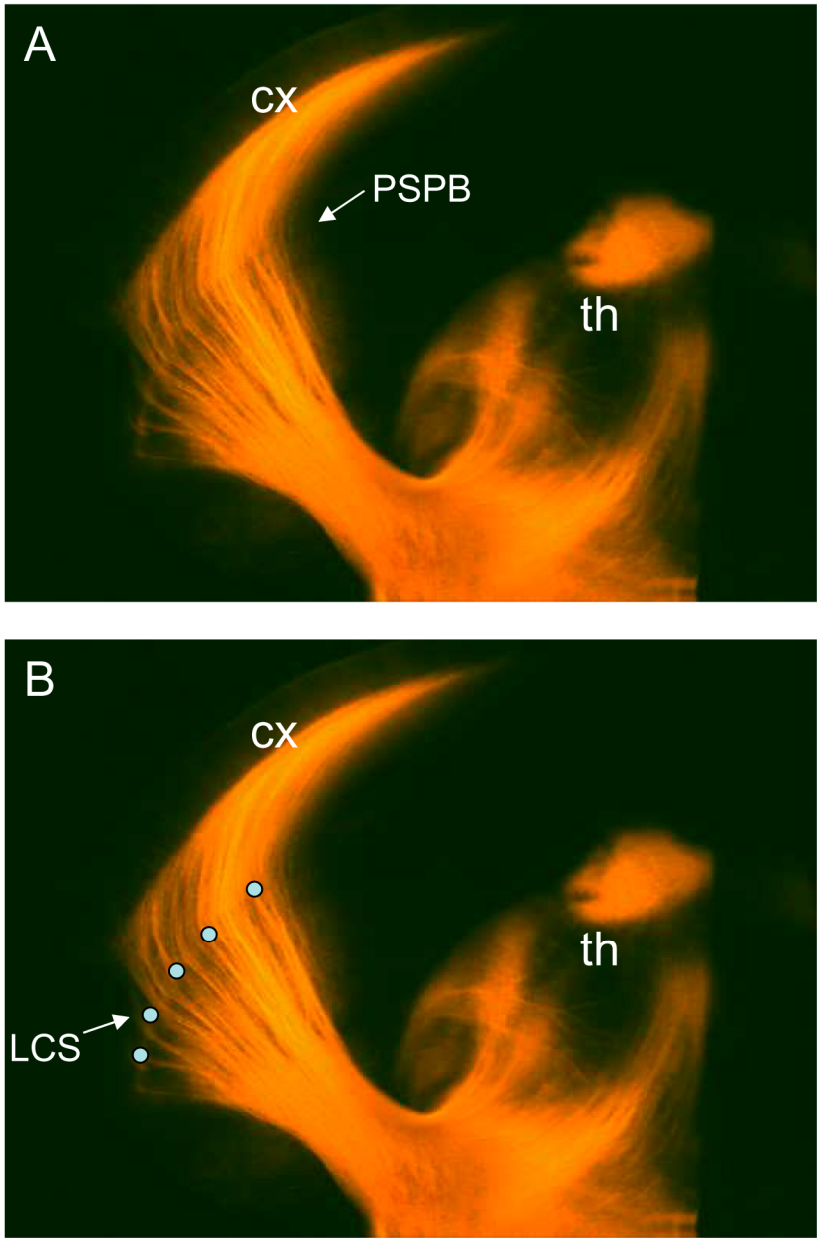

Figure 2. The patterns of CTAs and TCAs in relation to the LCS. (A) The spectacular comb-shape pattern of CTAs and TCAs at the PSPB appears to reveal the physical force generated by the ventrally-directed LCS cells. **(B)** The migratory LCS cells encounter CTAs and TCAs on their way towards the basal telencephalon, and they push CTAs and TCAs tangentially in a dorsal to ventral direction, which cause CTAs and TCAs to bend and make a unique curve specifically along the LCS route.

that the generation of LCS is dependent on the homeodomain-containing gene Gsh2 and that cell migration along the LCS was largely reduced in Gsh2-/- mutants (Carney et al., 2006). It would be interesting to examine the growth pattern of TCAs and CTAs in the Gsh2-/- mutants and see how these axons behave when there are less LCS cells blocking their trajectory.

6.3 The angle region of the cerebral cortex has a growth promoting effect on TCAs

It has been proposed that the angle region in the most ventral region of the pallium has important functions in TCA navigation. *Ig-Nrg1*, the diffusible isoform of *Nrg1*, is highly expressed in the angle region and is suggested to play long-range roles in attracting TCAs towards the cortex (Lopez-Bendito et al., 2006). In brain slice culture experiments where the angle region was ablated, TCAs failed to reach the cortex. Interestingly, addition of Ig-Nrg1-expressing COS cells to the ablated angle region in the slice cultures rescued the growth of TCAs toward the cortex (Lopez-Bendito et al., 2006).

In the current study, *Ig-Nrg1* is still present in the angle region of the *Emx1*-Cre/*Apc*-LoxP conditional mutants. Additionally, thalamic axonal outgrowth was largely increased when thalamic explant was cultured with the angle region from both the control and *Emx1*-Cre/*Apc*-LoxP conditional mutants, indicating that the angle region of both the control and the mutant have growth promoting effects on TCAs. Nevertheless, thalamic axons did not particularly grow towards the angle region explant of either the control or *Emx1*-Cre/*Apc*-LoxP conditional mutants, consistent with previous findings where thalamic axons projecting from thalamic explants did not specifically extend towards the source of Ig-Nrg1-expressing COS cell aggregates (Lopez-Bendito et al., 2006). These results show that Ig-Nrg1 expression in the angle region can promote the growth of TCAs, but it does not affect the direction of thalamic axonal outgrowth. Therefore additional factors are needed to direct TCAs into the cerebral cortex, which might be the descending CTAs.

In conclusion, my data reveal a choice point for TCAs at the PSPB. Guidance factors from the cortex are needed for TCAs to cross the PSPB, which are absent in the *Emx1*-Cre/*Apc*-LoxP conditional mutants. TCAs may need the direct contact with cortical axons and use them as an axonal scaffold to navigate into the cerebral cortex, in addition to the growth promoting effect from Ig-Nrg1 (Figure 3).

In the *Emx1*-Cre/*Apc*-LoxP conditional mutants, no corticofugal axons grow out of the cerebral cortex, and thalamic axons fail to cross the PSPB into the cortex. For future experiments, inducible *Emx1*-Cre strategy can be used to delete *Apc* at later ages, which may allow the outgrowth of a small population of cortical efferents and the arrival of some corresponding thalamocortical afferents in the cortex. Additionally, there are potential use of other Cre lines such as subplate specific Cre's or *Nex1* Cre (active in differentiating neurons) to remove *Apc* from subplate and/or cortical plate neurons, which may result in the disruption of cortical axonal outgrowth and subsequently affect the guidance of thalamic afferents. In the current study, the PSPB appears to be a non-permissive boundary for TCAs, and guidance cues are needed for TCAs to cross this territory. For future work, the PSPB may be removed by using PSPB specific Cre's such as *Gsh2* Cre or in the *in vitro* brain slice culture experiments, so that the growth patterns of cortical and thalamic axons can be examined in the absence of this boundary,

Figure 3

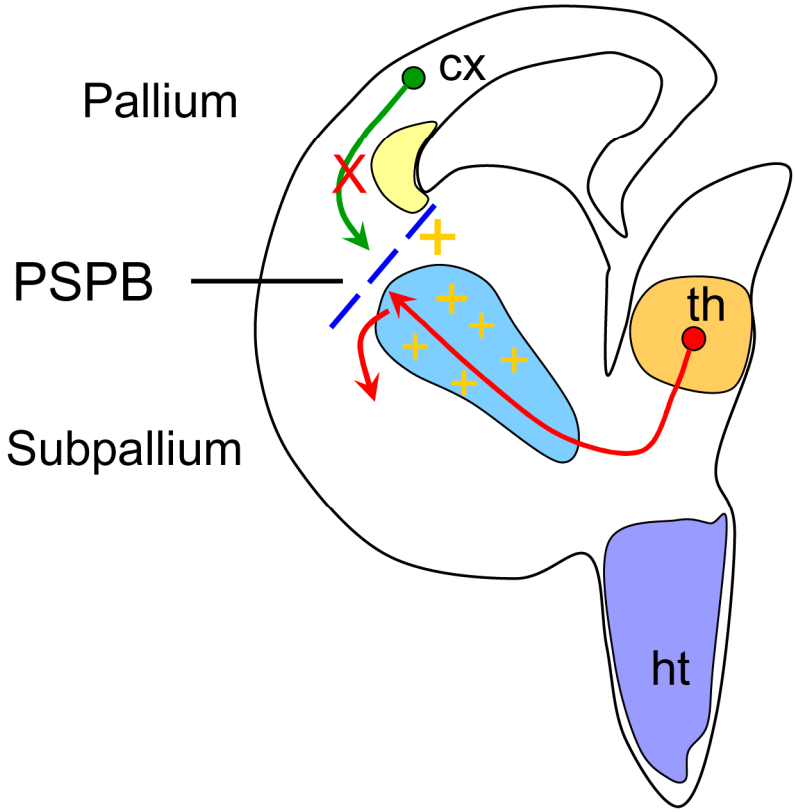

Figure 3. Diagram of the thalamocortical axonal development in the *Emx1*-Cre/*Apc*-LoxP conditional mutant animal model. In the cerebral cortex of the conditional mutants, cortical axons are absent and that TCAs initially navigate into the ventral telencephalon normally but fail to complete their journey into the cortex. They stop as they approach the PSPB, although the PSPB doesn't seem to be affected by the deletion of *Apc* in the cortex. Additionally, Ig-Nrg1 (Neuregulin-1), the secreted protein that was suggested to play long-range roles in attracting TCAs towards the cortex, is present in the ventricular angle of the mutant cortex. This implies that Ig-Nrg1 does not account for the TCA defects in the conditional mutant. It also indicates that Ig-Nrg1 is not sufficient for the extension of TCAs in the conditional mutant, and that additional factors are needed to guide these axons into the cortex. The conditional mutant cortex lacks these guidance factors, which might be the cortical axons. In conclusion, my data reveal a choice point for TCAs at the PSPB. Guidance factors from the cortex are needed for TCAs to cross the PSPB, which are absent in the conditional mutant. TCAs may need the direct contact with cortical axons and use them as an axonal scaffold to navigate into the cerebral cortex, in addition to the growth promoting effect from Ig-Nrg1. cx – cortex, th – thalamus, ht – hypothalamus, PSPB-pallial-subpallial boundary.

Bibliography

Allendoerfer, K. L., and Shatz, C. J. (1994). The subplate, a transient neocortical structure: its role in the development of connections between thalamus and cortex. Annu Rev Neurosci *17*, 185-218.

Andrews, W., Liapi, A., Plachez, C., Camurri, L., Zhang, J., Mori, S., Murakami, F., Parnavelas, J. G., Sundaresan, V., and Richards, L. J. (2006). Robo1 regulates the development of major axon tracts and interneuron migration in the forebrain. Development *133*, 2243-2252.

Auladell, C., Perez-Sust, P., Super, H., and Soriano, E. (2000). The early development of thalamocortical and corticothalamic projections in the mouse. Anat Embryol (Berl) *201*, 169-179.

Bagri, A., Marin, O., Plump, A. S., Mak, J., Pleasure, S. J., Rubenstein, J. L., and Tessier-Lavigne, M. (2002). Slit proteins prevent midline crossing and determine the dorsoventral position of major axonal pathways in the mammalian forebrain. Neuron *33*, 233-248.

Bagri, A., and Tessier-Lavigne, M. (2002). Neuropilins as Semaphorin receptors: in vivo functions in neuronal cell migration and axon guidance. Adv Exp Med Biol *515*, 13-31.

Bhat, R. V., Baraban, J. M., Johnson, R. C., Eipper, B. A., and Mains, R. E. (1994). High levels of expression of the tumor suppressor gene APC during development of the rat central nervous system. J Neurosci *14*, 3059-3071.

Bicknese, A. R., Sheppard, A. M., O'Leary, D. D., and Pearlman, A. L. (1994). Thalamocortical axons extend along a chondroitin sulfate proteoglycan-enriched pathway coincident with the neocortical subplate and distinct from the efferent path. J Neurosci *14*, 3500-3510.

Bielle, F., Griveau, A., Narboux-Neme, N., Vigneau, S., Sigrist, M., Arber, S., Wassef, M., and Pierani, A. (2005). Multiple origins of Cajal-Retzius cells at the borders of the developing pallium. Nat Neurosci *8*, 1002-1012.

Bishop, K. M., Rubenstein, J. L., and O'Leary, D. D. (2002). Distinct actions of Emx1, Emx2, and Pax6 in regulating the specification of areas in the developing neocortex. J Neurosci *22*, 7627-7638.

Bloom, A. J., Miller, B. R., Sanes, J. R., and DiAntonio, A. (2007). The requirement for Phr1 in CNS axon tract formation reveals the corticostriatal boundary as a choice point for cortical axons. Genes Dev *21*, 2593-2606.

Bolz, J., Uziel, D., Muhlfriedel, S., Gullmar, A., Peuckert, C., Zarbalis, K., Wurst, W., Torii, M., and Levitt, P. (2004). Multiple roles of ephrins during the formation of thalamocortical projections: maps and more. J Neurobiol *59*, 82-94.

Bonnin, A., Torii, M., Wang, L., Rakic, P., and Levitt, P. (2007). Serotonin modulates the response of embryonic thalamocortical axons to netrin-1. Nat Neurosci *10*, 588-597.

Braisted, J. E., Catalano, S. M., Stimac, R., Kennedy, T. E., Tessier-Lavigne, M., Shatz, C. J., and O'Leary, D. D. (2000). Netrin-1 promotes thalamic axon growth and is required for proper development of the thalamocortical projection. J Neurosci *20*, 5792-5801.

Braisted, J. E., Ringstedt, T., and O'Leary, D. D. (2009). Slits are chemorepellents endogenous to hypothalamus and steer thalamocortical axons into ventral telencephalon. Cereb Cortex *19 Suppl 1*, i144-151.

Braisted, J. E., Tuttle, R., and O'Leary D, D. (1999). Thalamocortical axons are influenced by chemorepellent and chemoattractant activities localized to decision points along their path. Dev Biol *208*, 430-440.

Briscoe, J., and Ericson, J. (2001). Specification of neuronal fates in the ventral neural tube. Curr Opin Neurobiol *11*, 43-49.

Carney, R. S., Alfonso, T. B., Cohen, D., Dai, H., Nery, S., Stoica, B., Slotkin, J., Bregman, B. S., Fishell, G., and Corbin, J. G. (2006). Cell migration along the lateral cortical stream to the developing basal telencephalic limbic system. J Neurosci *26*, 11562-11574.

Carney, R. S., Cocas, L. A., Hirata, T., Mansfield, K., and Corbin, J. G. (2009). Differential regulation of telencephalic pallial-subpallial boundary patterning by Pax6 and Gsh2. Cereb Cortex *19*, 745-759.

Cecchi, C., and Boncinelli, E. (2000). Emx homeogenes and mouse brain development. Trends Neurosci *23*, 347-352.

Chapouton, P., Schuurmans, C., Guillemot, F., and Gotz, M. (2001). The transcription factor neurogenin 2 restricts cell migration from the cortex to the striatum. Development *128*, 5149-5159.

Corbin, J. G., Rutlin, M., Gaiano, N., and Fishell, G. (2003). Combinatorial function of the homeodomain proteins Nkx2.1 and Gsh2 in ventral telencephalic patterning. Development *130*, 4895-4906.

Dufour, A., Seibt, J., Passante, L., Depaepe, V., Ciossek, T., Frisen, J., Kullander, K., Flanagan, J. G., Polleux, F., and Vanderhaeghen, P. (2003). Area specificity and topography of thalamocortical projections are controlled by ephrin/Eph genes. Neuron *39*, 453-465.

Flames, N., Long, J. E., Garratt, A. N., Fischer, T. M., Gassmann, M., Birchmeier, C., Lai, C., Rubenstein, J. L., and Marin, O. (2004). Short- and long-range attraction of cortical GABAergic interneurons by neuregulin-1. Neuron *44*, 251-261.

Garel, S., and Rubenstein, J. L. (2004). Intermediate targets in formation of topographic projections: inputs from the thalamocortical system. Trends Neurosci *27*, 533-539.

Groden, J., Thliveris, A., Samowitz, W., Carlson, M., Gelbert, L., Albertsen, H., Joslyn, G., Stevens, J., Spirio, L., Robertson, M., and et al. (1991). Identification and characterization of the familial adenomatous polyposis coli gene. Cell *66*, 589-600.

Hanson, C. A., and Miller, J. R. (2005). Non-traditional roles for the Adenomatous Polyposis Coli (APC) tumor suppressor protein. Gene *361*, 1-12.

Hebert, J. M., and Fishell, G. (2008). The genetics of early telencephalon patterning: some assembly required. Nat Rev Neurosci *9*, 678-685.

Hevner, R. F., Miyashita-Lin, E., and Rubenstein, J. L. (2002). Cortical and thalamic axon pathfinding defects in Tbr1, Gbx2, and Pax6 mutant mice: evidence that cortical and thalamic axons interact and guide each other. J Comp Neurol *447*, 8-17.

Hevner, R. F., Shi, L., Justice, N., Hsueh, Y., Sheng, M., Smiga, S., Bulfone, A., Goffinet, A. M., Campagnoni, A. T., and Rubenstein, J. L. (2001). Tbr1 regulates differentiation of the preplate and layer 6. Neuron *29*, 353-366.

Hoch, R. V., Rubenstein, J. L., and Pleasure, S. (2009). Genes and signaling events that establish regional patterning of the mammalian forebrain. Semin Cell Dev Biol *20*, 378-386.

Inoue, T., Tanaka, T., Takeichi, M., Chisaka, O., Nakamura, S., and Osumi, N. (2001). Role of cadherins in maintaining the compartment boundary between the cortex and striatum during development. Development *128*, 561-569.

Ivaniutsin, U., Chen, Y., Mason, J. O., Price, D. J., and Pratt, T. (2009). Adenomatous polyposis coli is required for early events in the normal growth and differentiation of the developing cerebral cortex. Neural Dev *4*, 3.

Iwasato, T., Datwani, A., Wolf, A. M., Nishiyama, H., Taguchi, Y., Tonegawa, S., Knopfel, T., Erzurumlu, R. S., and Itohara, S. (2000). Cortex-restricted disruption of NMDAR1 impairs neuronal patterns in the barrel cortex. Nature *406*, 726-731.

Jacobs, E. C., Campagnoni, C., Kampf, K., Reyes, S. D., Kalra, V., Handley, V., Xie, Y. Y., Hong-Hu, Y., Spreur, V., Fisher, R. S., and Campagnoni, A. T. (2007). Visualization of corticofugal projections during early cortical development in a tau-GFP-transgenic mouse. Eur J Neurosci *25*, 17-30.

Jones, E. G. (2001). The thalamic matrix and thalamocortical synchrony. Trends Neurosci *24*, 595-601.

Jones, L., Lopez-Bendito, G., Gruss, P., Stoykova, A., and Molnar, Z. (2002). Pax6 is required for the normal development of the forebrain axonal connections. Development *129*, 5041-5052.

Komuta, Y., Hibi, M., Arai, T., Nakamura, S., and Kawano, H. (2007). Defects in reciprocal projections between the thalamus and cerebral cortex in the early development of Fezl-deficient mice. J Comp Neurol *503*, 454-465.

Lakhina, V., Falnikar, A., Bhatnagar, L., and Tole, S. (2007). Early thalamocortical tract guidance and topographic sorting of thalamic projections requires LIM-homeodomain gene Lhx2. Dev Biol *306*, 703-713.

Lee, K. J., Mendelsohn, M., and Jessell, T. M. (1998). Neuronal patterning by BMPs: a requirement for GDF7 in the generation of a discrete class of commissural interneurons in the mouse spinal cord. Genes Dev *12*, 3394-3407.

Lett, R. L., Wang, W., and O'Connor, T. P. (2009). Semaphorin 5B is a novel inhibitory cue for corticofugal axons. Cereb Cortex *19*, 1408-1421.

Liang, Y., Annan, R. S., Carr, S. A., Popp, S., Mevissen, M., Margolis, R. K., and Margolis, R. U. (1999). Mammalian homologues of the Drosophila slit protein are ligands of the heparan sulfate proteoglycan glypican-1 in brain. J Biol Chem *274*, 17885-17892.

Lim, Y., and Golden, J. A. (2007). Patterning the developing diencephalon. Brain Res Rev *53*, 17-26.

Little, G. E., Lopez-Bendito, G., Runker, A. E., Garcia, N., Pinon, M. C., Chedotal, A., Molnar, Z., and Mitchell, K. J. (2009). Specificity and plasticity of thalamocortical connections in Sema6A mutant mice. PLoS Biol *7*, e98.

Liu, Y., Ford, B. D., Mann, M. A., and Fischbach, G. D. (2005). Neuregulin-1 increases the proliferation of neuronal progenitors from embryonic neural stem cells. Dev Biol *283*, 437-445.

Lopez-Bendito, G., Cautinat, A., Sanchez, J. A., Bielle, F., Flames, N., Garratt, A. N., Talmage, D. A., Role, L. W., Charnay, P., Marin, O., and Garel, S. (2006). Tangential neuronal migration controls axon guidance: a role for neuregulin-1 in thalamocortical axon navigation. Cell *125*, 127-142.

Lopez-Bendito, G., Chan, C. H., Mallamaci, A., Parnavelas, J., and Molnar, Z. (2002). Role of Emx2 in the development of the reciprocal connectivity between cortex and thalamus. J Comp Neurol *451*, 153-169.

Lopez-Bendito, G., Flames, N., Ma, L., Fouquet, C., Di Meglio, T., Chedotal, A., Tessier-Lavigne, M., and Marin, O. (2007). Robo1 and Robo2 cooperate to control the guidance of major axonal tracts in the mammalian forebrain. J Neurosci *27*, 3395-3407.

Lopez-Bendito, G., and Molnar, Z. (2003). Thalamocortical development: how are we going to get there? Nat Rev Neurosci *4*, 276-289.

Ma, L., Harada, T., Harada, C., Romero, M., Hebert, J. M., McConnell, S. K., and Parada, L. F. (2002). Neurotrophin-3 is required for appropriate establishment of thalamocortical connections. Neuron *36*, 623-634.

Magnani, D., Hasenpusch-Theil, K., Jacobs, E. C., Campagnoni, A. T., Price, D. J., and Theil, T. (2010). The Gli3 hypomorphic mutation Pdn causes selective impairment in the growth, patterning, and axon guidance capability of the lateral ganglionic eminence. J Neurosci *30*, 13883-13894.

Marin, O., Baker, J., Puelles, L., and Rubenstein, J. L. (2002). Patterning of the basal telencephalon and hypothalamus is essential for guidance of cortical projections. Development *129*, 761-773.

Menezes, J. R., and Luskin, M. B. (1994). Expression of neuron-specific tubulin defines a novel population in the proliferative layers of the developing telencephalon. J Neurosci *14*, 5399-5416.

Metin, C., Denizot, J. P., and Ropert, N. (2000). Intermediate zone cells express calcium-permeable AMPA receptors and establish close contact with growing axons. J Neurosci *20*, 696-708.

Metin, C., and Godement, P. (1996). The ganglionic eminence may be an intermediate target for corticofugal and thalamocortical axons. J Neurosci *16*, 3219-3235.

Miller, B., Chou, L., and Finlay, B. L. (1993). The early development of thalamocortical and corticothalamic projections. J Comp Neurol *335*, 16-41.

Molnar, Z., Adams, R., and Blakemore, C. (1998a). Mechanisms underlying the early establishment of thalamocortical connections in the rat. J Neurosci *18*, 5723-5745.

Molnar, Z., Adams, R., Goffinet, A. M., and Blakemore, C. (1998b). The role of the first postmitotic cortical cells in the development of thalamocortical innervation in the reeler mouse. J Neurosci *18*, 5746-5765.

Molnar, Z., and Blakemore, C. (1995). How do thalamic axons find their way to the cortex? Trends Neurosci *18*, 389-397.

Molnar, Z., and Butler, A. B. (2002). The corticostriatal junction: a crucial region for forebrain development and evolution. Bioessays *24*, 530-541.

Molnar, Z., and Cordery, P. (1999). Connections between cells of the internal capsule, thalamus, and cerebral cortex in embryonic rat. J Comp Neurol *413*, 1-25.

Molnar, Z., Metin, C., Stoykova, A., Tarabykin, V., Price, D. J., Francis, F., Meyer, G., Dehay, C., and Kennedy, H. (2006). Comparative aspects of cerebral cortical development. Eur J Neurosci *23*, 921-934.

Nakagawa, Y., and O'Leary, D. D. (2003). Dynamic patterned expression of orphan nuclear receptor genes RORalpha and RORbeta in developing mouse forebrain. Dev Neurosci *25*, 234-244.

Pinon, M. C., Tuoc, T. C., Ashery-Padan, R., Molnar, Z., and Stoykova, A. (2008). Altered molecular regionalization and normal thalamocortical connections in cortex-specific Pax6 knock-out mice. J Neurosci *28*, 8724-8734.

Powell, A. W., Sassa, T., Wu, Y., Tessier-Lavigne, M., and Polleux, F. (2008). Topography of thalamic projections requires attractive and repulsive functions of Netrin-1 in the ventral telencephalon. PLoS Biol *6*, e116.

Pratt, T., Quinn, J. C., Simpson, T. I., West, J. D., Mason, J. O., and Price, D. J. (2002). Disruption of early events in thalamocortical tract formation in mice lacking the transcription factors Pax6 or Foxg1. J Neurosci *22*, 8523-8531.

Pratt, T., Vitalis, T., Warren, N., Edgar, J. M., Mason, J. O., and Price, D. J. (2000). A role for Pax6 in the normal development of dorsal thalamus and its cortical connections. Development *127*, 5167-5178.

Price, D. J., Kennedy, H., Dehay, C., Zhou, L., Mercier, M., Jossin, Y., Goffinet, A. M., Tissir, F., Blakey, D., and Molnar, Z. (2006). The development of cortical connections. Eur J Neurosci *23*, 910-920.

Puelles, L., Kuwana, E., Puelles, E., Bulfone, A., Shimamura, K., Keleher, J., Smiga, S., and Rubenstein, J. L. (2000). Pallial and subpallial derivatives in the embryonic chick and mouse telencephalon, traced by the expression of the genes Dlx-2, Emx-1, Nkx-2.1, Pax-6, and Tbr-1. J Comp Neurol *424*, 409-438.

Puelles, L., and Rubenstein, J. L. (2003). Forebrain gene expression domains and the evolving prosomeric model. Trends Neurosci *26*, 469-476.

Ronca, F., Andersen, J. S., Paech, V., and Margolis, R. U. (2001). Characterization of Slit protein interactions with glypican-1. J Biol Chem *276*, 29141-29147.

Schuurmans, C., and Guillemot, F. (2002). Molecular mechanisms underlying cell fate specification in the developing telencephalon. Curr Opin Neurobiol *12*, 26-34.

Sherman, S. M., and Guillery, R. W. (2011). Distinct functions for direct and transthalamic corticocortical connections. J Neurophysiol *106*, 1068-1077.

Sierra, J., Yoshida, T., Joazeiro, C. A., and Jones, K. A. (2006). The APC tumor suppressor counteracts beta-catenin activation and H3K4 methylation at Wnt target genes. Genes Dev *20*, 586-600.

Simpson, T. I., Pratt, T., Mason, J. O., and Price, D. J. (2009). Normal ventral telencephalic expression of Pax6 is required for normal development of thalamocortical axons in embryonic mice. Neural Dev *4*, 19.

Stoykova, A., Gotz, M., Gruss, P., and Price, J. (1997). Pax6-dependent regulation of adhesive patterning, R-cadherin expression and boundary formation in developing forebrain. Development *124*, 3765-3777.

Stoykova, A., Treichel, D., Hallonet, M., and Gruss, P. (2000). Pax6 modulates the dorsoventral patterning of the mammalian telencephalon. J Neurosci *20*, 8042-8050.

Swanson, L. W., and Petrovich, G. D. (1998). What is the amygdala? Trends Neurosci *21*, 323-331.

Tian, N. M., Pratt, T., and Price, D. J. (2008). Foxg1 regulates retinal axon pathfinding by repressing an ipsilateral program in nasal retina and by causing optic

chiasm cells to exert a net axonal growth-promoting activity. Development *135*, 4081-4089.

Tissir, F., Bar, I., Jossin, Y., De Backer, O., and Goffinet, A. M. (2005). Protocadherin Celsr3 is crucial in axonal tract development. Nat Neurosci *8*, 451-457.

Torii, M., and Levitt, P. (2005). Dissociation of corticothalamic and thalamocortical axon targeting by an EphA7-mediated mechanism. Neuron *48*, 563-575.

Tuttle, R., Nakagawa, Y., Johnson, J. E., and O'Leary, D. D. (1999). Defects in thalamocortical axon pathfinding correlate with altered cell domains in Mash-1-deficient mice. Development *126*, 1903-1916.

Uemura, M., Nakao, S., Suzuki, S. T., Takeichi, M., and Hirano, S. (2007). OL-Protocadherin is essential for growth of striatal axons and thalamocortical projections. Nat Neurosci *10*, 1151-1159.

Wang, Y., Thekdi, N., Smallwood, P. M., Macke, J. P., and Nathans, J. (2002). Frizzled-3 is required for the development of major fiber tracts in the rostral CNS. J Neurosci *22*, 8563-8573.

Wilson, S. W., and Houart, C. (2004). Early steps in the development of the forebrain. Dev Cell *6*, 167-181.

Wright, A. G., Demyanenko, G. P., Powell, A., Schachner, M., Enriquez-Barreto, L., Tran, T. S., Polleux, F., and Maness, P. F. (2007). Close homolog of L1 and neuropilin 1 mediate guidance of thalamocortical axons at the ventral telencephalon. J Neurosci *27*, 13667-13679.

Yokota, Y., Kim, W. Y., Chen, Y., Wang, X., Stanco, A., Komuro, Y., Snider, W., and Anton, E. S. (2009). The adenomatous polyposis coli protein is an essential regulator of radial glial polarity and construction of the cerebral cortex. Neuron *61*, 42-56.

Yun, K., Potter, S., and Rubenstein, J. L. (2001). Gsh2 and Pax6 play complementary roles in dorsoventral patterning of the mammalian telencephalon. Development *128*, 193-205.

Zhou, C., Qiu, Y., Pereira, F. A., Crair, M. C., Tsai, S. Y., and Tsai, M. J. (1999). The nuclear orphan receptor COUP-TFI is required for differentiation of subplate neurons and guidance of thalamocortical axons. Neuron *24*, 847-859.

Zhou, F. Q., Zhou, J., Dedhar, S., Wu, Y. H., and Snider, W. D. (2004). NGF-induced axon growth is mediated by localized inactivation of GSK-3beta and functions of the microtubule plus end binding protein APC. Neuron *42*, 897-912.

Zhou, L., Bar, I., Achouri, Y., Campbell, K., De Backer, O., Hebert, J. M., Jones, K., Kessaris, N., de Rouvroit, C. L., O'Leary, D., *et al.* (2008). Early forebrain wiring: genetic dissection using conditional Celsr3 mutant mice. Science *320*, 946-949.